Industrial Electrical Engineering and Automation

Differential Protection for Arbitrary Three-Phase Power Transformers

Zoran Gajić

Department of Industrial Electrical Engineering and Automation
Lund University

Differential Protection for Arbitrary Three-Phase Power Transformers

Zoran Gajić

LUND UNIVERSITY

Doctoral Dissertation
Department of Industrial Electrical Engineering and Automation

2008

Department of Industrial Electrical Engineering and Automation
Lund University
Box 118
221 00 LUND
SWEDEN

http://www.iea.lth.se

ISBN: 978-91-88934-47-5
CODEN:LUTEDX/(TEIE-1055)/1-226/(2008)

Printed in Sweden by Media-Tryck, Lund University
Lund 2008

Abstract

This thesis describes how to provide standardized, current based, differential protection for any three-phase power transformer, including phase-shifting transformers with variable phase angle shift and transformers of all construction types and internal on-load tap-changer configurations. The use of standard transformer differential protection for such applications is considered impossible in the protective relaying standards and practices currently applied.

The first part of the thesis provides the background for different types of power transformers and the differential protection schemes currently applied. After that a complete mathematical proof for the new, universal transformer differential protection principle, based on theory of symmetrical components, is derived. It is demonstrated that it is possible to make numerical differential protection relays which can properly calculate differential currents for any power transformer, regardless of whether it is of fixed or variable phase angle shift construction and whether current magnitude variations are caused by on-load tap-changer(s).

It is shown how to correctly calculate differential currents by simultaneously providing on-line compensation for current magnitude variations, on-line compensation for arbitrary phase angle shift variations and settable zero-sequence current reduction on any power transformer side. By using this method differential protection for arbitrary power transformers will be ideally balanced for all symmetrical and non-symmetrical through-load conditions and external faults. The method is independent of individual transformer winding connection details (i.e. star, delta or zigzag), but dependent on having the correct information about actual on-load tap-changer(s) position if they are built-in within the protected power transformer.

The implementation and practical use of this new universal principle is quite simple, as all necessary transformer data is commonly available on the protected power transformer rating plate. Practical application of the universal method for the differential protection of standard transformers,

special transformers and phase shifting transformer is presented. Detailed testing of this new universal differential protection method is given and it is based on actual field recordings captured by numerical relays in existing phase-shifting transformer installations and on simulations from the Real Time Digital Simulator for a practical dual-core, symmetrical phase-shifting transformer. The implementation of the universal transformer differential method for analogue and numerical transformer differential relays is also described.

Problems for the differential protection caused by transformer inrush currents are discussed. The mathematical relationship between differential protection and directional protection is derived. Then it is shown that through the addition of supplementary directional criteria security and speed of the operation of the transformer differential protection can be improved. Finally, the use of additional directional criteria to significantly improve the sensitivity of the differential protection for transformer winding turn-to-turn faults is suggested. Captured disturbance files from numerical differential relays in actual power transformer installations, during internal and external faults, have been used to demonstrate the performance of additional directional criteria.

Acknowledgements

I would like to express my sincere gratitude to Professor Sture Lindahl, my supervisor, for his guidance and support throughout my studying at Lund University and also for his help during my relocation and inhabitancy in Sweden. Furthermore I would like to thank to Dr. Olof Samuelsson, Dr. Daniel Karlsson and Professor Gustaf Olsson for their help and advice during my studying at Lund.

Many thanks go as well to my employer ABB AB, Substation Automation Products for permission to use this work for my thesis and their financial support for my travelling to Lund. I specially would like to thanks my direct supervisors Mr. Claudio Marchetti and Mr. Kent Wikström for their understanding and support during my studies. I would also like to thank my colleagues Mr. Birger Hillström and Mr. Ivo Brnčić for the many useful discussions I had with them.

I specially would like to thank Mr. Igor Ivanković from Croatian Power Utility-HEP for his willingness to share disturbance files captured by existing numerical differential relays in the first PST installation in Croatia. From these recordings the first ideas about the presented differential protection method has been discovered and visualized.

I am also very grateful to Dr. Dietrich Bonmann from ABB AG Transformatoren, located in Bad Honnef, Germany, for all his patience and time to discuss with me all details regarding PSTs and his eagerness to give me his simulation files, rating plates and other design parameters for practical PSTs and special power transformers.

Finally, I would like to thank my dear wife Dragica and our three children Ružica, Petar and Maja for all their love, patience, understanding and support throughout my years of studies. I love you all four so much.

"If you want truly to understand something, try to change it."

Kurt Lewin

"Храбре прати срећа."

Српска народна пословица

Preface - The Whole Story

The author had the privilege to work as a member of the ABB development team for a numerical, current based, transformer differential protection relay [11]. The relay was able to automatically compensate for the power transformer vector group connection and even to compensate for the current magnitude differences caused by on-load tap-changer (OLTC) operation. Thus, one could say that I had some good insight into "the stuff", or at least I thought so.

Then, sometime at the end of 2002, a customer called me and asked about the protection of a special transformer. The transformer was a "strange mix" between an auto-transformer and a phase shifting transformer. "Can we use standard differential protection?" was their first question. I looked around and all I could find on the subject was the IEEE/PSRC working group K1 report [37] regarding protection of phase shifting transformers (PST). There it is written that standard differential protection can not be used for a PST. Thus, my first answer was: "No, you probably need to install buried current transformers within the tank and in one or another way follow the IEEE rapport". But the customer came back and said: "But we have no budget for that. Our phase shift is quite small, around 7^{o}; we use a different transformer construction than the one presented in the IEEE paper and we will not install buried CTs. By the way, the transformer manufacturer is starting with its construction soon. Can we use standard differential protection? The relay can read the OLTC position!"

Then the work for this thesis started. First, I tried to calculate how big false differential current would appear if we would apply the differential relay which reads the OLTC position but only can compensate for the current magnitude variations (i.e. not for the phase angle variation) caused by OLTC operation. It took me a while (about a week) to do it. Not much literature was available. Finally I concluded that it is possible, but the relay had to be desensitized. Most problems for the relay will of course be for external single phase to ground faults.

Then the second problem came. From the customer I got steady-state currents (phasors) calculated for an external single phase to ground fault by the short-circuit calculation program using the PST model. The customer asked two questions "Will the differential relay remain stable? Please check if these currents are properly calculated?". "Properly

calculated! How I am going to check this? I do not even have source impedances! Only PST rated quantities! The individual phase currents did not rotate for just 7^{o}!" were my thoughts. After some thinking I concluded that the currents seem reasonable, but I was not really 100% sure. After a while a transformer was manufactured and the first transformer short-circuits tests with the connected differential protection were performed in the transformer manufacturer premises. The differential relay was stable! My calculations were approximately correct!

As soon as the substation was commissioned, the customer performed the primary testing of the PST protection by applying close-by primary single phase to ground faults. The differential relay was stable! For the first time I got the actual disturbance recordings for an external fault captured on such a special transformer.

In the mean time some other enquires came for other PST projects and I got in touch with ABB Transformatoren AG, the ABB centre of excellence for constructions of special transformers and PSTs. At least I got a speaking partner for these "strange devices"! I as well got realistic construction data which were used to simulate such special transformers. They were also able to provide me with some additional disturbance recording files from "their existing PST installations".

Approximately at the same time, more and more often, enquiries for differential protection of special converter transformers came to my table. The interesting thing was that most of them had additional phase shift of 7.5^{o}. Almost the same as the maximum phase angle shift of that PST. "Can we use standard transformer differential protection? Will the error be the same?"

One day when I was looking for some other information, I by chance found out that in the old Westinghouse Transmission & Distribution Reference Book [25] (published in 1950!) there are stated rules of how no-load voltage and load current sequence components (positive, negative and zero sequence) are transferred across any phase shifting transformer. "Very useful information! Now I could check if the customer external fault current calculations were correct. But wait a moment; I could as well check that these rules were valid by evaluating captured disturbance recordings! Yes the rules were valid. Good. What about the phase comparison protection across PST using these rules? Could it be used? Let me check! Yes it seemed to work based on the data from the available field recordings!"

“But wait a little bit! I knew how the sequence current components were transferred across a PST, actually across any three-phase power transformer in accordance with this old book. If I started from there, I should be able to derive a relationship between the phase currents from the two PST sides. I had learned symmetrical components and matrix based mathematics once upon a time. It should be quite easy to perform such a task! Yes of course!” Unfortunately it took at least a week to go through all equations without making any error during the derivation process. Finally the equation was in front of me.
Then I checked the equation on captured field data. “It works! It works even for normal standard power transformers! It works for converter transforms too! It works with phasors but what about inrush currents? Do I need second and fifth harmonic blocking? I then looked once more into the matrix.” Surprisingly I realised that the phase angle shift compensation matrix contained only real numbers. “But, I have started from positive, negative and zero sequence phasors (i.e. complex numbers)! If only real numbers are used then I can use it for sampled phase current values from the two sides! What about sampling rate? Is this matrix transformation frequency invariant? I checked it on all available recording data. It works!”

Yes, it was so simple!

“And what about turn to turn faults? Yes, I think that I have some good insight into “the stuff”… Now maybe I just need to wait for another customer call!?”

Contents

Chapter 1

Introduction

In this chapter, a short overview of the thesis is given.

1.1 Main Purpose of Power Transformers

The main principle of a transformer was first demonstrated in 1831 by Michael Faraday, although he only used it to present the principle of electromagnetic induction and did not foresee its practical uses. During the initial years of electricity distribution in the United States, a direct current based electrical distribution system was used. However, during the "War of Currents" era (sometimes as well called "Battle of Currents") in the late 1880s, George Westinghouse and Thomas Edison became adversaries due to Edison's promotion of the direct current (DC) system over an alternating current (AC) system for electricity distribution advocated by Westinghouse and Nikola Tesla.

Power is the product of current and voltage ($P = U \cdot I$). For a given amount of power, a low voltage requires a higher current and a higher voltage requires a lower current. Since metal conducting wires have a certain resistance, some power will be wasted as heat in the wires of the distribution system. This power loss is given by $P_{Loss} = R \cdot I^2$. Thus, if the overall transmitted power is the same, and given the constraints of practical conductor sizes, a low-voltage, high-current based electricity distribution system will have a much greater power loss than a high-voltage, low-current based one. This holds true whether DC or AC electricity distribution system is used.

However, it is quite difficult to transform DC power to a high-voltage, low-current form efficiently, whereas with AC system this can be done

with a simple and efficient device called a power transformer. Power transformer can transfer practically all of its input AC power (given by product $U_1 \cdot I_1$) to its output power (given by $U_2 \cdot I_2$). However, voltage and current magnitudes will be changed in accordance with power transformer design details. Thus, the power transformer was one of the most important reasons for the success of the AC electrical power system, which was for the first time commercially used on 1896-11-16. On that day AC power was sent from the Niagara Falls to industries in Buffalo, over a distance of 35km, indicating the final triumph of the AC based distribution system.

Consequently, transformers have shaped the electricity supply industry, permitting generation (e.g. thermal and hydro power stations) to be located remotely from points of energy demand (e.g. cities). Today, all but a fraction of the world's produced electrical power has passed through a series of transformers by the time it finally reaches the consumer.

Transformers are some of the most efficient electrical machines, with some large units able to transfer 99.5% of their input power as their output power. Power transformers come in a range of sizes from a palm-sized transformer inside mobile telephone chargers to a huge giga-volt-ampere rated unit used to interconnect parts of national power grid. All of them operate on the same basic principle of electromagnetic induction, though a variety of designs exist to perform specialized roles for domestic and industrial applications [9].

Transformers, just like generators, lines and other elements of the power system, need to be protected from damages caused by a fault. This task is performed by relay protection which detects the fault situation and gives command to the relevant circuit breaker(s) to disconnect the faulty equipment from the rest of the power system. Power transformers are normally protected by differential protection relays.

1.2 Objectives

The primary objective of this work is to investigate the possibility to use a differential protection for standard three-phase power transformers for protection of special and non-standard three-phase transformers. At the end of the thesis supplementary criteria are presented which can improve the performance of the traditional power transformer differential protection for low level internal faults such as turn-to-turn faults. These

supplementary criteria can be applied on any type of the three-phase power transformer.

1.3 Contributions of the Thesis

The main contribution of the work is included in Chapter 4, where the complete theoretical background for a differential protection for an arbitrary, three-phase power transformer is presented. It is shown that a differential protection for standard power transformers can be applied, with minor modifications, as differential protection for phase shifting transformers and special converter transformers with fixed, but non-standard phase angle shift (e.g. 22.5^{o}). Any previous publications regarding such use of the differential protection could not be found. Thus, it seems that this work is unique and completely new in the field of power transformer protective relaying.

A number of secondary objectives can be enunciated as briefly shown in the following short list:

- better understanding of numerical differential protection principles to the protective relaying community;
- possibility to use standardized differential protection principle for all types of phase shifting transformers and special converter transformers;
- buried CTs are no longer required for PST protection schemes;
- improved principles for detection of transformer winding turn-to-turn faults; and
- possibility to check the output calculations from any short-circuit software package for power systems with PSTs and special transformers.

Research results from this thesis have resulted in two international patent applications with the following publication numbers:

- WO2007057240
- WO2005064759

1.4 Outline of the Thesis

In the Chapter 1 introduction to the thesis is given. The Chapter 2 presents a brief overview about different types of power transformers used in modern power systems, in accordance with the IEC standard. In Chapter 3 a brief historical overview about existing differential schemes, currently used for protection of power transformers, is presented.
In Chapter 4 a complete mathematical proof for the new universal transformer differential protection method, based on theory of symmetrical components, is derived. It is shown how to correctly calculate differential currents by simultaneously providing on-line compensation for current magnitude variations, on-line compensation for arbitrary phase angle shift variations and settable zero-sequence current reduction on any power transformer side. By using this method differential protection for arbitrary power transformers will be ideally balanced for all symmetrical and non-symmetrical through-load conditions and external faults. The method is independent of individual transformer winding connection details (i.e. star, delta, zigzag), but dependent on having the correct information about actual on-load tap-changer(s) position, if they are built-in within the protected power transformer.
Chapter 5 gives detailed instruction, how to apply the new universal differential protection method to different types of three-phase, power transformers. In Chapter 6 evaluation and testing of the new differential method with disturbance files captured in the field in existing phase shifting transformer installations is presented. Evaluation and testing of the new differential method with data files obtained from the Real Time Digital Simulator is presented in Chapter 7. Practical application and implementation possibilities of the new universal differential protection method, for analogue and numerical transformer differential protection relays, are given in Chapter 8.
Chapter 9 gives insight about transformer inrush currents and problems encounter by the transformer differential protection because of them. In Chapter 10 the relationship between differential and directional protection principles is presented. It as well shows how to use directional protection as a supplementary criterion in order to improve the performance of the traditional power transformer differential protection. Chapter 11 gives a possible solution which improves the sensitivity of the traditional differential protection for turn-to-turn faults in the power transformer windings.

Main conclusions about the performed work are given in Chapter 12, while the Chapter 13 suggests the possible future work on this subject.

1.5 Publications

This work has resulted in several publications:

Journal Papers:

Z. Gajić, "Universal Transformer Differential Protection, Part I: Theory", Submitted to IET Generation, Transmission & Distribution Journal, Manuscript ID: GTD-2007-0417.

Z. Gajić, "Universal Transformer Differential Protection, Part II: Application and Testing", Submitted to IET Generation, Transmission & Distribution Journal, Manuscript ID: GTD-2007-0419.

Z. Gajić, "Differential Protection for Special Industrial Transformers", IEEE Transactions on Power Delivery, Vol. 22, Issue 4, pp. 2126-2131, Oct. 2007. Paper no. TPWRD-00528-2006. Digital Object Identifier 10.1109/TPWRD.2007.905561.

Conference Papers:

Z. Gajić, "Differential Protection Methodology for Arbitrary Three-Phase Power Transformers," IET, The 9th International Conference on Developments in Power System Protection, Glasgow, UK, March 2008. Accepted for publishing.

Z. Gajić, S. Holst, D. Bonmann, D. Baars, "Influence of Stray Flux on Protection Systems," IET, The 9th International Conference on Developments in Power System Protection, Glasgow, UK, March 2008. Accepted for publishing.

Z. Gajić, "Differential Protection Solution for Arbitrary Phase Shifting Transformer", International Conference on Relay Protection and Substation Automation of Modern EHV Power Systems, Moscow – Cheboksary, Russia, September 2007.

Z. Gajić, I. Ivanković, B. Filipović-Grčić, R. Rubeša, "New General Method for Differential Protection of Phase Shifting Transformers", 2nd International Conference on Advanced Power System Automation and Protection, Jeju-South Korea, April 2007.

F. Mekic, R. Girgis, Z. Gajić, Ed teNyenhuis, " Power Transformer Characteristics and Their Effect on Protective Relays", 33rd Western Protective Relay Conference, October 17-19, 2006, Spokane – USA.

Z. Gajić, I. Ivanković, B. Filipović-Grčić, R. Rubeša, "New Method for Differential Protection of Phase Shifting Transformers", 15th International Conference on Power System protection, Bled-Slovenia, September 2006.

I. Brnčić, Z. Gajić, T. Einarson, "Transformer Differential Protection Improved by Implementation of Negative-Sequence Currents", 15th International Conference on Power System protection, Bled-Slovenia, September 2006.

Z. Gajić, I. Brnčić, B. Hillström, I. Ivanković, "Sensitive Turn-to-Turn Fault Protection for Power Transformers," CIGRÉ Study Committee B5 Colloquium, Calgary, Canada, Sep. 2005.

I. Ivanković, B. Filipović-Grčić, Z. Gajić, " Operational Experience with the Differential Protection of Phase Shifting Transformer", 7th Regional CIGRÉ Conference, Cavtat, Croatia, November 2005, (in Croatian language).

Z. Gajić, I. Ivanković, V. Bodiš, "Sensitivity of Transformer Differential Protection for the Internal Faults", 7th Regional CIGRÉ Conference, Cavtat, Croatia, November 2005, (in Croatian language).

Z. Gajić, I. Ivanković, B. Filipović-Grčić, "Differential Protection Issues for Combined Autotransformer – Phase Shifting Transformer," IEE Conference on Developments in Power System Protection, Amsterdam, Netherlands, April 2004.

Chapter 2

Three-Phase Power Transformers

"Power transformer is a static piece of apparatus with two or more windings which, by electromagnetic induction, transforms a system of alternating voltage and current into another system of voltage and current usually of different values and at the same frequency for the purpose of transmitting electrical power." (Definition of Power Transformer; taken from IEC 600761 standard).

Many different types of power transformers are presently used in electrical power systems worldwide. Short summary of most commonly used types, as defined by IEC standards, will be given in this Chapter.

2.1 General-purpose Power Transformers

Most commonly used types of general-purpose power transformers will be described in this section.

Two-winding Transformers

The two-winding power transformer has two separate electrical windings. It is used to interconnect two electrical networks with typically different voltage levels. Two-winding power transformers with rating bigger than 5MVA are typically star (wye) connected or delta connected, and less frequently, zigzag connected. Such power transformers introduce a fixed phase angle displacement (i.e. phase angle shift) Θ between the two windings. The phase angle displacement Θ can have a value of $n \cdot 30^o$, where n is an integer between 0 and 11, and depends on the winding connection details for the specific power transformer. Typically the high

voltage winding is used as reference for the phase angle displacement. Commonly used connections for two-winding, three-phase power transformers are shown in Figure 1 (from [58]). More information can be found in references [9], [58] and [62].

Multi-winding Transformers

The multi-winding power transformer has more than two separate electrical windings. In practice by far the most used type is a three-winding power transformer. Such power transformer is used to interconnect three electrical networks with typically different voltage levels. The three windings are typically star (wye) connected or delta connected. Such power transformers introduce a fixed phase angle shift between each pair of its windings. The phase angle displacement can have a value of $n \cdot 30^o$, where n is an integer between 0 and 11, and depends on the individual winding connection details for the specific winding pair. Typically the high voltage winding is used as reference for phase angle displacement. Two examples of three-winding, three-phase power transformer connections are YNyn0d1 and Yd11d11.

Auto-transformers

An auto-transformer is a power transformer in which at least two windings have a common part. Auto-transformers are most often used to interconnect EHV and/or HV networks. It can be shown that they are less expensive than normal two-winding transformers if the voltage difference between the two windings (e.g. networks) is relatively small [29]. For power system applications auto-transformers are typically used with a third, delta connected winding. Vector group connection for a three-winding auto-transformer can for example be designated as YNautod5.

Regulating Transformers

Such transformers are typically used to vary the voltage magnitude on one or more sides of the power transformer. This is achieved by constructing one (or more) winding with taps. A separate device called Tap-Changer (TC) is then used to select one of the winding taps and to connect it with the other electrical parts of the power transformer. Two types of tap-changers are commonly used:

- on-load tap-changer (OLTC) which can change a winding tap while the power transformer is in service; and

- off-circuit tap-changer which can change a winding tap only when the power transformer is de-energized.

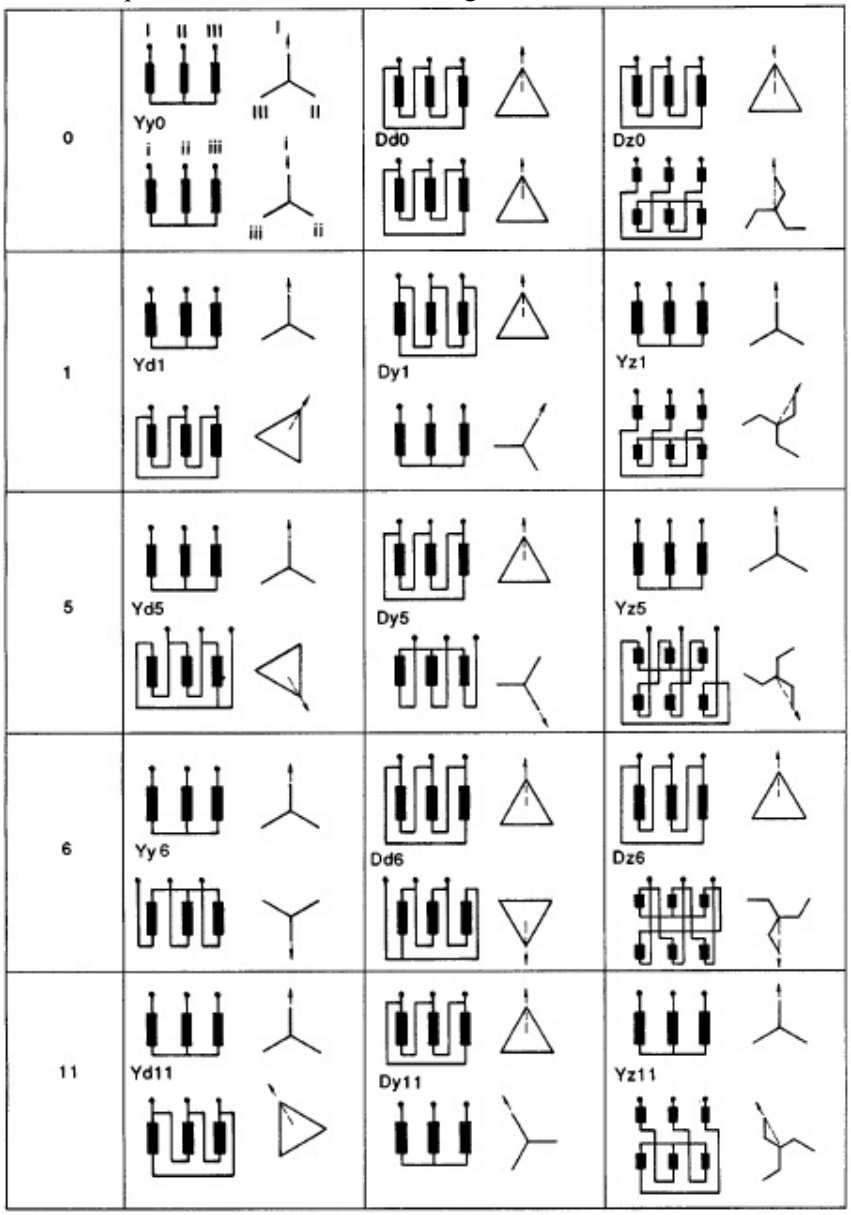

Figure 1: Commonly used connections for two-winding power transformers [58].

More information about tap-changers can be found in IEC 60214 standard. Note that any previously described type of general-purpose power transformer can be constructed as a regulating transformer. In such case it is the most common to use OLTC to select appropriate winding tap. With such a design it is possible to step-wise regulate the voltage magnitude, typically on the LV side of the power transformer. The standard OLTC typically offers in between ±9 and ±17 positions. Each OLTC step can change the no-load transformer LV side voltage for certain value (typically 1-2%).

2.2 Converter Transformers

Converter transformers are power transformers intended for operation with power electronic converters. A short summary of the most commonly used types, as defined by IEC 61378 standard, are given in this section.

Transformers for Industrial Applications

This type of transformer is intended for operation with power converters not exceeding 36kV. They can be of standard construction regarding the winding connection (e.g. either star or delta) and phase angle displacement (multiple of 30^o), but there are also such transformers with a quite special construction. Such special industrial power transformers can have a phase angle shift Θ different from 30º or a multiple of 30º [22]. The overall phase angle shift Θ differs from the standard $n \cdot 30^o$ shift for additional angle Ψ ($0^o < \Psi < 15^o$). A typical example is a 24-pulse converter transformer with an additional phase angle shift Ψ of $\pm 7.5^o$. Such special transformers typically have three windings, but sometimes even up to five windings [9], [15]. They are used to supply different electrical equipment fed by power converter such as MV drives [13], [15] and FACTS devices [59]. Such power electronic equipment injects significant harmonics into the utility power system. The application of converter transformers with special phase angle shift can substantially reduce the current harmonic content in the utility supply system [6], [36] and [49].

Due to power quality issues, the use of special industrial transformers has been increased over the last years. Special industrial transformers with rated power of up to 100MVA have been installed [14]. The additional phase angle shift Ψ is typically obtained by special connections of the HV winding [54]. This HV winding is typically connected either as extended-

delta (as shown in Figure 2) or as zigzag (as shown in Figure 3). Obviously the special "HV winding extensions" are used in both designs in order to provide the required additional phase angle shift Ψ. Other converter transformer windings (i.e. LV windings) are connected in the standard way (e.g. star or delta). Note that the design in Figure 2 is a variation of a Dy11d0 standard power transformer, and the design in Figure 3 is a variation of an Yy0d1 standard power transformer.

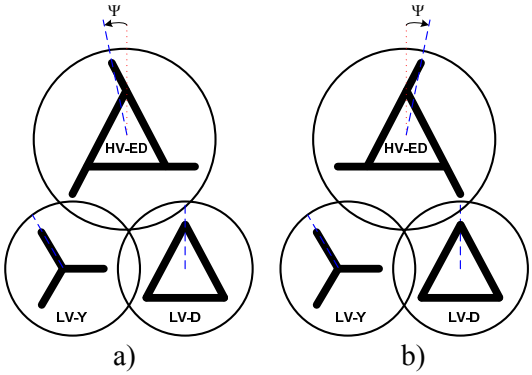

Figure 2: Transformer winding connections for extended delta design.

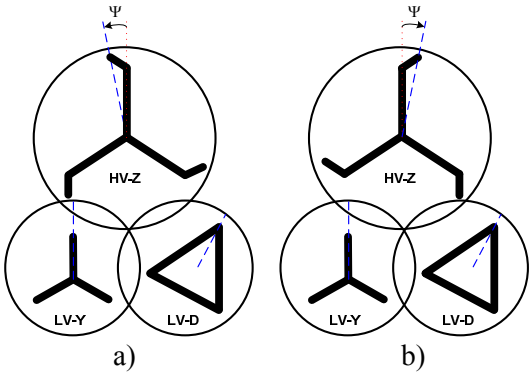

Figure 3: Transformer winding connections for zigzag design.

The phasor diagram for positive sequence quantities for the converter transformer shown in Figure 2a is given in Figure 4. Figure 4a shows the phasor diagram which directly corresponds to the winding arrangements shown in Figure 2a. However, the power transformer phasor diagram is

typically shown with the HV winding positive sequence quantity at position zero, as shown in Figure 4b. In a similar way the phasor diagrams for converter transformers shown in Figure 2b, 3a and 3b can be constructed.

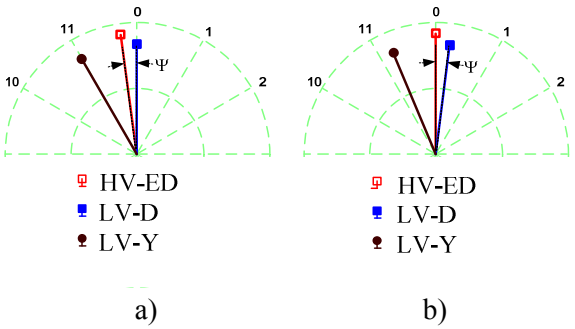

a) b)

Figure 4: Positive sequence phasor diagram for the special converter transformer shown in Figure 2a.

In the rest of this thesis, power transformers with fixed but non-standard phase angle displacement will be referred to as "special converter transformers".

Transformers for HVDC Applications

This type of transformer is intended for use in station for High Voltage Direct Current (HVDC) power transmission. Presently, such transformers are using standard construction regarding the winding connection (either star or delta) and phase angle displacement (multiple of 30^{o}). Thus, differential protection can be applied by using the same rules as for standard multi-winding transformers.

Transformers for Traction Applications

This type of transformer is intended for use in railway substations and railway locomotives. They are often of a special design, and they are used to supply one-phase or two-phase railway supply systems. More information about traction transformers can be found in IEC 60310 standard. Differential protection for such transformers will not be considered in this thesis.

2.3 Phase-Shifting Transformers

A phase-shifting transformer (PST) is a regulating transformer with one or more OLTCs which primary task is to regulate the phase angle displacement across the transformer. Actually, a PST creates a step-wise variable phase angle shift Θ across its primary (**S**ource) and secondary (**L**oad) terminals [35]. For a PST one or more OLTCs are used [48] and [60] to obtain the variable phase angle shift. In practice multiple OLTCs with as many as 70 combined steps can be used to obtain the PST variable phase angle shift Θ of up to ±75°. The standard OLTC typically offers in between ±9 and ±17 positions (i.e. altogether from 19 to 35 positions). If more positions are required it is necessary to add a second OLTC in series. Such constructions make the practical design of a PST quite complicated.
The main purpose of the phase-shifting transformer is the real-time control of the active power flow in a complex power network. The phase angle shift change governs the flow of active power. Thus, PSTs are typically used to:

- control power exchange between two networks without influencing power flow to third parties [23];
- control load sharing between parallel transmission paths [59];
- increase total power transfer through specific interconnection lines
- force active power flow on contract path(s) ;
- block parasitic power flow due to phase angle differences in feeding network(s) ;
- force power flow from LV to HV side of a power transformer;
- distribute power to different customers in a pre-defined way;
- avoid circulating power flows in interconnected power systems; and,
- special applications [38].

Phase-Shifting Transformer Design

Phase-shifting transformers have some characteristics in common with auto-transformers [64]. One of which is that in most practical designs the primary and secondary terminals are galvanically connected. In addition the size and therefore also the cost of a PST and auto-transformer is not only dependent on power rating and voltage. In the case of an auto-transformer, the voltage ratio has a major impact, while for a PST the

maximum possible phase angle shift determines the size of the transformer.

Note that the maximum transformer rating and phase angle shift, is often constrained by the availability of an appropriate OLTC [4]. The most commonly used PST designs in modern power systems are:

- single-core design (symmetrical/asymmetrical);
- two-core design (symmetrical/asymmetrical); and
- special constructions (typically asymmetrical).

A more detailed description of the terms "symmetrical" and "asymmetrical" might be useful [35]. The term "symmetrical" means that under no-load condition the absolute values of the source and load voltage are the same irrespective of the actual phase angle shift Θ. The term "asymmetrical" means that under no load conditions the voltage magnitude on the load side is different than the voltage magnitude on the source side. Typically this difference is bigger as the phase angle shift Θ increases.

Single-Core PST Design

A simple example for an asymmetric, single-core phase-shifting transformer is given in Figure 5 (from [64]), which in principle is probably the simplest type of PST. The advantage of this solution is that it does not need a separate excitation transformer. On the other hand, the on-load tap-changer and the regulating windings are connected in series with the power system. Thus they are directly exposed to system disturbances and fault currents, which might involve costly OLTC design.
Based on the same principle and with a marginal increase in complexity, a symmetric design is also possible with the addition of a regulating winding and an additional OLTC. This design provides for a significant increase in the maximum possible phase angle shift. The basic design scheme is shown in Figure 6.

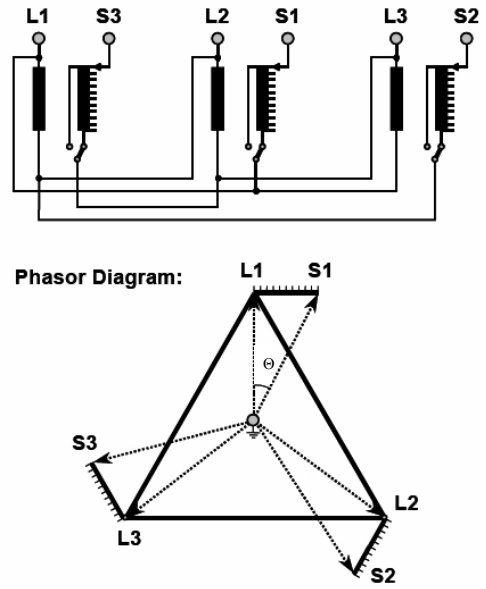

Figure 5: Asymmetric type, single-core PST design [64].

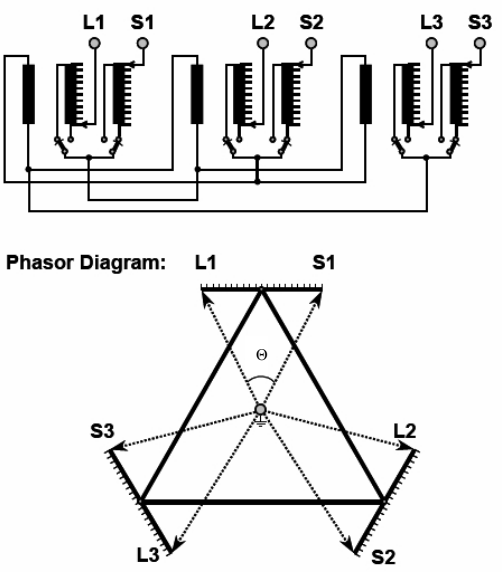

Figure 6: Symmetric type, single-core PST design [64].

Additional impedance, typically a series reactor connected to the PST load side terminals, might be necessary. It is used to protect the OLTCs from short circuit currents, because no PST impedance is present at phase angle shift of zero degree.

Two-Core PST Design

The most commonly implemented and "classic" solution is the symmetric, dual-core PST with separate series transformer and excitation transformer. The principle scheme for the dual-core PST is shown in Figure 7 (from [64]). The series transformer primary winding is serially connected with the primary system in between source and load terminals. This winding is split into two halves, and the primary winding of the exciting transformer is connected to the mid point between these two half-windings. Thus, total symmetry between source and load side no-load voltages is achieved. The regulating circuit consists of a secondary tapped winding in the excitation transformer and a delta connected secondary winding in the series transformer. Ratings of these two windings can be optimized independently from the main circuit with regard to the voltage level. This provides more freedom for the selection of the OLTC, which can sometimes determine the limit for a specific design [4].

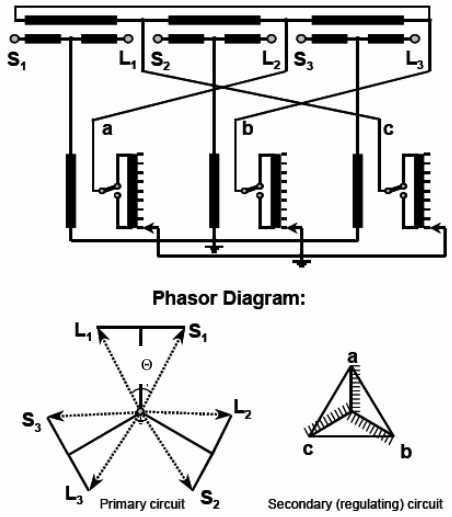

Figure 7: Symmetric type, dual-core PST design [64].

Depending on the rated power, voltage and maximum no-load phase angle shift of the PST, series and excitation transformers can be designed as:

- two three-phase, five-limb transformers located in the same tank;
- two three-phase, five-limb transformers located in two separate tanks interconnected with oil ducts or HV cables; or,
- six single-phase transformers located in six separate tanks interconnected with oil ducts or HV cables.

If one of the two half-windings in the series transformer is omitted, an asymmetric design can be achieved. Such PSTs are used in practice (see Section 5.6), but with asymmetric design the maximum phase shift angle is limited to approximately 20^{o} because otherwise a too big voltage magnitude difference between the two PST sides will be obtained.

Special PST Design

Special PST constructions are typically based on an auto-transformer design. As an example the PST installed in the Croatian power system will be presented [67]. This power transformer is constructed as a conventional auto-transformer with a tertiary delta-connected, equalizer winding [58]. The OLTC winding is located at the auto-transformer neutral point. The auto-transformer rating data is 400/400/(130)MVA; 400/231/(10.5)kV; YNa0(d5). The main difference from the typical auto-transformer construction is a two position switch located in-between the OLTC winding and the common auto-transformer winding as shown in Figure 8. The position of this switch can be changed only when the power transformer is de-energized.

When this switch position is as shown in Figure 8, the power transformer is in auto-transformer operating mode. In this operation mode the common winding, serial winding and OLTC winding, mounted on the same magnetic core limb, are connected in series. Phase A windings connections for auto-transformer operating mode and the corresponding power transformer no-load voltage phasor diagram are shown in Figure 9.

When the switch position is changed, the OLTC winding in phase C (mounted around the third magnetic core limb) is connected in series with the common and serial auto-transformer windings in phase A (mounted around the first magnetic core limb). This switch arrangement converts the auto-transformer to a phase-shifting transformer. The phase A winding connections for PST operating mode and the corresponding power

transformer no-load voltage phasor diagram are shown in Figure 10. For more information about different PST constructions please refer to [35], [41], [56], [60] and [64].

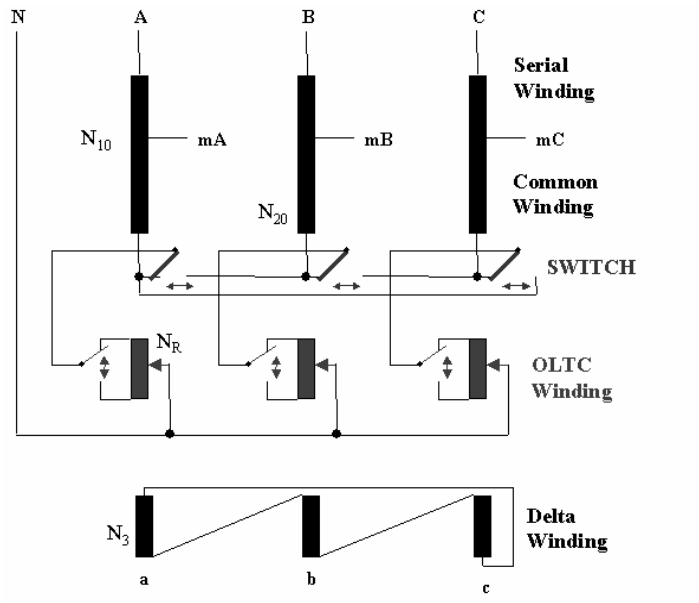

Figure 8: Construction details for the PST installed in Croatia [67].

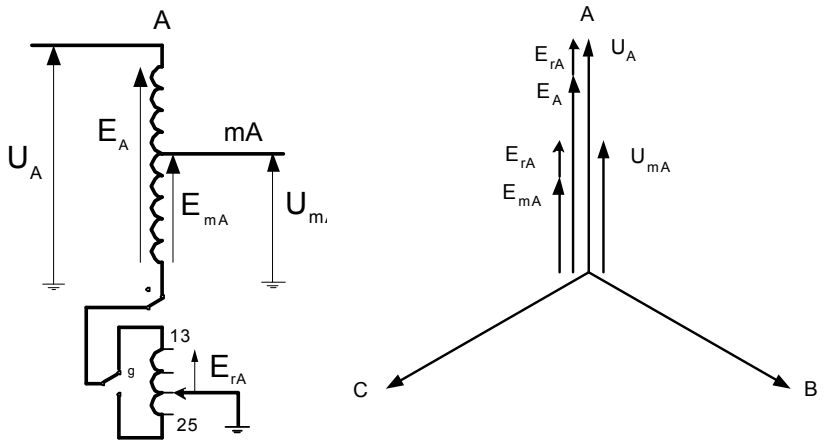

Figure 9: Auto-transformer operating mode [67].

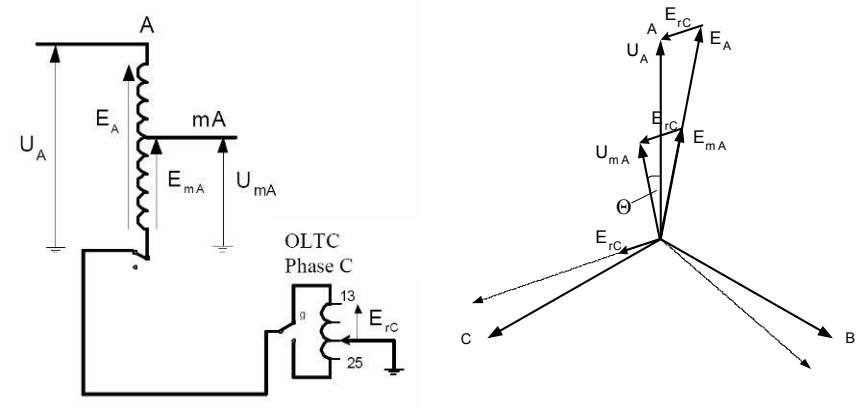

Figure 10: PST operating mode [67].

In Sweden there is only one PST installed in 1988 at Charlottenberg substation. It is of a special design and is used to interconnect 132kV networks in Sweden and Norway. More information about it can be found in [19].

2.4 Power Transformer as Nonlinear Device

All power transformers inherently have a magnetic core. Due to magnetic properties of the core (e.g. hysteresis, saturation), the whole power transformer becomes a non-linear device. This non-linearity from the differential protection point of view manifests itself as a magnetizing current which is present whenever the power transformer is connected to the electrical power system. The magnetizing current is used to produce necessary magnetic flux in the transformer core. The magnetizing currents can be divided into two categories:

- Steady-state magnetizing currents; and
- Transient magnetizing current.

Steady State Magnetizing Currents

The steady state magnetic flux in the core is proportional to the ratio of the voltage and frequency applied to the power transformer winding, as shown by the following equation:

$$\Phi = C \cdot \frac{U}{f} \tag{2.1}$$

where:

- Φ is the magnetic flux in the core;
- C is a constant dependent on the particular power transformer construction details;
- U is the voltage; and
- f is the frequency of the voltage signal.

Typically, a power transformer magnetic core is designed in such way that it will tolerate 110% of rated U/f ratio being applied to the power transformer without saturation [58]. Under such steady state operating condition (e.g. U/f < 110%) the magnetizing current drawn by the power transformer will be quite small. A typical RMS value of the magnetizing current is from 0.2% to 0.5% for power transformers with a rating above 30MVA [1]. However, if the 110% over-excitation limit is exceeded the magnetic core will start to saturate. This will result in a sharp magnitude increase of the magnetizing current.

Transient Magnetizing Currents

Transient magnetizing currents will appear every time the magnitude or phase angle of the voltage, applied to the power transformer, is suddenly changed. Transient magnetizing currents can have quite a big magnitude (e.g. 300%) and can cause unwanted operation of the protection relays. Additional information about transient magnetizing currents is given in Chapter 9.

Chapter 3

Differential Protection for Power Transformers

Current based differential protection has been applied in power systems since the end of the 19th century [32], and was one of the first protection systems ever used. Faults are detected by comparing the currents flowing into and out of the protected object as shown in Figure 11.

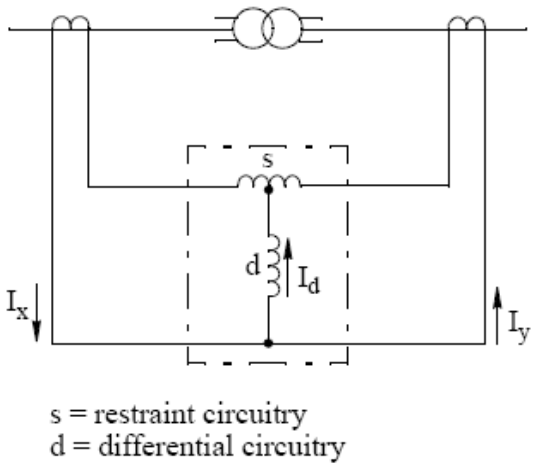

Figure 11: Principal connections for transformer differential protection [10].

Within the differential relay two quantities are derived:

- the stabilizing current (often as well called bias or restraining current) which flows through the restraining circuitry "s" shown in Figure 11; and
- the differential current (i.e. the current Id shown in Figure 11).

The magnitudes of these two quantities are typically used in order to determine whether the differential relay will operate (trip) or restrain from operation. A typical numerical differential relay tripping characteristic is shown in Figure 12.

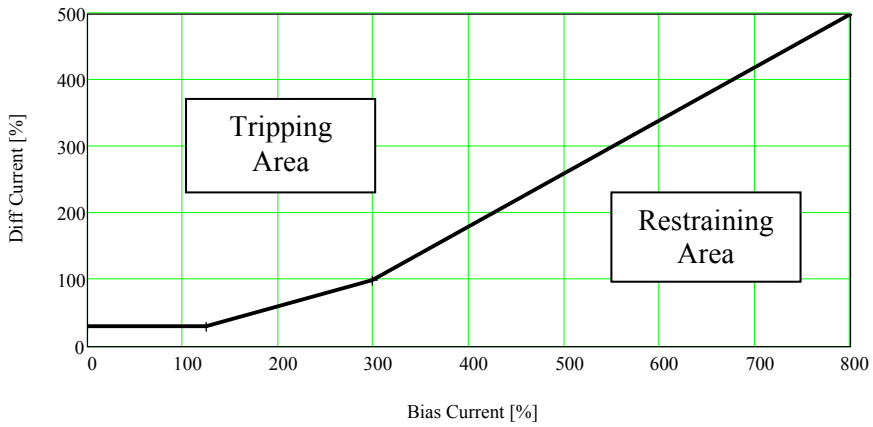

Figure 12: Differential relay tripping characteristic [12].

Typically, differential protection provides for fast tripping with absolute selectivity for internal, high-level shunt faults when the relay operating point defined by the current pair [Ibias, Idiff] is above the tripping characteristic (see Figure 12). Differential relays are often used as main protection for all important elements of the power system such as generators, transformers, buses, cables and short overhead lines. The protected zone is clearly defined by the positioning of the main current transformers to which the differential relay is connected.
Transformer differential protection is as well quite specific because it has to cope with non-linearity of the power transformer explained in Section 2.4. This is traditionally achieved by 2^{nd} and 5^{th} harmonic blocking/restraining features which are typically found in all power transformer differential relays [5] and [32].

3.1 Differential Protection for Standard Transformers

Current based differential protection for standard power transformers has been used for decades. It is based on ampere-turn-balance of all windings mounted on the same magnetic core limb. In order to correctly apply transformer differential protection it is necessary to properly compensate for:

- primary current magnitude difference on different sides of the protected transformer (i.e. current magnitude compensation);
- power transformer phase angle shift (i.e. phase angle shift compensation); and provide
- zero sequence current elimination (i.e. zero sequence current compensation).

Static Differential Relays

With static (or even electromechanical) differential relays such compensations were performed by using interposing CTs or special connection of main CTs (i.e. delta connected CTs) [10]. Well-known characteristics for electromechanical or static power transformer differential relays are as follows:

- correct selection of interposing CT ratios, makes it possible to compensate for current magnitude differences on different sides of the protected transformer;
- correct selection of interposing CT winding connections makes it possible to compensate for power transformer phase angle shift; and
- the use of interposing CT connections, makes it possible to remove zero sequence current from any power transformer side.

Maximum power transformer rated apparent power was used to calculate the interposing CT ratios [10]. However, the interposing CTs could only be calculated for the mid-position of the on-load tap-changer. Thus, as soon as the OLTC is moved from the mid-position, false differential currents would appear. Note as well that all interposing CTs required for one particular application are calculated by taking the maximum rated power of all windings within the protected power transformer as a base for

the calculations. A typical differential protection scheme with interposing CTs is given in Figure 13.

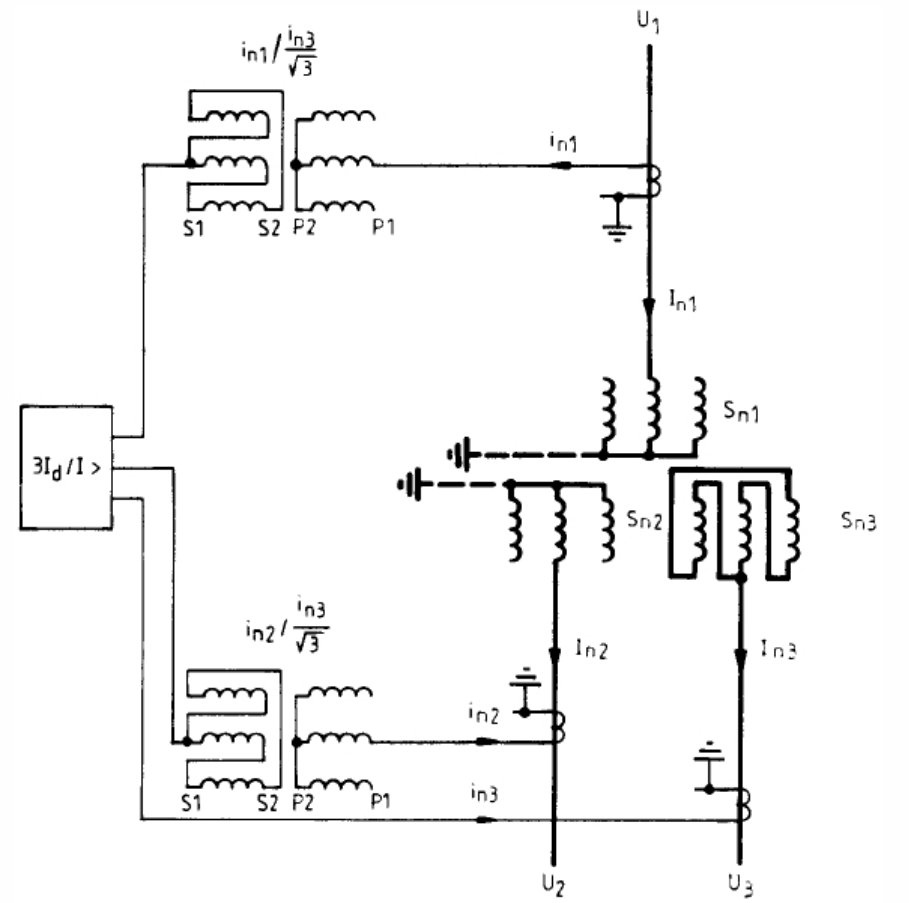

Figure 13: Power transformer differential protection scheme with interposing CTs [10].

Numerical Differential Relays

The first papers about microprocessor based transformer protection were published at the beginning of the eighties [7], [45]. With modern numerical transformer differential relays [11], [12], [17] and [32] external

interposing CTs are not required because relay software enables the user to:

- compensate for current magnitude differences on the different sides of the protected power transformer;
- compensate for standard power transformer phase angle shift (i.e. multiple of 30˚); and
- use all star connected primary CTs and still remove zero sequence currents from any transformer side by parameter setting.

In addition to this, it is possible to on-line monitor the OLTC position and automatically compensate for it in the calculation of differential currents [11], [12] and [34]. Thus, the numerical differential relay can be ideally balanced regardless of the actual OLTC position. A typical differential protection scheme with a numerical differential relay is shown in Figure 14.

In some recent publications it was suggested to include the voltage measurement from only one or even from all sides of the protected power transformer into the differential protection [65], [66]. However, in this thesis only the current based differential protection will be considered.

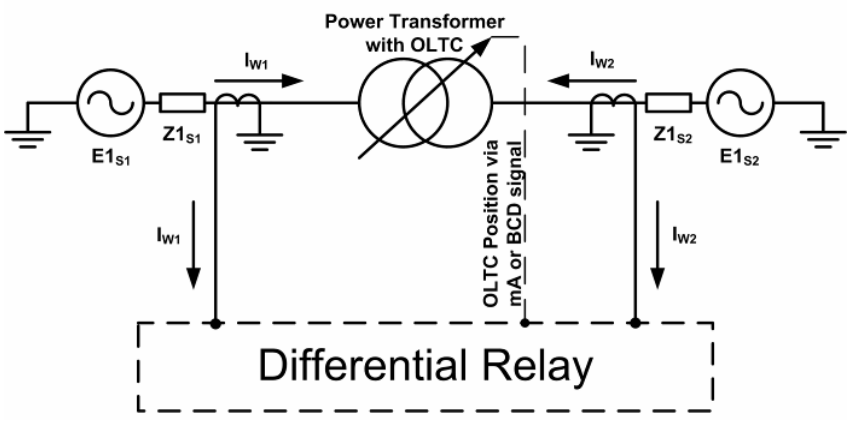

Figure 14: Typical connections for modern numerical differential relay.

3.2 Differential Protection for Special Converter Transformers

Standard three-phase power transformers can be protected without any external interposing CTs with numerical differential protection as described in Section 3.1.
However, if the numerical differential relay is directly applied for differential protection of a special converter transformer, and set to compensate for the nearest standard transformer vector group, it will not be able to compensate for additional, non-standard phase angle shift Ψ caused by special winding connections. As a result a permanent false differential current would appear. The false differential current magnitude can be estimated by using the following formula:

$$I_{d\_false} = 2 \cdot \sin(\frac{\Psi}{2}) \cdot I_{Load} \approx \sin(\Psi) \cdot I_{Load} \qquad (3.1)$$

where:

- I_{d_false} is the false differential current magnitude;
- I_{Load} is the through-going load current magnitude; and
- Ψ is a non-standard phase angle shift.

For the worst case when $\Psi = 15^{o}$ a false differential currents of up to 26% of the through-load current will appear. As a consequence the minimum pickup of the differential protection must be increased to at least twice this value and consequently the differential relay will not be sensitive for the low level internal faults within the protected power transformer.

3.3 Differential Protection for PST

If a numerical power transformer differential relay is directly applied for the differential protection of a PST, and set for Yy0 vector group compensation, the differential relay will not be able to compensate for the variable phase angle shift Θ caused by OLTC operation. As a result a false differential current will exist which will vary in accordance with the coincident PST phase angle shift, as already shown in equation (3.1). As a consequence the minimum pickup of the differential protection must be increased and consequently the differential relay will not be sensitive for the low level internal faults.

Thus, diverse differential protection schemes for phase-shifting transformers are presently used [2], [37] and [67]. These schemes tend to be dependent on the particular construction details and maximum phase angle shift of the protected PST. A special report has been written by IEEE-PSRC which describes possible protection solutions for PST applications [37].
In references [51] and [52] a PST differential protection scheme, based only on individual positive and negative sequence current components, is proposed. However such a solution has the following drawbacks:

- It can be applied to PSTs with two ends only.
- It must be blocked during PST energizing.
- It must be blocked when an external fault is cleared (i.e. current reversal blocking logic shall be used).
- It can't provide the faulty phase indication.

Presently, there is no commercially available differential relay that can provide complete phase-wise differential protection, in accordance with Figure 14, for any PST regardless of its construction details.

3.4 Main CT Connections

In some countries (e.g. USA) delta connected main CTs are even used with numerical differential protection relays. This is not in accordance with IEC standards due to personal safety related issues, as the delta connected CTs can not be earthed in the main CT junction box but only in the relay protection cubicle. The three most typical main CT connections used for transformer differential protection around the world are shown in Figure 15. It is assumed that the primary phase sequence is L1-L2-L3 (i.e. ANSI ABC).
For star/wye connected main CTs, secondary currents fed to the differential relay:

- are directly proportional to the measured primary currents;
- are in phase with the measured primary currents; and
- contain all sequence components including the zero sequence current component.

For delta DAC connected main CTs (DAC means that the difference between A and C phase currents is generated as the first phase current by

the main CT delta connection), secondary currents fed to the differential relay:

- are increased $\sqrt{3}$ times in comparison with star/wye connected CTs;
- lag the primary winding currents by 30^o (i.e. this CT connection rotates currents by 30^o in clockwise direction); and
- do not contain any zero sequence current component.

For delta DAB connected main CTs (DAB means that the difference between A and B phase currents is generated as the first phase current by the main CT delta connection), secondary currents fed to the differential relay:

- are increased $\sqrt{3}$ times in comparison with star/wye connected CTs;
- lead the primary winding currents by 30^o (i.e. this CT connection rotates currents by 30^o in anticlockwise direction)
- do not contain any zero sequence current component.

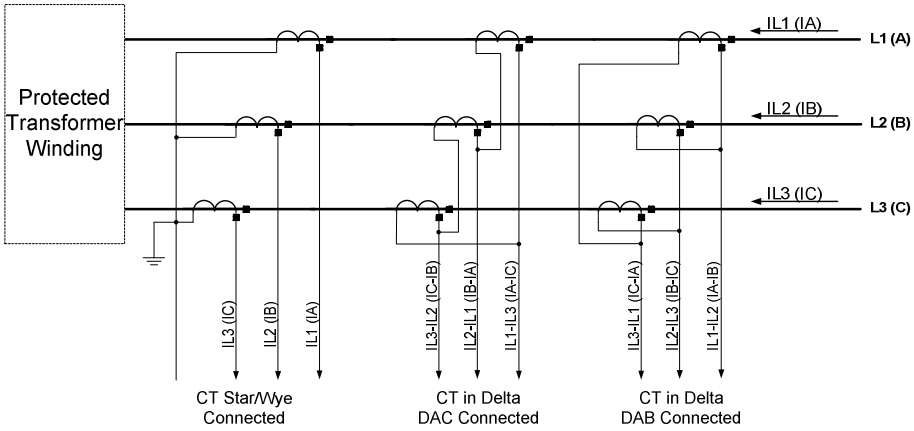

Figure 15: Used CT connections for transformer differential protection.

Note that the influence of delta connected main CTs can be taken into account in the method shown in Chapter 4, but this is not done in this thesis. In this thesis it will always be assumed that all main CTs connected to the differential protection are star/wye connected.

Chapter 4

New Universal Method

To provide universal differential protection for all variants of three-phase power transformers it is necessary to provide three types of compensation (see Section 3.1), which are described in the following sections.

4.1 Current Magnitude Compensation

In order to achieve current magnitude compensation, the individual phase currents must be normalized on all power transformer sides by dividing them by the so-called base current. The base current in primary amperes can be calculated for each power transformer winding via the following equation.

$$I_{Base\_Wi} = \frac{S_{rMax}}{\sqrt{3} \cdot U_{rWi}} \tag{4.1}$$

where:

- I_{Base_Wi} is winding i base current in primary amperes.
- S_{rMax} is the maximum rated apparent power among all power transformer windings. The maximum value, as stated on the protected power transformer rating plate, is typically used.
- U_{rWi} is winding i rated phase-to-phase no-load voltage; Values for all windings are typically stated on the transformer rating plate.

For the winding with power rating equal to S_{rMax} the base current is equal to the winding rated current which is usually stated on the power transformer rating plate.
Note that when a power transformer incorporates an OLTC, U_{rWi} typically has different values for different OLTC positions on at least one side of the power transformer. Therefore the base current will have different values on that side of the protected power transformer for different OLTC

positions as well. Typically, for the winding where the OLTC is located, different I_{Base} values shall be used for every OLTC position, in order to correctly compensate for the winding current magnitude variations caused by OLTC operation. Once this normalization of the measured phase currents is performed, the phase currents from the two sides of the protected power transformer are converted to the same per unit scale and can be used to calculate the transformer differential currents.
Note that the base current in (4.1) is in primary amperes. Differential relays may use currents in secondary amperes to perform their algorithm. In such case the base current in primary amperes obtained from equation (4.1), shall be converted to the CT secondary side by dividing it by the ratio of the main current transformer located on that power transformer side. For an example see Section 5.1.

4.2 Phase Angle Shift across Power Transformer

In order to comprehend the phase angle shift compensation it is important to understand the property of power transformers described in this section. Typical voltage and current definitions used for three-phase power transformers are shown in Figure 16, where:

- IL1_W1 is winding 1 (side 1) current in phase L1;
- UL1_W1 is winding 1 (side 1) phase-to-earth voltage in phase L1;
- IL1_W2 is winding 2 (side 2) current in phase L1; and
- UL1_W2 is winding 2 (side 2) phase-to-earth voltage in phase L1.

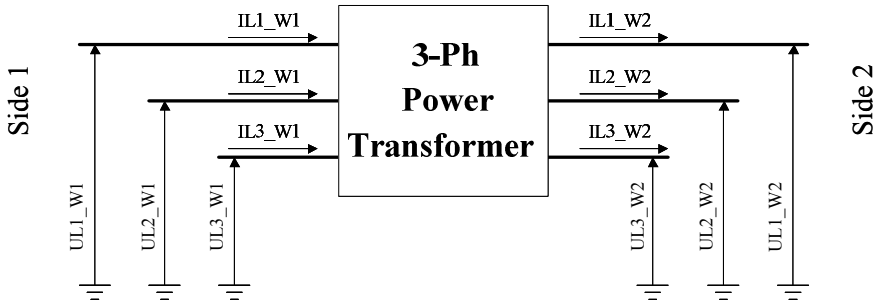

Figure 16: Typical voltage and current reference directions for a transformer.

The common characteristic for all types of three-phase power transformers is that they introduce a phase angle shift Θ between winding 1 and winding 2 side no-load voltages, as shown in Figure 17. Note that the magnitude difference typically induced by the power transformer is not shown in Figure 17. It can be assumed that voltage phasors are shown in the per-unit (pu) system.

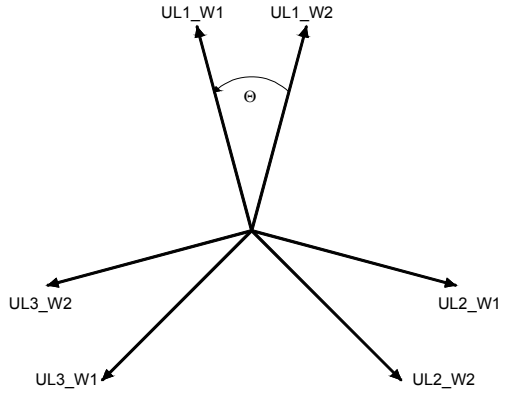

Figure 17: Phasor diagram for individual no-load, phase voltages.

The only difference among the variants of three-phase power transformers is that:

- general-purpose three-phase power transformers introduce a fixed phase angle shift Θ of $n \cdot 30^o$ (n=0, 1, 2, …, 11) between its terminal no-load voltages;
- special converter transformers introduce a fixed phase angle shift Θ different from 30º or a multiple of 30º between its terminal no-load voltages (e.g. 22.5º); and
- phase-shifting transformers introduce a variable phase angle shift Θ between its terminal no-load voltages (e.g. 0º - 18º in fifteen steps of 1.2º).

It can be shown [25] that strict rules do exist for the phase angle shift between the sequence components of the no-load voltage from the two sides of the power transformer, as shown in Figure 18, but not for individual phase voltages from the two sides of the power transformer.

Note that the following symbols (abbreviations) will be used for the sequence quantities:

- PS – positive sequence quantity;
- NS – negative sequence quantity; and
- ZS – zero sequence quantity.

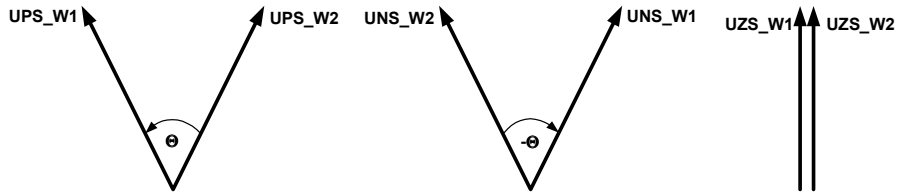

Figure 18: Phasor diagram for no-load positive, negative and zero sequence voltage components from the two sides of the power transformer.

As shown in Figure 18 the following will hold true for the positive, negative and zero sequence no-load voltage components:

- the positive sequence no-load voltage component from winding 1 (UPS_W1) will lead the positive sequence no-load voltage component from winding 2 (UPS_W2) by angle Θ;
- the negative sequence no-load voltage component from winding 1 (UNS_W1) will lag the negative sequence no-load voltage component from winding 2 (UNS_W2) by angle Θ; and
- the zero sequence no-load voltage component from winding 1 (UZS_W1) will be exactly in phase with the zero sequence no-load voltage component from winding 2 (UZS_W2), when the zero sequence no-load voltage components are at all transferred across the power transformer.

However, as soon as the power transformer is loaded, this *voltage* relationship will no longer be valid, due to the voltage drop across the power transformer impedance. However it can be shown that the same phase angle relationship, as shown in Figure 18, will be valid for the sequence *current* components, as shown in Figure 19, which flow into the power transformer winding 1 and flow out from the winding two [25].

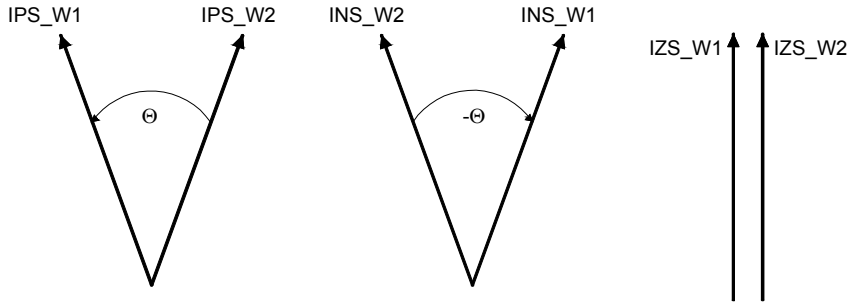

Figure 19: Phasor diagram for positive, negative and zero sequence current components from the two sides of the power transformers.

As shown in Figure 19, the following will hold true for the sequence current components from the two power transformer sides:

- the positive sequence current component from winding 1 (IPS_W1) will lead the positive sequence current component from winding 2 (IPS_W2) by angle Θ (the same relationship as for the positive sequence no-load voltage components);
- the negative sequence current component from winding 1 (INS_W1) will lag the negative sequence current component from winding 2 (INS_W2) by angle Θ (the same relationship as for the negative sequence no-load voltage components); and
- the zero sequence current component from winding 1 (IZS_W1) will be exactly in phase with the zero sequence current component from winding 2 (IZS_W2), when the zero sequence current components are at all transferred across the transformer (the same relationship as for the zero sequence no-load voltage components).

Therefore the following equations can be written for positive, negative and zero sequence current components from the two sides of the power transformer:

$$IPS\_W1 = e^{j\Theta} \cdot IPS\_W2 \tag{4.2}$$

$$INS\_W1 = e^{-j\Theta} \cdot INS\_W2 \tag{4.3}$$

$$IZS\_W1 = IZS\_W2 \tag{4.4}$$

4.3 Phase Angle Shift Compensation

In this section it will be assumed that current magnitude compensation of individual phase currents from the two power transformer sides has been performed. Hence, only the procedure for phase angle shift compensation will be presented.

For a differential protection scheme, currents from all sides of the protected object are typically measured with the same reference direction (e.g. towards the protected object), as shown in Figure 14. From this point, all equations will be written for the current reference direction as shown in Figure 14.

According to the equations (4.2), (4.3) and (4.4) the sequence differential currents can be calculated with the following equations (note new current reference directions!):

$$Id\_PS = IPS\_W1 + e^{j\Theta} \cdot IPS\_W2 \tag{4.5}$$ Positive sequence differential current

$$Id\_NS = INS\_W1 + e^{-j\Theta} \cdot INS\_W2 \tag{4.6}$$ Negative sequence differential current

$$Id\_ZS = IZS\_W1 + IZS\_W2 \tag{4.7}$$ Zero sequence differential current

By using the basic relationship between sequence and phase quantities the following matrix relationship can be written for phase-wise differential currents:

$$\begin{bmatrix} Id\_L1 \\ Id\_L2 \\ Id\_L3 \end{bmatrix} = A \cdot \begin{bmatrix} Id\_ZS \\ Id\_PS \\ Id\_NS \end{bmatrix} \tag{4.8}$$

where from [21] and [43]:

$$A = \begin{bmatrix} 1 & 1 & 1 \\ 1 & a^2 & a \\ 1 & a & a^2 \end{bmatrix} \tag{4.9}$$

$$A^{-1} = \frac{1}{3} \cdot \begin{bmatrix} 1 & 1 & 1 \\ 1 & a & a^2 \\ 1 & a^2 & a \end{bmatrix} \tag{4.10}$$

$$a = e^{j120°} = cos(120°) + j \cdot sin(120°) = -\frac{1}{2} + j \cdot \frac{\sqrt{3}}{2} \tag{4.11}$$

$$a^2 = e^{-j120°} = cos(-120°) + j \cdot sin(-120°) = -\frac{1}{2} - j \cdot \frac{\sqrt{3}}{2} \tag{4.12}$$

By combining equations (4.5), (4.6) and (4.7) into equation (4.8) and doing some basic rearrangements the following equations can be derived:

$$\begin{bmatrix} Id\_L1 \\ Id\_L2 \\ Id\_L3 \end{bmatrix} = A \cdot \begin{bmatrix} IZS\_W1 \\ IPS\_W1 \\ INS\_W1 \end{bmatrix} + A \cdot \begin{bmatrix} IZS\_W2 \\ e^{j\Theta} \cdot IPS\_W2 \\ e^{-j\Theta} \cdot INS\_W2 \end{bmatrix} \tag{4.13}$$

$$\begin{bmatrix} Id\_L1 \\ Id\_L2 \\ Id\_L3 \end{bmatrix} = A \cdot \begin{bmatrix} IZS\_W1 \\ IPS\_W1 \\ INS\_W1 \end{bmatrix} + A \cdot \begin{bmatrix} 1 & 0 & 0 \\ 0 & e^{j\Theta} & 0 \\ 0 & 0 & e^{-j\Theta} \end{bmatrix} \cdot \begin{bmatrix} IZS\_W2 \\ IPS\_W2 \\ INS\_W2 \end{bmatrix} \tag{4.14}$$

By further elementary mathematical manipulation and using the basic relationship between phase and sequence quantities the following equations can be derived:

$$\begin{bmatrix} Id\_L1 \\ Id\_L2 \\ Id\_L3 \end{bmatrix} = A \cdot \begin{bmatrix} IZS\_W1 \\ IPS\_W1 \\ INS\_W1 \end{bmatrix} + A \cdot \begin{bmatrix} 1 & 0 & 0 \\ 0 & e^{j\Theta} & 0 \\ 0 & 0 & e^{-j\Theta} \end{bmatrix} \cdot (A^{-1} \cdot A) \cdot \begin{bmatrix} IZS\_W2 \\ IPS\_W2 \\ INS\_W2 \end{bmatrix} \quad (4.15)$$

$$\begin{bmatrix} Id\_L1 \\ Id\_L2 \\ Id\_L3 \end{bmatrix} = \begin{bmatrix} IL1\_W1 \\ IL2\_W1 \\ IL3\_W1 \end{bmatrix} + A \cdot \begin{bmatrix} 1 & 0 & 0 \\ 0 & e^{j\Theta} & 0 \\ 0 & 0 & e^{-j\Theta} \end{bmatrix} \cdot A^{-1} \cdot \begin{bmatrix} IL1\_W2 \\ IL2\_W2 \\ IL3\_W2 \end{bmatrix} \quad (4.16)$$

The equation (4.16) now represents the basic relationship between phase – wise differential currents and individual phase currents from the two sides of the protected object.
To simplify equation (4.16) the new matrix transformation M(Θ) is defined and further developed in the following equations:

$$M(\Theta) = A \cdot \begin{bmatrix} 1 & 0 & 0 \\ 0 & e^{j\Theta} & 0 \\ 0 & 0 & e^{-j\Theta} \end{bmatrix} \cdot A^{-1} \quad (4.17)$$

$$M(\Theta) = \frac{1}{3} \cdot \begin{bmatrix} 1 & 1 & 1 \\ 1 & a^2 & a \\ 1 & a & a^2 \end{bmatrix} \cdot \begin{bmatrix} 1 & 0 & 0 \\ 0 & e^{j\Theta} & 0 \\ 0 & 0 & e^{-j\Theta} \end{bmatrix} \cdot \begin{bmatrix} 1 & 1 & 1 \\ 1 & a & a^2 \\ 1 & a^2 & a \end{bmatrix} \quad (4.18)$$

$$\mathrm{M}(\Theta) = \frac{1}{3} \cdot \begin{bmatrix} 1 + e^{j\Theta} + e^{-j\Theta} & 1 + a \cdot e^{j\Theta} + a^2 \cdot e^{-j\Theta} & 1 + a^2 \cdot e^{j\Theta} + a \cdot e^{-j\Theta} \\ 1 + a^2 \cdot e^{j\Theta} + a \cdot e^{-j\Theta} & 1 + a^3 \cdot e^{j\Theta} + a^3 \cdot e^{-j\Theta} & 1 + a^4 \cdot e^{j\Theta} + a^2 \cdot e^{-j\Theta} \\ 1 + a \cdot e^{j\Theta} + a^2 \cdot e^{-j\Theta} & 1 + a^2 \cdot e^{j\Theta} + a^4 \cdot e^{-j\Theta} & 1 + a^3 \cdot e^{j\Theta} + a^3 \cdot e^{-j\Theta} \end{bmatrix} \quad (4.19)$$

$$M(\Theta) = \frac{1}{3} \cdot \begin{bmatrix} 1+2 \cdot \cos(\Theta) & 1 - \cos(\Theta) - \sqrt{3} \cdot \sin(\Theta) & 1 - \cos(\Theta) + \sqrt{3} \cdot \sin(\Theta) \\ 1 - \cos(\Theta) + \sqrt{3} \cdot \sin(\Theta) & 1+2 \cdot \cos(\Theta) & 1 - \cos(\Theta) - \sqrt{3} \cdot \sin(\Theta) \\ 1 - \cos(\Theta) - \sqrt{3} \cdot \sin(\Theta) & 1 - \cos(\Theta) + \sqrt{3} \cdot \sin(\Theta) & 1+2 \cdot \cos(\Theta) \end{bmatrix} \quad (4.20)$$

Using the trigonometric relationship

$$cos(x \pm y) = cos(x) \cdot cos(y) \mp sin(x) \cdot sin(y)$$

the following form can be obtained:

$$\mathrm{M}(\Theta) = \frac{1}{3} \cdot \begin{bmatrix} 1+2 \cdot cos(\Theta) & 1 + 2 \cdot cos(\Theta + 120°) & 1 + 2 \cdot cos(\Theta - 120°) \\ 1 + 2 \cdot cos(\Theta - 120°) & 1+2 \cdot cos(\Theta) & 1 + 2 \cdot cos(\Theta + 120°) \\ 1 + 2 \cdot cos(\Theta + 120°) & 1 + 2 \cdot cos(\Theta - 120°) & 1+2 \cdot cos(\Theta) \end{bmatrix} \quad (4.21)$$

Due to a fact that $M(0^o)$ is a unit matrix, the equation (4.16) can be re–written as follows:

$$\begin{bmatrix} Id\_L1 \\ Id\_L2 \\ Id\_L3 \end{bmatrix} = \begin{bmatrix} IL1\_W1 \\ IL2\_W1 \\ IL3\_W1 \end{bmatrix} + M(\Theta) \cdot \begin{bmatrix} IL1\_W2 \\ IL2\_W2 \\ IL3\_W2 \end{bmatrix} = M(0°) \cdot \begin{bmatrix} IL1\_W1 \\ IL2\_W1 \\ IL3\_W1 \end{bmatrix} + M(\Theta) \cdot \begin{bmatrix} IL1\_W2 \\ IL2\_W2 \\ IL3\_W2 \end{bmatrix} \quad (4.22)$$

It shall be observed that Θ is the angle for which the winding two positive sequence, no-load voltage component shall be rotated in order to overlay with the positive sequence, no-load voltage component from winding one side. Refer to Figure 18 for more information. The angle Θ has a positive value when rotation is in an anticlockwise direction. Note that $M(0^o)$ is a unit matrix, which can be assigned to the first power transformer winding which is taken as the reference winding for phase angle compensation. Thus, the *reference winding* is a winding to which:

- all other winding currents are aligned; and
- its currents are not rotated (i.e. rotated by zero degrees).

Note that it is as well equally possible to select winding two as the reference winding for the differential protection phase angle shift compensation. In that case the negative value for angle Θ shall be associated with winding one. See Section 5.1 for an example.

4.4 Zero Sequence Current Compensation

Sometimes it is necessary to remove the zero sequence current component from one or possibly both sides of the protected transformer because the zero sequence current is not properly transferred from one side of the transformer to the other. In these cases the following, more general form of equation (4.22), can be used:

$$\begin{bmatrix} Id\_L1 \\ Id\_L2 \\ Id\_L3 \end{bmatrix} = M(0°) \cdot \begin{bmatrix} IL1\_W1 - k_{w1} \cdot IZS\_W1 \\ IL2\_W1 - k_{w1} \cdot IZS\_W1 \\ IL3\_W1 - k_{w1} \cdot IZS\_W1 \end{bmatrix} + M(\Theta) \cdot \begin{bmatrix} IL1\_W2 - k_{w2} \cdot IZS\_W2 \\ IL2\_W2 - k_{w2} \cdot IZS\_W2 \\ IL3\_W2 - k_{w2} \cdot IZS\_W2 \end{bmatrix} \quad (4.23)$$

where:

- IZS_W1 is the zero sequence current on side 1 of the protected object.
- IZS_W2 is the zero sequence current on side 2 of the protected object.
- k_{w1} and k_{w2} are setting parameters which can have values 1 or 0 and are set by the end user in order to enable or disable the zero sequence current reduction on any of the two sides.

By closer examination of equation (4.23) it is obvious that it is actually possible to deduct the zero sequence currents in the following two ways:

- by measuring the zero-sequence current at the winding common neutral point as described in [44]; or,
- by internally calculating zero-sequence current from the individually measured three-phase winding currents using the well-known formula from [21] and [43].

$$IZS = \frac{I_{L1} + I_{L2} + I_{L3}}{3} \quad (4.24)$$

When internal calculation of the zero-sequence current is used, it is possible to include equation (4.24) into the M(Θ) matrix transform by defining a new matrix transform M0(Θ), which simultaneously performs the phase angle shift compensation and the required zero sequence current elimination:

$$M0(\Theta) = M(\Theta) - \frac{1}{3} \cdot \begin{bmatrix} 1 & 1 & 1 \\ 1 & 1 & 1 \\ 1 & 1 & 1 \end{bmatrix} \tag{4.25}$$

$$M0(\Theta) = \frac{2}{3} \cdot \begin{bmatrix} \cos(\Theta) & \cos(\Theta + 120°) & \cos(\Theta - 120°) \\ \cos(\Theta - 120°) & \cos(\Theta) & \cos(\Theta + 120°) \\ \cos(\Theta + 120°) & \cos(\Theta - 120°) & \cos(\Theta) \end{bmatrix} \tag{4.26}$$

Therefore now (4.23) can be re-written as follows:

$$\begin{bmatrix} Id\_L1 \\ Id\_L2 \\ Id\_L3 \end{bmatrix} = M0(0°) \begin{bmatrix} IL1\_W1 \\ IL2\_W1 \\ IL2\_W1 \end{bmatrix} + M0(\Theta) \begin{bmatrix} IL1\_W2 \\ IL2\_W2 \\ IL2\_W2 \end{bmatrix} \tag{4.27}$$

Note that equations (4.22) and (4.27) actually have the same form. The only difference is the matrix transformation (i.e. M(Θ) or M0(Θ)) actually used. Thus, it is possible to select matrix transformation M0(Θ) to allow for the removal of the zero sequence currents on the relevant side of the protected transformer, or to select M(Θ) for phase angle shift compensation only in the differential current calculations.

Note that matrix transform M0(Θ) is actually the numerical equivalent of the generalized normalization transform presented in reference [42]. However, when the M0(Θ) matrix transformation is always applied on all sides of the protected transformer, as suggested in [42]:

- the differential protection sensitivity is unnecessarily reduced on the sides where it is not required to remove the zero sequence currents; and
- the calculation of the instantaneous differential currents can be unnecessarily corrupted, which can cause problems for proper operation of the 2nd and 5th harmonic blocking criteria, as shown in reference [12].

4.5 Universal Differential Current Calculation Method

If now all compensation techniques described in the previous sections are combined in one equation, the following universal equation for differential current calculations for any two winding, three-phase power transformer or PST can be written:

$$\begin{bmatrix} Id\_L1 \\ Id\_L2 \\ Id\_L3 \end{bmatrix} = \sum_{i=1}^{2} \frac{1}{Ib\_Wi} \cdot M(\Theta Wi) \cdot \begin{bmatrix} I_{L1\_Wi} - kWi \cdot I_{ZS\_Wi} \\ I_{L2\_Wi} - kWi \cdot I_{ZS\_Wi} \\ I_{L3\_Wi} - kWi \cdot I_{ZS\_Wi} \end{bmatrix} \tag{4.28}$$

where:

- Id_Lx are phase-wise differential currents;
- I_{b_Wi} is the base current of winding i (it can be a variable value if the winding incorporates OLTC);
- $M(\Theta_{Wi})$ is a 3x3 matrix that performs on-line phase angle shift compensation on winding i measured phase currents (it can have variable element values for some PST windings depending on the OLTC location within the PST);
- Θ_{Wi} is the angle for which winding i positive sequence, no-load *voltage* component shall be rotated in order to overlay with the positive sequence, no-load voltage component from the chosen reference winding (typically the first star winding as shown in Section 5.1); Θ_{Wi} has a positive value when rotation is performed in the anticlockwise direction;
- I_{Lx_Wi} are measured winding i phase currents (primary amperes);
- k_{Wi} is a setting which determines whether the zero sequence current shall be subtracted from the winding i phase currents (settable to zero or one); and
- I_{zs_Wi} is either the measured or the calculated winding i zero sequence current.

By using the superposition principle the most general equation to calculate the differential currents for any n-winding power transformer or PST can be written:

$$\begin{bmatrix} Id\_L1 \\ Id\_L2 \\ Id\_L3 \end{bmatrix} = \sum_{i=1}^{n} \frac{1}{I_{b\_Wi}} \cdot M(\Theta_{Wi}) \cdot \begin{bmatrix} I_{L1\_Wi} - k_{Wi} \cdot I_{ZS\_Wi} \\ I_{L2\_Wi} - k_{Wi} \cdot I_{ZS\_Wi} \\ I_{L3\_Wi} - k_{Wi} \cdot I_{ZS\_Wi} \end{bmatrix} \tag{4.29}$$

where:

- n is the number of windings of the protected power transformer (typically n≤6).

Alternatively, when zero sequence reduction is performed by internal calculations (4.25), the following equation can be written:

$$\begin{bmatrix} Id\_L1 \\ Id\_L2 \\ Id\_L3 \end{bmatrix} = \sum_{i=1}^{n} \frac{1}{I_{b\_Wi}} \cdot MX_{Wi} \cdot \begin{bmatrix} I_{L1\_Wi} \\ I_{L2\_Wi} \\ I_{L3\_Wi} \end{bmatrix} \tag{4.30}$$

where:

- MX_{Wi} is equal to either $M(\Theta_{Wi})$ on sides where zero sequence current is not removed or $M0(\Theta_{Wi})$ on sides where zero sequence current shall be removed.

A new quantity, DCC_{Wi}, described as the Differential Current Contribution set for winding i, can be defined by the following equation:

$$DCC_{Wi} = \begin{bmatrix} DCC\_L1_{Wi} \\ DCC\_L2_{Wi} \\ DCC\_L3_{Wi} \end{bmatrix} = \frac{1}{I_{b\_Wi}} \cdot MX_{Wi} \cdot \begin{bmatrix} I_{L1\_Wi} \\ I_{L2\_Wi} \\ I_{L3\_Wi} \end{bmatrix} \tag{4.31}$$

where:

- DCC_L1_{Wi} is the phase L1 differential current contribution from winding i.

Thus, equation (4.30) can now be re-written as follows:

$$\begin{bmatrix} Id\_L1 \\ Id\_L2 \\ Id\_L3 \end{bmatrix} = \sum_{i=1}^{n} DCC_{Wi} = \sum_{i=1}^{n} \begin{bmatrix} DCC\_L1_{Wi} \\ DCC\_L2_{Wi} \\ DCC\_L3_{Wi} \end{bmatrix} \tag{4.32}$$

Note that the elements of the M(Θ) and M0(Θ) matrices are always real numbers. Therefore, the presented differential current calculation method can be used to calculate the fundamental frequency phase-wise differential currents, the sequence-wise differential currents and the instantaneous differential currents for the protected power transformer [11] and [12].
For example, starting from equation (4.30) the negative sequence component differential current can be calculated in accordance with the following equation:

$$\begin{bmatrix} IdNS\_L1 \\ IdNS\_L2 \\ IdNS\_L3 \end{bmatrix} = \sum_{i=1}^{n} \frac{1}{I_{b\_Wi}} \cdot MX_{Wi} \cdot \begin{bmatrix} I_{NS\_Wi} \\ a \cdot I_{NS\_Wi} \\ a^2 \cdot I_{NS\_Wi} \end{bmatrix} = \sum_{i=1}^{n} \begin{bmatrix} DCCNS\_L1_{Wi} \\ DCCNS\_L2_{Wi} \\ DCCNS\_L3_{Wi} \end{bmatrix} \tag{4.33}$$

where:

- IdNS_L1 is the negative sequence differential current for phase L1
- I_{NS_Wi} is the winding i negative sequence current component in primary amperes (phase L1 used as reference phase);
- DCCNS_L1Wi is the negative sequence differential current contribution for phase L1 from winding I; and
- $a = e^{j120^o}$ is a sequence operator.

Note that the three differential currents based on the negative sequence current components will have equal magnitudes but they will be phase displaced by 120^o. Thus in practical applications it is sufficient to calculate the negative sequence component differential current for phase L1 only. Therefore, by using the concept of differential current contributions explained above the following equation can be written:

$$IdNS = IdNS\_L1 = \sum_{i=1}^{n} DCCNS\_L1_{Wi} \tag{4.34}$$

The above mentioned properties mean that all features of existing numerical differential protection for standard power transformers [11] and [12] can be directly applied to the new principle including:

- bias current calculation;
- operate-restraint characteristic;
- unrestraint operational level;

- 2^{nd} and 5^{th} harmonic blocking;
- waveform blocking;
- cross blocking; and
- negative sequence based internal/external fault discriminator.

Equation (4.29) is the main innovation in the differential current measurement system. With numerical technology it is possible to provide power transformer differential protection, which can simultaneously:

- provide on-line current magnitude compensation for every side;
- provide on-line phase angle compensation for arbitrary phase shift between different sides of the protected object;
- provide optional zero-sequence current compensation for every side; and
- compensate for multiple OLTCs located within the same power transformer.

Therefore it will be possible to provide differential protection, in accordance with Figure 14, for any three-phase power transformer or PST with arbitrary phase angle shift and current magnitude variations caused by OLTC(s) operation. This universal method for differential current calculations eliminates any need for buried current transformers within the PST tank, as usually required by presently used PST differential protection schemes [37]. Thus, any PST or special converter transformer can be protected with this differential protection scheme which is very similar to the presently used differential protection scheme for general-purpose three-phase power transformers.

4.6 Phase Sequence and Vector Group Compensation

Declared vector group (e.g. YNd5) on a power transformer rating plate is always stated with the assumption that the primary phase sequence connected to this three-phase power transformer is L1-L2-L3 (i.e. ANSI ABC). In other words, the power transformer vector group is always declared for the positive sequence system [33], [58].
From the transformer differential protection point of view the most important thing is that the phase sequence of the currents connected to the differential relay follows the phase sequence connected to the protected power transformer. Such arrangement, which is most commonly used in

the protective relaying practice, is shown in Figure 20a. For such connections the differential relay shall be set to compensate for the vector group as stated on the protected power transformer rating plate (e.g. YNd5 for application shown in Figure 20a), irrespective of the actual phase sequence used in this power system (e.g. either L1-L2-L3 or L3-L2-L1).

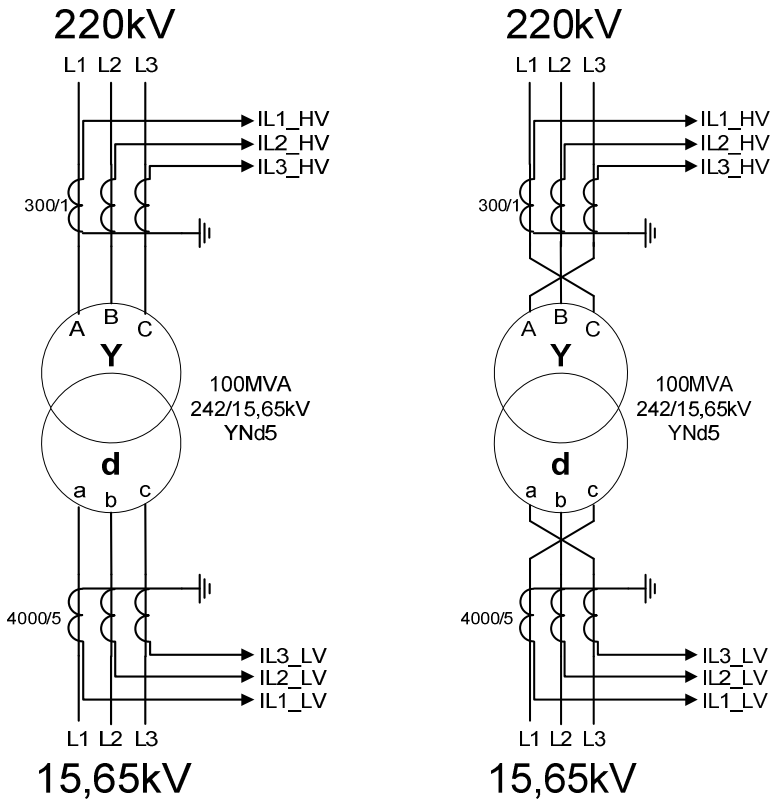

a) b)

Figure 20: Influence of the primary connections on the differential protection.

Sometimes, due to easier mechanical design, connections as shown in Figure 20b are used. As shown in this figure, two phases (e.g. L1 and L3 in this example) are swopped on both power transformer sides within the protected zone of the differential relay. Note that from the power system

point of view the two connections shown in Figure 20a and Figure 20b are fully equivalent. However the differential relay will not be stable if it is set to compensate for the YNd5 vector group. The reason is that the phase sequence connected to the differential relay (e.g. L1-L2-L3) is different on both sides from the phase sequence connected to the protected power transformer (e.g. L3-L2-L1). For such connections, the differential relay shall be set to compensate for the YNd7 vector group in order to remain stable for all through load conditions. Such setting is required irrespective of the actual phase sequence used in the power system (e.g. either L1-L2-L3 or L3-L2-L1).
Thus, for connections shown in Figure 20b, the protected power transformer vector group effectively becomes equal to twelve minus vector group number stated on the rating plate. Note that the same rule applies to all variants of three-phase power transformers (i.e. general-purpose transformers, converter transformers and phase-shifting transformers).

Connections shown in Figure 20b are taken from an actual installation and results from the differential protection primary testing are available to prove the presented principles. The same "setting problem" has been reported from other sites as well. For another practical example see Section 10.3/Field Case #1).
In this thesis it will always be assumed that the differential relay connections and the protected power transformer connections have the same phase sequence (i.e. as shown in Figure 20a).

4.7 Properties of M and M0 Matrix Transformations

Only three different numerical elements are present in any M and M0 matrix. Thus, the following two equations can be written:

$$M(\theta) = \frac{1}{3} \cdot \begin{bmatrix} 1+2\cdot\cos(\Theta) & 1+2\cdot\cos(\Theta+120^{O}) & 1+2\cdot\cos(\Theta-120^{O}) \\ 1+2\cdot\cos(\Theta-120^{O}) & 1+2\cdot\cos(\Theta) & 1+2\cdot\cos(\Theta+120^{O}) \\ 1+2\cdot\cos(\Theta+120^{O}) & 1+2\cdot\cos(\Theta-120^{O}) & 1+2\cdot\cos(\Theta) \end{bmatrix} = \begin{bmatrix} x & y & z \\ z & x & y \\ y & z & x \end{bmatrix} \quad (4.35)$$

$$M0(\theta)=\frac{2}{3}\cdot\begin{bmatrix}\cos(\Theta) & \cos(\Theta+120^{O}) & \cos(\Theta-120^{O})\\ \cos(\Theta-120^{O}) & \cos(\Theta) & \cos(\Theta+120^{O})\\ \cos(\Theta+120^{O}) & \cos(\Theta-120^{O}) & \cos(\Theta)\end{bmatrix}=\begin{bmatrix}x0 & y0 & z0\\ z0 & x0 & y0\\ y0 & z0 & x0\end{bmatrix} \tag{4.36}$$

These three numerical elements are interrelated. For the M matrix transformation elements the following equation is always valid.

$$x+y+z=1 \tag{4.37}$$

For the M0 matrix transformation elements the following equation is always valid.

$$x0+y0+z0=0 \tag{4.38}$$

The inverse matrix of the M (Θ) transformation is equal to:

$$M^{-1}(\Theta)=M(-\Theta)=M^{T}(\Theta)=\begin{bmatrix}x & z & y\\ y & x & z\\ z & y & x\end{bmatrix} \tag{4.39}$$

The matrix M0(Θ) is a singular matrix so a unique inverse matrix cannot be derived. However, it is possible to define the pseudo-inverse matrix (Moore-Penrose Matrix Inverse) $M0^{\dagger}(\Theta)$ [24]. This matrix can be used to calculate the three-phase currents if all three differential currents are known. Note that in such case the calculated phase currents will not contain any zero-sequence current component.

$$M0^{\dagger}(\Theta)=M0(-\Theta)=M0^{T}(\Theta)=\begin{bmatrix}x0 & z0 & y0\\ y0 & x0 & z0\\ z0 & y0 & x0\end{bmatrix} \tag{4.40}$$

These matrix transformations have the following interesting properties:

$$M(\Theta1+\Theta2)=M(\Theta1)\otimes M(\Theta2) \tag{4.41}$$

$$M0(\Theta1+\Theta2)=M0(\Theta1)\otimes M0(\Theta2) \tag{4.42}$$

$$M0(\Theta1+\Theta2)=M(\Theta1)\otimes M0(\Theta2)=M0(\Theta1)\otimes M(\Theta2) \tag{4.43}$$

where $\otimes$ is the symbol for matrix multiplication

The last property of the M and M0 transformations means that in practice the three-phase currents, which shall be rotated by angle $\Theta 1+\Theta 2$, can first be rotated by phase angle $\Theta 1$ and then subsequently be rotated by phase angle $\Theta 2$. The overall result will be exactly the same as if the rotation by the overall angle has been performed at once. A practical use of this property is shown in Section 8.1.

4.8 Correct Values for Base Current and Angle Θ

The proposed differential current calculation method is dependent on the correct values of the base current and phase angle shift for every power transformer side being available to the differential protection algorithm. These values can be obtained in one of the following ways:

- as fixed values, determined from the protected power transformer rated data and vector group, which are entered as setting parameters by the end user (see Section 5.1 for an example);
- from a look-up table which describes the relationship between different OLTC positions and the corresponding Ibase and Θ values (see Section 5.6 for an example);
- from two, three or more look-up tables, similar to the one described in the previous point, for devices with more than one OLTC [19], [48] and [60];
- from a two- or three-dimensional look-up table, similar to the one described in the previous points, for devices with more than one OLTC [19], [48] and [60];
- by an algorithm internal to the differential protection, which during steady state operating conditions measures the phase angle difference between the positive sequence no-load voltages from the two power transformer sides when the transformer is not loaded, or alternatively by measuring the phase angle difference between positive sequence currents from the two power transformer sides when the transformer is loaded. Note that this is possible only for power transformers with two sides; or
- via a communication link from the protected object control system in case of more complicated FACTs devices.

Chapter 5

Application of the Method

Examples of how to calculate the differential currents in accordance with the new universal method for some practical transformer applications will be presented in this chapter.

5.1 Standard Two–winding, YNd1 Transformer

The transformer rating data, relevant application data for the differential protection and the vector diagram for the voltage quantities for this power transformer are given in Figure 21. The maximum power (i.e. base power) for this transformer is 20.9MVA, and against this value, the base primary currents and base currents on the CT secondary side are calculated as shown in Table 1. Note that the calculation of the base currents on the CT secondary side is limited to this example and subsequent cases will mainly be presented with primary base currents.

Table 1: Base current calculations for an YNd1 transformer

	Primary Base Current	Base current on CT secondary side
W1, 69kV-Star	$\frac{20.9\text{MVA}}{\sqrt{3}\times 69\text{kV}}=174.9\text{A}$	$\frac{174.9}{300/1}=0.583\text{A}$
W2, 12.5kV-Delta	$\frac{20.9\text{MVA}}{\sqrt{3}\times 12.5\text{kV}}=965.3\text{A}$	$\frac{965.3}{1000/5}=4.827\text{A}$

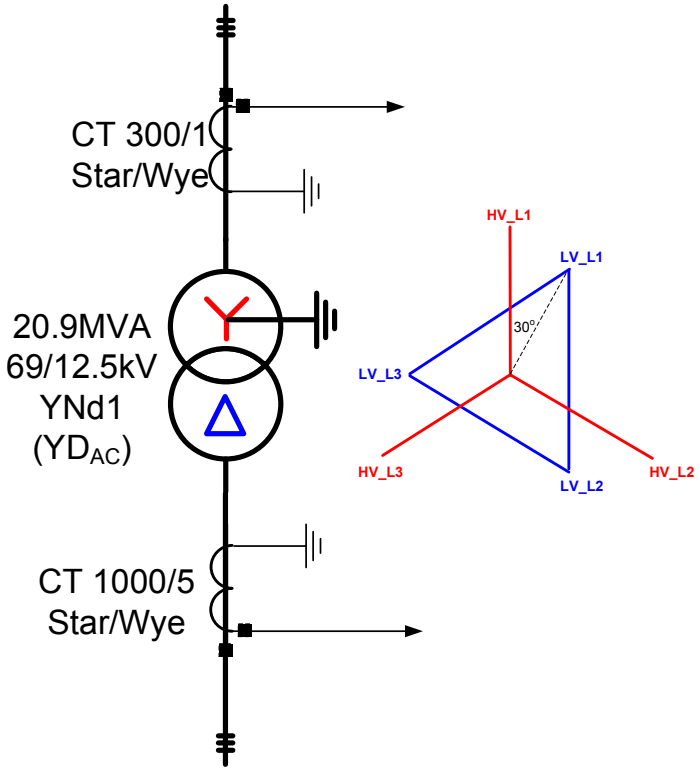

Figure 21: Relevant application data for an YNd1 power transformer.

Regarding phase angle compensation two solutions are possible (in general for an n-winding transformer at least n possible solutions exist). The first solution is to take W1 side as the reference side (i.e. with 0^o phase angle shift). The vector group of the protected transformer is Yd1 (ANSI designation YD_{AC}), thus the W2 (delta winding) positive sequence voltage component shall be rotated by 30^o in an anticlockwise direction in order to coincide with the W1 positive sequence voltage component. For this first phase angle compensation solution the required matrices for both windings are shown in Table 2. Note that the zero sequence current shall be removed from the W1 side, because the HV star winding neutral point is solidly grounded.

Table 2: First solution for phase angle compensation for an YNd1 transformer

	Compensation matrix Mx
W1, 69kV-Star, selected as reference winding	$M0(0^o) = \frac{1}{3} \cdot \begin{bmatrix} 2 & -1 & -1 \\ -1 & 2 & -1 \\ -1 & -1 & 2 \end{bmatrix}$
W2, 12.5kV-Delta	$M(30^o) = \begin{bmatrix} 0.9107 & -0.2440 & 0.3333 \\ 0.3333 & 0.9107 & -0.2440 \\ -0.2440 & 0.3333 & 0.9107 \end{bmatrix}$

The second solution is to take W2 side as the reference side (with 0^o phase angle shift). The vector group of the protected transformer is Yd1, thus the W1 (star winding) positive sequence voltage component shall be rotated by 30^o in a clockwise direction (see Figure 21) in order to coincide with the W2 positive sequence voltage component. For this second phase angle compensation solution the required matrices for both windings are shown in Table 3.

Table 3: Second solution for phase angle compensation for an YNd1 transformer

	Compensation matrix Mx
W1, 69kV-Star	$M0(-30^o) = \frac{1}{\sqrt{3}} \cdot \begin{bmatrix} 1 & 0 & -1 \\ -1 & 1 & 0 \\ 0 & -1 & 1 \end{bmatrix}$
W2, 12.5kV-Delta, selected as reference winding	$M(0^o) = \begin{bmatrix} 1 & 0 & 0 \\ 0 & 1 & 0 \\ 0 & 0 & 1 \end{bmatrix}$

Note that the second solution is identical to the traditionally applied transformer differential protection schemes that utilize analogue differential relays and interposing CTs. In such schemes, the y/d connected interposing CTs are used on star-connected power transformer windings, while y/y connected interposing CTs are used on delta-connected power transformer windings.

Note, however, that the first solution correlates better with the physical winding layout around the magnetic core limbs within the protected power transformer. In the case of an internal fault in phase L1 of the HV star connected winding for the second solution, equally large differential currents would appear in phases L1 and L3 and the differential relay would operate in both phases. However, for the first solution, the biggest differential current would appear in phase L1 clearly indicating the actual faulty phase. It can also be shown that a slightly larger magnitude of the differential current would be calculated for such an internal fault by using the first solution (i.e. for phase-to-ground faults, the ratio of the differential currents will be $1^{st}\_Solution : 2^{nd}\_Solution = \frac{2}{3} : \frac{1}{\sqrt{3}} = 0.667 : 0.577$). Thus, the first solution is recommended for the numerical differential protection and it can be simply formulated using the following guidelines:

- the first star (i.e. wye) connected power transformer winding shall preferably be selected as the reference winding (with 0^o phase angle shift) for the transformer differential protection;
- the first delta connected power transformer winding shall be selected as the reference winding only for power transformers without any star connected windings;
- the first delta connected winding within the protected power transformer can be selected as the reference winding only if a solution similar with traditionally applied transformer differential protection schemes utilizing analogue differential relays and interposing CTs is required;
- for special converter transformers (see Section 5.4 and Section 5.5), a zigzag connected power transformer winding might be selected as reference winding; and
- for PST applications typically the S-side shall be selected as the reference side.

The first guideline will be followed for all applications shown in this document, with exception of Sections 5.2 and 5.8 where still two solutions for phase angle shift compensation will be presented.
Once the base currents and MX matrices are determined the overall equation to calculate differential currents can be written in accordance with equation (4.30). Equation using primary base currents and the first solution for phase angle compensation will only be presented here.

$$\begin{bmatrix} Id\_L1 \\ Id\_L2 \\ Id\_L3 \end{bmatrix} = \frac{1}{174.9} \cdot \frac{1}{3} \cdot \begin{bmatrix} 2 & -1 & -1 \\ -1 & 2 & -1 \\ -1 & -1 & 2 \end{bmatrix} \cdot \begin{bmatrix} I_{L1\_69} \\ I_{L2\_69} \\ I_{L3\_69} \end{bmatrix} +$$

$$+ \frac{1}{965.3} \cdot \begin{bmatrix} 0.9107 & -0.2440 & 0.3333 \\ 0.3333 & 0.9107 & -0.2440 \\ -0.2440 & 0.3333 & 0.9107 \end{bmatrix} \cdot \begin{bmatrix} I_{L1\_12.5} \\ I_{L2\_12.5} \\ I_{L3\_12.5} \end{bmatrix}$$

5.2 Auto-transformers

The application of the differential protection to auto-transformers is somewhat special because the schemes can be arranged in a number of ways, as described below. The following auto-transformer rating data will be used for all examples in this section: 300/300/100MVA; 400/115/10.5kV; YNautod5. The maximum power (i.e. base power) for this auto-transformer is 300MVA. The phase shift between the tertiary delta winding and the other two windings is 150^{o}.

Auto-transformer with not Loaded Tertiary Delta Winding

Quite often the auto-transformer tertiary winding is not loaded and it is used as a delta-connected equalizer winding [58]. Typical CT locations for the differential protection of such an auto-transformer are shown in Figure 22. In this scenario the auto-transformer is protected as a two-winding power transformer. Thus, the base primary currents are calculated as shown in Table 4.

Table 4: Base current calculations

	Primary Base Current
W1, 400kV-Star	$\frac{300\text{MVA}}{\sqrt{3}\times 400\text{kV}} = 433\text{A}$
W2, 115kV-Star	$\frac{300\text{MVA}}{\sqrt{3}\times 115\text{kV}} = 1506\text{A}$

Regarding phase angle compensation, two solutions are possible. The first solution is to take W1 side as the reference side (with 0^o phase angle shift). The vector group of the protected auto-transformer is Yy0, thus the W2 positive sequence, no-load voltage component is in phase with W1 positive sequence, no-load voltage component. Due to the existence of a tertiary delta winding the zero sequence current must be eliminated from both sides, thus M0(0^o) matrices shall be used on both auto-transformer sides. The required compensation matrices for both windings are shown in Table 5.

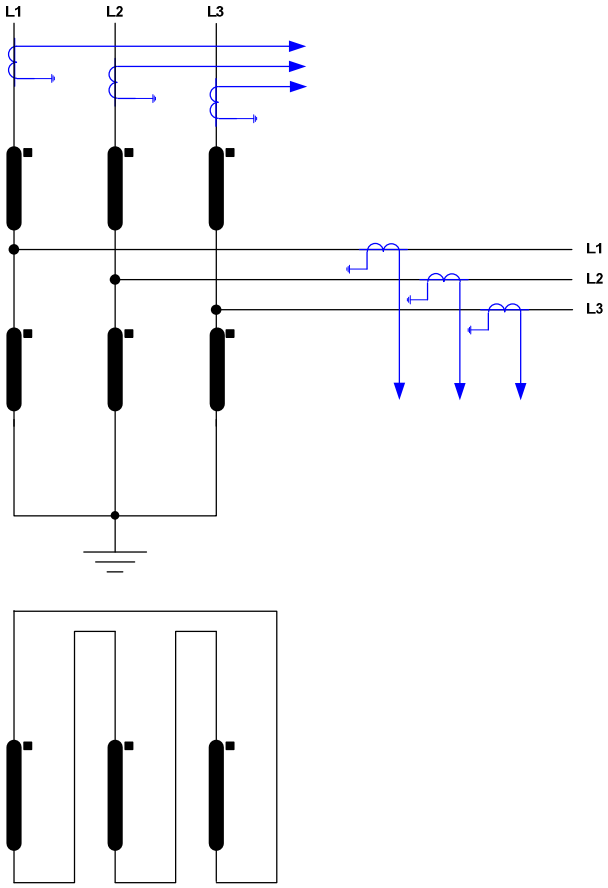

Figure 22: YNautod5 connected auto-transformer with unloaded tertiary delta winding.

Table 5: The first solution for the phase angle compensation

	Compensation matrix Mx
W1, 400kV-Star, selected as reference winding	$M0(0^o) = \frac{1}{3} \cdot \begin{bmatrix} 2 & -1 & -1 \\ -1 & 2 & -1 \\ -1 & -1 & 2 \end{bmatrix}$
W2, 115kV-Star	$M0(0^o) = \frac{1}{3} \cdot \begin{bmatrix} 2 & -1 & -1 \\ -1 & 2 & -1 \\ -1 & -1 & 2 \end{bmatrix}$

The second solution is identical to traditionally used solutions with analogue transformer differential relays and y/d connected interposing CTs. In the case of an auto-transformer it is only important to take the same compensation angle on both sides. The vector group of the protected auto-transformer is Yy0d5, thus both sides can be, for example, rotated by 150^o in the clockwise direction in order to prepare for the inclusion of W3 into the differential protection if so would be required in the future. The required compensation matrices for both windings are shown in Table 6.

Table 6: The second solution for the phase angle compensation

	Compensation matrix Mx
W1, 400kV-Star	$M0(-150^o) = \frac{1}{\sqrt{3}} \cdot \begin{bmatrix} -1 & 1 & 0 \\ 0 & -1 & 1 \\ 1 & 0 & -1 \end{bmatrix}$
W2, 115kV-Star	$M0(-150^o) = \frac{1}{\sqrt{3}} \cdot \begin{bmatrix} -1 & 1 & 0 \\ 0 & -1 & 1 \\ 1 & 0 & -1 \end{bmatrix}$

The second solution to calculate differential currents for this auto-transformer has the same drawbacks as explained in Section 5.1. Once the base currents and MX matrices are determined the overall equation to calculate differential currents can be written in accordance with equation (4.30).

Auto-transformer with Loaded Tertiary Delta Winding

In some countries the tertiary delta winding is used to provide reactive power compensation (i.e. shunt reactors or shunt capacitors) to the rest of the system. Typical CT locations for differential protection of such auto-transformers are shown in Figure 23. In such applications three-winding differential protection shall be used. Thus, the base primary currents are calculated as shown in Table 7.

Table 7: Base current calculations

	Primary Base Current
W1, 400kV-Star	$\frac{300\text{MVA}}{\sqrt{3}\times 400\text{kV}}=433\text{A}$
W2, 115kV-Star	$\frac{300\text{MVA}}{\sqrt{3}\times 115\text{kV}}=1506\text{A}$
W3, 10.5kV-Delta	$\frac{300\text{MVA}}{\sqrt{3}\times 10.5\text{kV}}=16496\text{A}$

Phase angle compensation matrixes as shown in Table 8 shall be used.

Table 8: Solution for the phase angle compensation

	Compensation matrix Mx
W1, 400kV-Star, selected as reference winding	$M0(0^o)=\frac{1}{3}\cdot\begin{bmatrix}2 & -1 & -1\\ -1 & 2 & -1\\ -1 & -1 & 2\end{bmatrix}$
W2, 115kV-Star	$M0(0^o)=\frac{1}{3}\cdot\begin{bmatrix}2 & -1 & -1\\ -1 & 2 & -1\\ -1 & -1 & 2\end{bmatrix}$
W3, 10.5kV-Delta	$M(150^o)=\begin{bmatrix}-0.2440 & 0.3333 & 0.9107\\ 0.9107 & -0.2440 & 0.3333\\ 0.3333 & 0.9107 & -0.2440\end{bmatrix}$

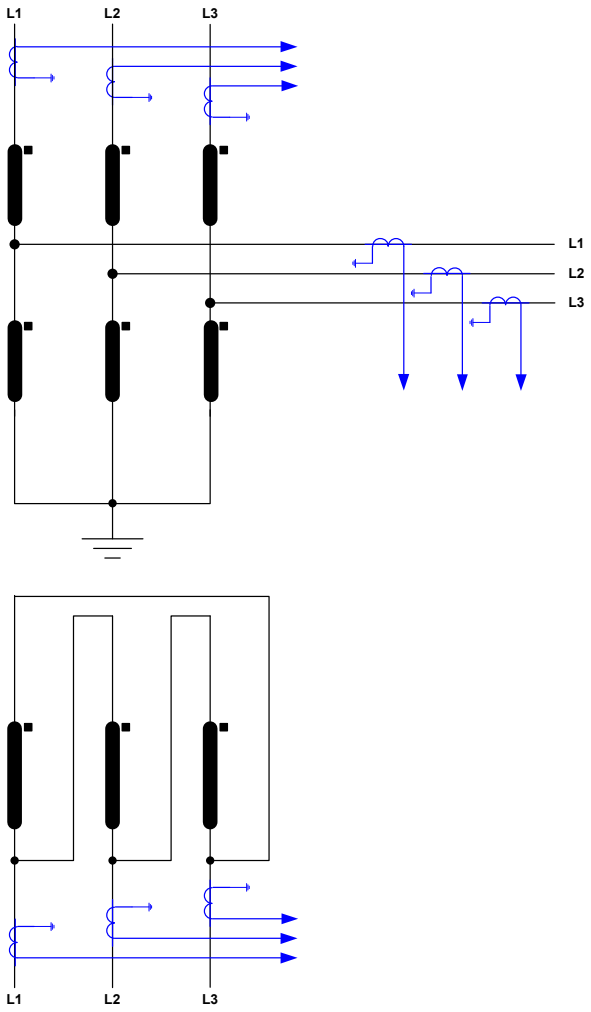

Figure 23: YNautod5 connected auto-transformer with loaded tertiary delta winding.

Auto-transformer Built from Three Single-phase Units

Due to easier transportation to site and cheaper reserve units big auto-transformers are sometimes built as three single-phase units. Typical CT locations for differential protection of such auto-transformers are shown in

Figure 24. Note the position of CTs inside the tertiary delta winding. In such applications three-winding differential protection shall be used. Thus, the base primary currents are calculated as shown in Table 9.

Table 9: Base current calculations

	Primary Base Current
W1, 400kV-Star	$\frac{300\text{MVA}}{\sqrt{3}\times 400\text{kV}}=433\text{A}$
W2, 115kV-Star	$\frac{300\text{MVA}}{\sqrt{3}\times 115\text{kV}}=1506\text{A}$
W3, 10.5kV-Star	$\frac{300\text{MVA}}{3\times 10.5\text{kV}}=9524\text{A}$

Phase angle compensation matrixes as shown in Table 10 shall be used. Zero sequence current reduction is not required due to the fact that every unit has its own magnetic core. The same is also valid for five-limb, three-phase auto-transformers [29].

Table 10: Solution for the phase angle compensation

	Compensation matrix Mx
W1, 400kV-Star, selected as reference winding	$M(0^o)=\begin{bmatrix}1 & 0 & 0\\ 0 & 1 & 0\\ 0 & 0 & 1\end{bmatrix}$
W2, 115kV-Star	$M(0^o)=\begin{bmatrix}1 & 0 & 0\\ 0 & 1 & 0\\ 0 & 0 & 1\end{bmatrix}$
W3, 10.5kV-Star	$M(0^o)=\begin{bmatrix}1 & 0 & 0\\ 0 & 1 & 0\\ 0 & 0 & 1\end{bmatrix}$

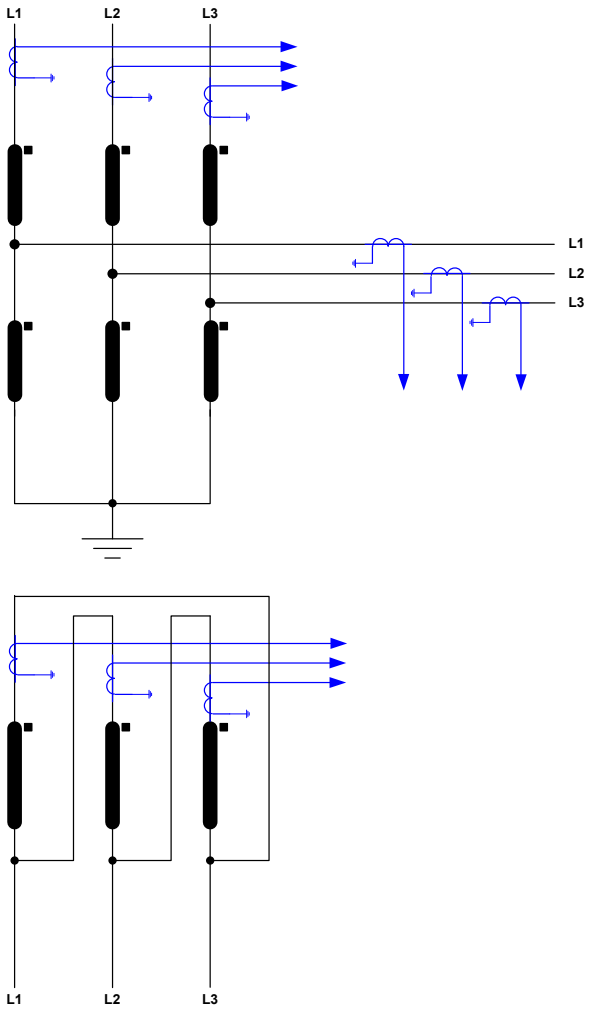

Figure 24: YNautod5 connected auto-transformer with CTs inside the loaded tertiary delta winding.

Auto-transformer Built from Three Single-phase Units and CTs in the Common Winding Neutral Point

Sometimes CTs are even available in the neutral point of the common winding of single-phase transformers. CT locations for such differential protection applications are shown in Figure 25. Three-winding differential protection shall be used. Thus, the base primary currents are calculated as shown in Table 11.

Table 11: Base current calculations

	Primary Base Current
W1, 400kV-Star	$\frac{300\text{MVA}}{\sqrt{3}\times 400\text{kV}}=433\text{A}$
W2, Common Winding NP-Star	1506-433=1073A
W3, 10.5kV-Star	$\frac{300\text{MVA}}{3\times 10.5\text{kV}}=9524\text{A}$

Phase angle compensation matrixes as shown in Table 12 shall be used. Zero sequence current reduction is not required due to the fact that every unit has its own magnetic core. The same is also valid for five-limb, three-phase auto-transformers [29].

Table 12: Solution for the phase angle compensation

	Compensation matrix Mx
W1, 400kV-Star, selected as reference winding	$M(0^o)=\begin{bmatrix}1 & 0 & 0\\ 0 & 1 & 0\\ 0 & 0 & 1\end{bmatrix}$
W2, Common Winding NP-Star	$M(0^o)=\begin{bmatrix}1 & 0 & 0\\ 0 & 1 & 0\\ 0 & 0 & 1\end{bmatrix}$
W3, 10.5kV-Delta	$M(0^o)=\begin{bmatrix}1 & 0 & 0\\ 0 & 1 & 0\\ 0 & 0 & 1\end{bmatrix}$

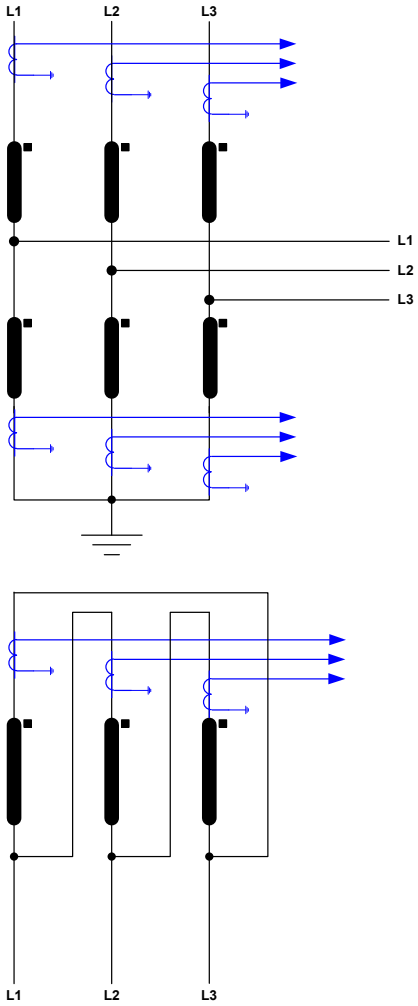

Figure 25: YNautod5 connected auto-transformer with CTs inside the loaded tertiary delta winding and in the common winding neutral point.

Differential protection in this application has increased the sensitivity for earth-faults within the auto-transformer due to the measuring point in the common winding neutral point, where increased current during internal earth-faults will occur.

5.3 Four – winding Power Transformer

The rated quantities for a four winding power transformer are given on the transformer rating plate shown in Figure 26.

Type	SDOG 63 030/145	Rated frequency	50 Hz	Insulation level		HV	LV1	LV2	Filter
Serial no.	118000189	Vector group	Y yn0 d1 d1			U, V, W	u, v, w, n	x, y, z	A, B, C
Year of manuf.	2005	Type of cooling	ONAN	Um	kV	145	12	12	24
Standard	IEC 60076	Oiltemperature rise max.	60 K	AC	kV	275	28	28	50
				LI	kV	650	75	75	125

Rated power	Rated voltage				Rated current			
	HV	LV1	LV2	Filter	HV	LV1	LV2	Filter
	U, V, W	u, v, w, n	x, y, z	A, B, C	U, V, W	u, v, w, n	x, y, z	A, B, C
55.53 MVA	132 kV	–	–	–	242.9 A	–	–	–
27.765 MVA	–	7 kV	7 kV	–	–	2290 A	2290 A	–
15.0 MVA	–	–	–	11 kV	–	–	–	787.3 A

Short–circuit impedance per phase				Impedance voltage			
HV–LV1(star)	Ohm	LV1(star)–Filter	Ohm	HV–LV1(star) (27.765 MVA)	%	LV1(star)–Filter (27.765 MVA)	%
HV–LV2(delta)	Ohm	LV2(delta)–Filter	Ohm	HV–LV2(delta) (27.765 MVA)	%	LV2(delta)–Filter (27.765 MVA)	%
HV–Filter	Ohm	HV–LV1//LV2	Ohm	HV–Filter (27.765 MVA)	%	HV–LV1//LV2 (55.53 MVA)	%

Figure 26: Rating plate for a four-winding transformer.

The rated power for the calculation of the base currents is the maximum power of all four windings, and it has a value of 55.53MVA. From the power transformer vector group Yyn0d1d1, stated on the rating plate, the angles for phase angle compensation can be extracted.

First winding:

Vector group: Y
Phase shift: 0^o (this winding is taken as the reference winding)
Rated voltage: 132kV
Rated power: 55.53MVA
Rated current: 242.9A

From this data the base current for the magnitude compensation is calculated:

$$I_{b\_W1}=\frac{S_b}{\sqrt{3}\times U_{b\_W1}}=\frac{55.53\text{MVA}}{\sqrt{3}\times 132\text{kV}}=242.9\text{A}$$

As the first winding is not earthed, then the subtraction of the zero sequence current is not required. Thus

$$MX_{W1} = M(0°) = \begin{bmatrix} 1 & 0 & 0 \\ 0 & 1 & 0 \\ 0 & 0 & 1 \end{bmatrix}$$

Second winding:

Vector group:	yn0
Phase shift:	0^o (the second winding no-load voltage is in phase with the first winding no-load voltage. Thus there is no need to rotate these winding currents)
Rated voltage:	7kV
Rated power:	27.765MVA
Rated current:	2290A

The base current is calculated as:

$$I_{b\_W2} = \frac{S_b}{\sqrt{3} \times U_{b\_W2}} = \frac{55.53\text{MVA}}{\sqrt{3} \times 7\text{kV}} = 4580\text{A}$$

Notice that for the calculation of the base current the maximum rated power of all windings within the protected transformer is used (in this case Sb = 55.53MVA).
As the winding is earthed, the zero sequence current must be removed.

$$MX_{W2} = M0(0°) = \frac{1}{3} \cdot \begin{bmatrix} 2 & -1 & -1 \\ -1 & 2 & -1 \\ -1 & -1 & 2 \end{bmatrix}$$

Third winding:

Vector group:	d1
Phase shift:	30^o (the third winding no-load voltage lags the first winding no-load voltage. To get the two windings correlated the third winding voltage has to be rotated anticlockwise by 30^o)
Rated voltage:	7kV
Rated power:	27.765MVA

Rated current: 2290A

The base current is calculated:

$$I_{b\_W3}=\frac{S_b}{\sqrt{3}\times U_{b\_W3}}=\frac{55.53\text{MVA}}{\sqrt{3}\times 7\text{kV}}=4580\text{A}$$

As the winding is delta connected the subtraction of the zero sequence current is not required.

$$MX_{W3}=M(30°)=\begin{bmatrix} 0.9107 & -0.2440 & 0.3333 \\ 0.3333 & 0.9107 & -0.2440 \\ -0.2440 & 0.3333 & 0.9107 \end{bmatrix}$$

Fourth winding:

Vector group: d1
Phase shift: 30^o (the fourth winding no-load voltage lags the first winding no-load voltage. To get the two windings correlated, the fourth winding voltage has to be rotated anticlockwise by 30^o)
Rated voltage: 11kV
Rated power: 15.0MVA
Rated current: 787.3A

The base current is calculated:

$$I_{b\_W4}=\frac{S_b}{\sqrt{3}\times U_{b\_W4}}=\frac{55.53\text{MVA}}{\sqrt{3}\times 11\text{kV}}=2914.6\text{A}$$

As the winding is delta connected the subtraction of the zero sequence current is not required.

$$MX_{W4}=M(30°)=\begin{bmatrix} 0.9107 & -0.2440 & 0.3333 \\ 0.3333 & 0.9107 & -0.2440 \\ -0.2440 & 0.3333 & 0.9107 \end{bmatrix}$$

Once all these base currents and MX matrices are determined the overall equation to calculate differential currents can be written in accordance with equation (4.30).

5.4 Special Converter Transformer

In this case, a design of a special converter transformer will be demonstrated that is a three–phase converter transformer with four windings with an additional phase angle shift Ψ of 7.5°. The rating plate of the transformer is presented in Figure 27.
The necessary data for the calculation of the differential currents can be easily obtained from the power transformer rating plate data. The vector group of the transformer is given on the rating plate as Y-7.5°yn0d1d1. Actually, this transformer vector group shall be given as Zyn11¾d0¾d0¾. The high voltage zigzag connected winding will be taken as the reference winding (i.e. with 0° phase shift for differential current calculation). From the phasor diagram on the rating plate the angles for phase angle compensation can be extracted.
The rated power for the calculation of the base currents is the maximum power of the four windings, and in this case it has a value of 61.44MVA.

First winding:

Vector group:	Z (i.e. Y on the rating plate)
Phase shift:	0° (this winding is taken as the reference winding)
Rated voltage:	132kV
Rated power:	61.44MVA
Rated current:	268.7A

The base current is calculated:

$$I_{b\_W1} = \frac{S_b}{\sqrt{3} \times U_{b\_W1}} = \frac{61.44\text{MVA}}{\sqrt{3} \times 132\text{kV}} = 268.7\text{A}$$

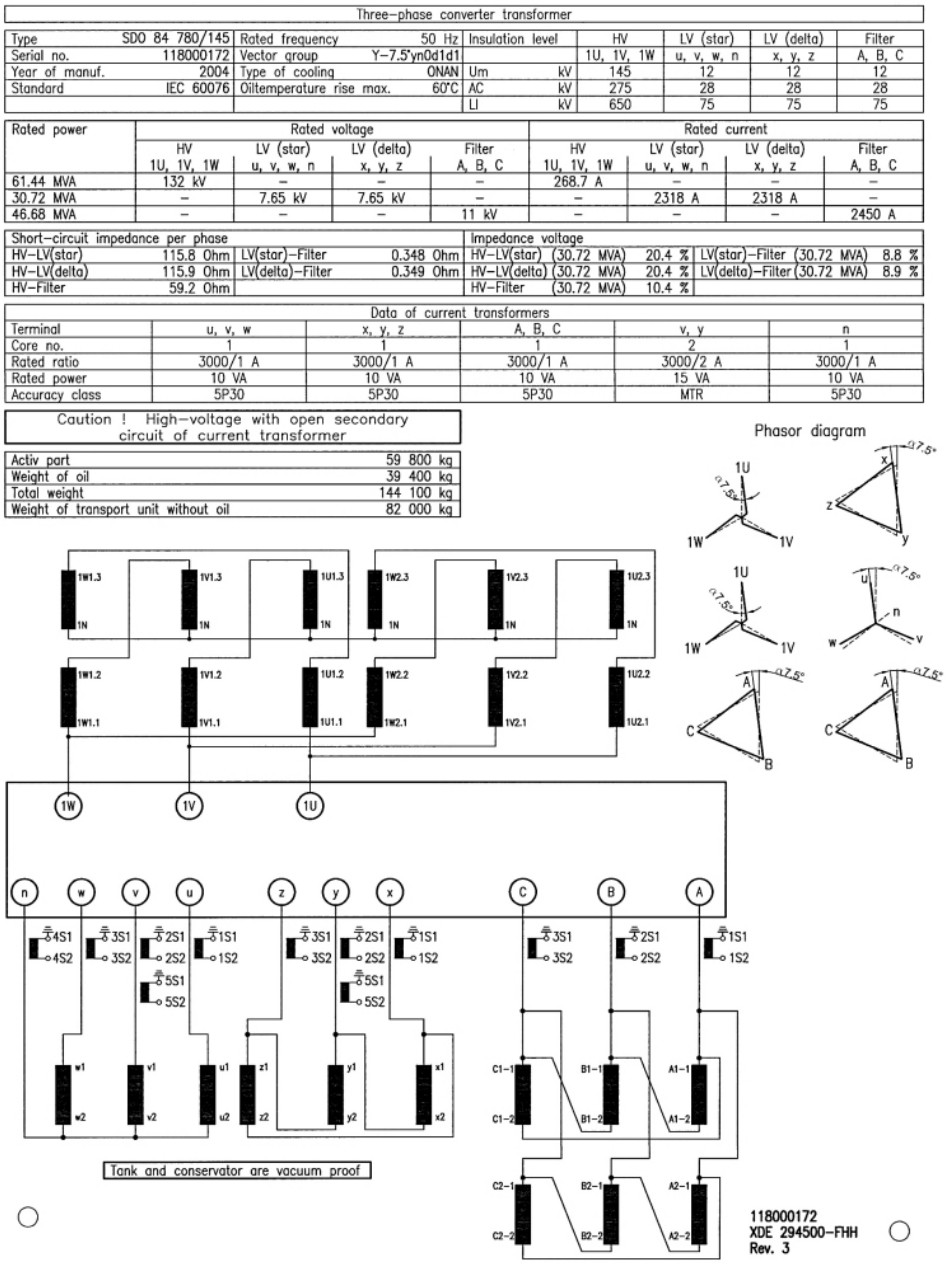

Three-phase converter transformer

Type	SDO 84 780/145	Rated frequency	50 Hz	Insulation level		HV	LV (star)	LV (delta)	Filter
Serial no.	118000172	Vector group	Y-7.5'yn0d1d1			1U, 1V, 1W	u, v, w, n	x, y, z	A, B, C
Year of manuf.	2004	Type of cooling	ONAN	Um	kV	145	12	12	12
Standard	IEC 60076	Oiltemperature rise max.	60°C	AC	kV	275	28	28	28
				LI	kV	650	75	75	75

Rated power	Rated voltage				Rated current			
	HV	LV (star)	LV (delta)	Filter	HV	LV (star)	LV (delta)	Filter
	1U, 1V, 1W	u, v, w, n	x, y, z	A, B, C	1U, 1V, 1W	u, v, w, n	x, y, z	A, B, C
61.44 MVA	132 kV	–	–	–	268.7 A	–	–	–
30.72 MVA	–	7.65 kV	7.65 kV	–	–	2318 A	2318 A	–
46.68 MVA	–	–	–	11 kV	–	–	–	2450 A

Short-circuit impedance per phase				Impedance voltage			
HV-LV(star)	115.8 Ohm	LV(star)-Filter	0.348 Ohm	HV-LV(star) (30.72 MVA)	20.4 %	LV(star)-Filter (30.72 MVA)	8.8 %
HV-LV(delta)	115.9 Ohm	LV(delta)-Filter	0.349 Ohm	HV-LV(delta) (30.72 MVA)	20.4 %	LV(delta)-Filter (30.72 MVA)	8.9 %
HV-Filter	59.2 Ohm			HV-Filter (30.72 MVA)	10.4 %		

Data of current transformers

Terminal	u, v, w	x, y, z	A, B, C	v, y	n
Core no.	1	1	1	2	1
Rated ratio	3000/1 A	3000/1 A	3000/1 A	3000/2 A	3000/1 A
Rated power	10 VA	10 VA	10 VA	15 VA	10 VA
Accuracy class	5P30	5P30	5P30	MTR	5P30

Caution ! High-voltage with open secondary circuit of current transformer

Activ part	59 800 kg
Weight of oil	39 400 kg
Total weight	144 100 kg
Weight of transport unit without oil	82 000 kg

Phasor diagram

Tank and conservator are vacuum proof

118000172
XDE 294500-FHH
Rev. 3

Figure 27: Part of the rating plate for a converter transformer.

The zigzag connected winding is not earthed so the subtraction of the zero sequence current is not required.

$$MX_{W1} = M(0°) = \begin{bmatrix} 1 & 0 & 0 \\ 0 & 1 & 0 \\ 0 & 0 & 1 \end{bmatrix}$$

Second winding:

Vector group: yn0
Phase shift : -7.5^o (the second winding no-load voltage leads the first winding no-load voltage. To get the two windings correlated the second winding voltage has to be rotated clockwise by 7.5^o)
Rated voltage: 7.65kV
Rated power: 30.72MVA
Rated current: 2318A

The base current is calculated:

$$I_{b\_W2} = \frac{S_b}{\sqrt{3} \times U_{b\_W2}} = \frac{61.44\text{MVA}}{\sqrt{3} \times 7.65\text{kV}} = 4636.9\text{A}$$

Because this winding star point is accessible the subtraction of the zero sequence current is needed.

$$MX_{W2} = M0(-7.5^o) = \begin{bmatrix} 0.6610 & -0.2551 & -0.4058 \\ -0.4058 & 0.6610 & -0.2551 \\ -0.2551 & -0.4058 & 0.6610 \end{bmatrix}$$

Third winding

Vector group: d1
Phase shift : 30^o-7.5^o=22.5^o (as the third winding vector group introduces a phase shift of 30^o, the phase shift angle of -7.5^o must be taken in consideration so the total phase shift is 22.5^o anticlockwise)
Rated voltage: 7.65kV
Rated power: 30.72MVA
Rated current: 2318A

The base current is calculated:

$$I_{b\_W3}=\frac{S_b}{\sqrt{3}\times U_{b\_W3}}=\frac{61.44\text{MVA}}{\sqrt{3}\times 7.65\text{kV}}=4636.9\text{A}$$

As the winding is delta connected the subtraction of the zero sequence current is not required.

$$MX_{W3}=M(22.5^o)=\begin{bmatrix} 0.9493 & -0.1956 & 0.2463 \\ 0.2463 & 0.9493 & -0.1956 \\ -0.1956 & 0.2463 & 0.9493 \end{bmatrix}$$

Fourth winding

Vector group: d1
Phase shift : 30^o-7.5^o=22.5^o (as the fourth winding vector group introduces a phase shift of 30^o, the phase shift angle of -7.5^o must be taken in consideration so the total phase shift is 22.5^o anticlockwise)
Rated voltage: 11kV
Rated power: 46.68MVA
Rated current: 2450A

The base current is calculated:

$$I_{b\_W4}=\frac{S_b}{\sqrt{3}\times U_{b\_W4}}=\frac{61.44\text{MVA}}{\sqrt{3}\times 11\text{kV}}=3224.8\text{A}$$

As the winding is delta connected the subtraction of the zero sequence current is not required.

$$MX_{W4}=M(22.5^o)=\begin{bmatrix} 0.9493 & -0.1956 & 0.2463 \\ 0.2463 & 0.9493 & -0.1956 \\ -0.1956 & 0.2463 & 0.9493 \end{bmatrix}$$

Once all these base currents and MX matrices are determined the overall equation to calculate differential currents can be written in accordance with equation (4.30).

5.5 24-pulse Converter Transformer

In this case, the 24-pulse converter transformer design will be presented. This 24-pulse converter transformer is quite special because within the same transformer tank two three-phase transformers, of very similar design, as shown in Figure 3a and Figure 3b, are put together. The first internal transformer has the vector group Zy11¾d10¾. The second internal transformer has the vector group Zy0¼d11¼. Such an arrangement gives an equivalent five-winding power transformer with a 15^o phase angle shift between the LV windings of the same connection type. For differential protection this is equivalent to a five winding power transformer with an additional phase angle shift Ψ of 7.5^o. The necessary information to apply the differential protection is given in Figure 28.

The high voltage, equivalent zigzag connected winding will be taken as the reference winding with 0º phase shift. The power for the calculation of the base currents is the maximum power of the five windings, and in this case it has a value of 2.6MVA.

First winding:

Vector group:	Z
Phase shift:	0^o (this winding is taken as the reference winding)
Rated voltage:	22kV
Rated power:	2.6MVA

The base current is calculated:

$$I_{b\_W1}=\frac{S_b}{\sqrt{3}\times U_{b\_W1}}=\frac{2.6\text{MVA}}{\sqrt{3}\times 22\text{kV}}=68.2\text{A}$$

The zigzag connected winding is not earthed so the subtraction of the zero sequence current is not required.

$$MX_{W1} = M(0°) = \begin{bmatrix} 1 & 0 & 0 \\ 0 & 1 & 0 \\ 0 & 0 & 1 \end{bmatrix}$$

Second winding LV1-Y:

Vector group: y
Phase shift : -7.5° (the second winding no-load voltage leads the first winding no-load voltage. To get the two windings correlated the second winding voltage has to be rotated clockwise by 7.5°)
Rated voltage: 705V
Rated power: 650kVA

The base current is calculated:

$$I_{b\_W2} = \frac{S_b}{\sqrt{3} \times U_{b\_W2}} = \frac{2.6MVA}{\sqrt{3} \times 705V} = 2129A$$

Because this winding star point is not accessible the subtraction of the zero sequence current is not required.

$$MX_{W2} = M(-7.5^o) = \begin{bmatrix} 0.9943 & 0.0782 & -0.0725 \\ -0.0725 & 0.9943 & 0.0782 \\ 0.0782 & -0.0725 & 0.9943 \end{bmatrix}$$

Third winding LV1-D:

Vector group: d
Phase shift : -37.5° (the third winding no-load voltage leads the first winding no-load voltage. To get the two windings correlated the third winding voltage has to be rotated clockwise by 37.5°)
Rated voltage: 705V
Rated power: 650kVA

The base current is calculated:

$$I_{b\_W3}=\frac{S_b}{\sqrt{3}\times U_{b\_W3}}=\frac{2.6MVA}{\sqrt{3}\times 705V}=2129A$$

Because this winding is delta connected the M matrix shall be used.

$$MX_{W3}=M(-37.5^o)=\begin{bmatrix} 0.8622 & 0.4204 & -0.2826 \\ -0.2826 & 0.8622 & 0.4204 \\ 0.4204 & -0.2826 & 0.8622 \end{bmatrix}$$

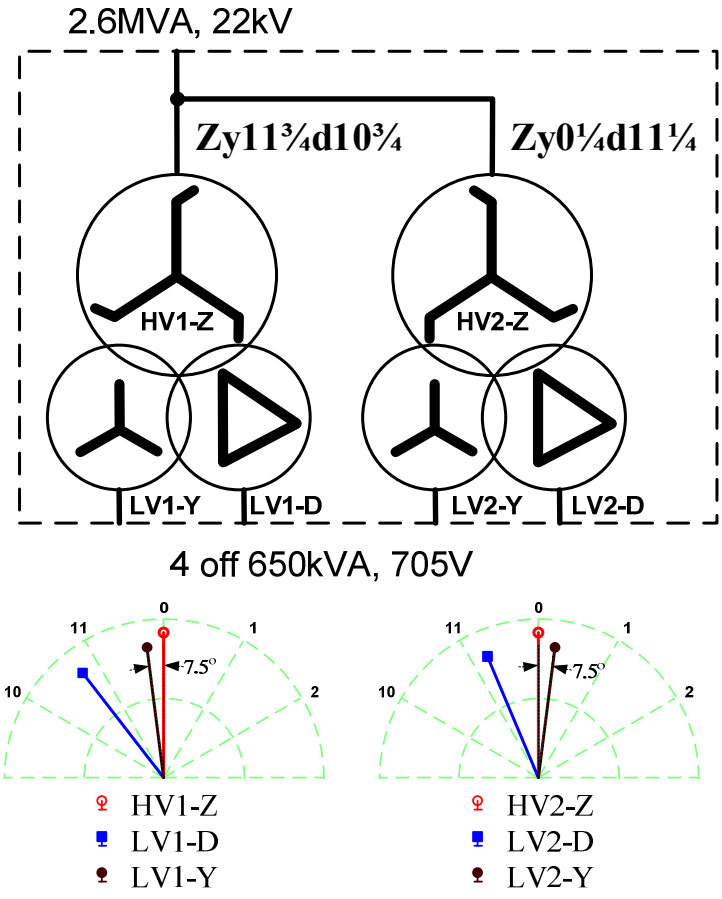

Figure 28: The 24-pulse converter transformer design.

Fourth winding LV2-Y:

Vector group: y
Phase shift: 7.5° (the fourth winding no-load voltage lags the first winding no-load voltage. To get the two windings correlated the fourth winding voltage has to be rotated anticlockwise by 7.5°)
Rated voltage: 705V
Rated power: 650kVA

The base current is calculated:

$$I_{b\_W4}=\frac{S_b}{\sqrt{3}\times U_{b\_W4}}=\frac{2.6\text{MVA}}{\sqrt{3}\times 705\text{V}}=2129\text{A}$$

Because this winding star point is not accessible the subtraction of the zero sequence current is not required.

$$MX_{W4}=M(7.5^o)=\begin{bmatrix} 0.9943 & -0.0725 & 0.0782 \\ 0.0782 & 0.9943 & -0.0725 \\ -0.0725 & 0.0782 & 0.9943 \end{bmatrix}$$

Fifth winding LV2-D:

Vector group: d
Phase shift : -22.5° (the fifth winding no-load voltage leads the first winding no-load voltage. To get the two windings correlated the fifth winding voltage has to be rotated clockwise by 22.5°)
Rated voltage: 705V
Rated power: 650kVA

The base current is calculated:

$$I_{b\_W5}=\frac{S_b}{\sqrt{3}\times U_{b\_W5}}=\frac{2.6\text{MVA}}{\sqrt{3}\times 705\text{V}}=2129\text{A}$$

Because this winding is delta connected the M matrix shall be used.

$$MX_{W5} = M(-22.5^o) = \begin{bmatrix} 0.9493 & 0.2463 & -0.1956 \\ -0.1956 & 0.9493 & 0.2463 \\ 0.2463 & -0.1956 & 0.9493 \end{bmatrix}$$

Once all these base currents and MX matrices are determined the overall equation to calculate differential currents can be written in accordance with equation (4.30).

5.6 Dual-core, Asymmetric Design of PST

In this example the application of the transformer differential protection method will be illustrated for an actual 1630MVA, 400kV, 50Hz, +18^o PST of asymmetric, two-core design. This type of PST is also known as the Quad Booster. For such an asymmetric PST design, the base current and the phase angle shift are functions of OLTC position. All necessary information for application of the method can be obtained directly from the PST rating plate. A relevant part of the PST rating plate is shown in Figure 29.

The first column in Figure 29 represents the available OLTC positions, in this case 33. From column three it is obvious that the base current for PST source side is constant for all positions and has a value of 2353A. Column five in Figure 29 gives the base current variation for the PST load side. Finally the fourteenth column in Figure 29 shows how the no-load phase angle shift varies across the PST for different OLTC positions.
Note that the phase angle shift on the PST rating plate is given as a positive value when the load side no-load voltage leads the source side no-load voltage [35] (i.e. advanced mode of operation). Therefore if the phase shift from Figure 29 is associated with the load side (i.e. source side taken as reference side with zero degree phase shift) the angle values from the rating plate must be taken with the minus sign.
This particular PST has a five-limb core construction for both internal transformers (i.e. serial and excitation transformer). Therefore the zero sequence current will be properly transferred across the PST and M(Θ) matrices shall be used on both PST sides.

Terminal	Source S8, S12, S4		Load L8, L12, L4		Series winding S8, S12, S4 L8, L12, L4		Booster winding A25,A26,B25,B26 C25,C26		Exciter winding S8, S12, S4 E0		Regulation winding A4, B4, C4 F0		Phase angle at no load
Pos.	Voltage V	Current A	Voltage V	Current A	Voltage V	Current A	Voltage V	Current A	Voltage V	Current A	Voltage V	Current A	advanced
33	400000	2353	420509	2238	74895	2238	121245	1382	400000	725.8	121245	2394	18.0°
32	400000	2353	419276	2245	72555	2245	117456	1386	400000	705.2	117456	2401	17.4°
31	400000	2353	418079	2251	70214	2251	113667	1390	400000	684.4	113667	2408	16.9°
30	400000	2353	416918	2257	67874	2257	109878	1394	400000	663.4	109878	2415	16.4°
29	400000	2353	415793	2263	65533	2263	106089	1398	400000	642.3	106089	2422	15.8°
28	400000	2353	414705	2269	63193	2269	102300	1402	400000	620.9	102300	2428	15.3°
27	400000	2353	413653	2275	60852	2275	98512	1405	400000	599.5	98512	2434	14.8°
26	400000	2353	412639	2281	58512	2281	94723	1409	400000	577.8	94723	2440	14.2°
25	400000	2353	411662	2286	56171	2286	90934	1412	400000	556.0	90934	2446	13.7°
24	400000	2353	410723	2291	53831	2291	87145	1415	400000	534.1	87145	2451	13.1°
23	400000	2353	409822	2296	51490	2296	83356	1418	400000	512.0	83356	2457	12.6°
22	400000	2353	408959	2301	49150	2301	79567	1421	400000	489.7	79567	2462	12.0°
21	400000	2353	408134	2306	46809	2306	75778	1424	400000	467.4	75778	2467	11.5°
20	400000	2353	407348	2310	44469	2310	71989	1427	400000	444.9	71989	2472	10.9°
19	400000	2353	406601	2315	42128	2315	68200	1430	400000	422.2	68200	2476	10.3°
18	400000	2353	405893	2319	39788	2319	64411	1432	400000	399.5	64411	2481	9.8°
17C	400000	2353	405225	2322	37448	2322	60623	1435	400000	376.6	60623	2485	9.2°
17B	400000	2353	405225	2322	37448	2322	60623	1435	400000	376.6	60623	2485	9.2°
17A	400000	2353	405225	2322	37448	2322	60623	1435	400000	376.6	60623	2485	9.2°
16	400000	2353	404595	2326	35107	2326	56834	1437	400000	353.6	56834	2489	8.6°
15	400000	2353	404006	2329	32767	2329	53045	1439	400000	330.5	53045	2492	8.1°
14	400000	2353	403457	2333	30426	2333	49256	1441	400000	307.3	49256	2496	7.5°
13	400000	2353	402947	2335	28086	2335	45467	1443	400000	284.0	45467	2499	6.9°
12	400000	2353	402478	2338	25745	2338	41678	1444	400000	260.7	41678	2502	6.4°
11	400000	2353	402049	2341	23405	2341	37889	1446	400000	237.2	37889	2504	5.8°
10	400000	2353	401660	2343	21064	2343	34100	1447	400000	213.7	34100	2507	5.2°
9	400000	2353	401313	2345	18724	2345	30311	1449	400000	190.1	30311	2509	4.6°
8	400000	2353	401005	2347	16383	2347	26522	1450	400000	166.5	26522	2511	4.1°
7	400000	2353	400739	2348	14043	2348	22733	1451	400000	142.8	22733	2513	3.5°
6	400000	2353	400513	2350	11702	2350	18945	1451	400000	119.1	18945	2514	2.9°
5	400000	2353	400329	2351	9362	2351	15156	1452	400000	95.3	15156	2515	2.3°
4	400000	2353	400185	2352	7021	2352	11367	1453	400000	71.5	11367	2516	1.7°
3	400000	2353	400082	2352	4681	2352	7578	1453	400000	47.7	7578	2517	1.2°
2	400000	2353	400021	2353	2340	2353	3789	1453	400000	23.8	3789	2517	0.6°
1	400000	2353	400000	2353	0	2353	0	1453	400000	0	0	2517	0°

Auxiliary winding	Voltage
	15000 V

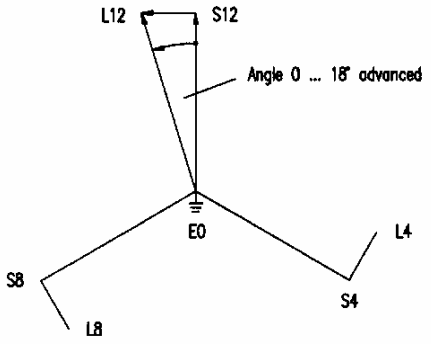

Figure 29: Part of rating plate for dual-core, asymmetric PST design.

Thus, for every OLTC position, the appropriate equation for differential current calculation can now be written. The equation for OLTC position 30 will be given here:

$$\begin{bmatrix} Id\_L1 \\ Id\_L2 \\ Id\_L3 \end{bmatrix} = \frac{1}{2353} \cdot M(0°) \cdot \begin{bmatrix} I_{L1\_S} \\ I_{L2\_S} \\ I_{L3\_S} \end{bmatrix} + \frac{1}{2257} \cdot M(-16.4°) \cdot \begin{bmatrix} I_{L1\_L} \\ I_{L2\_L} \\ I_{L3\_L} \end{bmatrix} \tag{5.1}$$

In a similar way this matrix equation can be written for any OLTC position if appropriate values from Figure 29 are given for the base current and the phase angle shift on the load side of the PST.

5.7 Single-core, Symmetric Design of PST

In this example the application of the transformer differential protection method will be illustrated for an actual 450MVA, 138kV, 60Hz, ±58^o PST of symmetric, single-core design. For symmetric PST design, only the phase angle shift is a function of the OLTC position. All necessary information for the application of the method can be obtained directly from the PST rating plate. A relevant part of the PST rating plate is shown in Figure 30.
The base currents for both sides have the same and constant value regardless the actual OLTC position. This value can be calculated by using the following equation:

$$I_b = \frac{S_b}{\sqrt{3} \times U_b} = \frac{450\text{MVA}}{\sqrt{3} \times 138\text{kV}} = 1882.6\text{A} \tag{5.2}$$

The fourth column in Figure 30 shows how the no-load phase angle shift varies across the PST for different OLTC positions. Note that the no-load phase angle shift shall be used for differential protection phase angle compensation and not the phase angle shift under load conditions which is given in column five. The no-load phase angle shift on the PST rating plate is given with positive values when the load side no-load voltage leads the source side no-load voltage [35] (i.e. advanced mode of operation). Therefore if the phase shift from Figure 30 is associated with the load side (i.e. source side taken as reference side with zero degree phase shift) the

angle values from the rating plate must be taken with the minus sign for advanced mode of operation.

Pos.	Voltage [kV]		Phase angle	Phase angle	
	Source	Load	Load leads Source (No load)	Load leads Source (Full load)	
33			58.0°	50.3°	
32			54.9°	47.6°	
31			51.7°	44.9°	
30			48.5°	42.1°	
29			45.1°	39.2°	
28			41.7°	36.1°	
27			38.2°	33.0°	ADVANCE
26			34.6°	29.7°	
25			31.0°	26.4°	
24			27.3°	22.9°	
23			23.5°	19.4°	
22			19.7°	15.7°	
21			15.8°	12.0°	
20			11.9°	8.3°	
19			7.9°	4.4°	
18			4.0°	0.5°	
17A			0°	3.4°	
17	138.0	138.0	0°	3.4°	
17B			0°	3.4°	
16			4.0°	7.4°	
15			7.9°	11.4°	
14			11.9°	15.5°	
13			15.8°	19.5°	
12			19.7°	23.6°	
11			23.5°	27.6°	
10			27.3°	31.6°	RETARD
9			31.0°	35.6°	
8			34.6°	39.6°	
7			38.2°	43.5°	
6			41.7°	47.3°	
5			45.1°	51.1°	
4			48.5°	54.9°	
3			51.7°	58.6°	
2			54.9°	62.2°	
1			58.0°	65.7°	

Figure 30: Part of rating plate for single-core, symmetric PST design.

This particular PST has no internal grounding points, thus the zero sequence current will be properly transferred across the PST, and $M(\Theta)$ matrices shall be used on both PST sides.

For every OLTC position the appropriate equation for differential current calculations can now be written. The equation for the OLTC position 8 is presented here:

$$\begin{bmatrix} Id\_L1 \\ Id\_L2 \\ Id\_L3 \end{bmatrix} = \frac{1}{1883} \cdot M(0°) \cdot \begin{bmatrix} I_{L1\_S} \\ I_{L2\_S} \\ I_{L3\_S} \end{bmatrix} + \frac{1}{1883} \cdot M(34.6°) \cdot \begin{bmatrix} I_{L1\_L} \\ I_{L2\_L} \\ I_{L3\_L} \end{bmatrix} \tag{5.3}$$

In a similar way this matrix equation can be written for any OLTC position if appropriate angle values from Figure 30 are given for the phase angle shift on the load side of the PST.

5.8 Combined Auto-transformer / PST in Croatia

In the Croatian Power network a special type of power transformer, which has two combined operating modes, is installed in the Žerjavinec substation. This transformer can be used as either a conventional 400MVA, 400/220/(10.5)kV, YNauto(d5) auto-transformer with an on-load tap-changer in the neutral point or as a phase-shifting transformer connecting 400kV and 220kV networks. The power transformer has a tertiary, unloaded delta winding. The relevant part of the rating plate in auto-transformer operating mode is given in Table 13.

In the auto-transformer operating mode no phase shift angle is introduced between the 400kV and 220kV no-load voltages. Thus, only the compensation for current magnitude variations caused by the OLTC movement shall be preformed. All necessary information for application of the new differential protection method can be obtained directly from the rating plate.

The first column in Table 13 represents the available OLTC positions, in this case 25. Column three defines the base current for the transformer 400kV side. The 220kV side base current is constant for all positions and has a fixed value of 999.7A. Due to the existence of a tertiary delta winding the zero sequence currents must be eliminated from both sides, thus M0(0^o) matrices shall be used on both power transformer sides. The equation for auto-transformer mode of operation for OLTC position 19 is presented here:

$$\begin{bmatrix} Id\_L1 \\ Id\_L2 \\ Id\_L3 \end{bmatrix} = \frac{1}{607.8} \cdot M0(0°) \cdot \begin{bmatrix} I_{L1\_400} \\ I_{L2\_400} \\ I_{L3\_400} \end{bmatrix} + \frac{1}{999.7} \cdot M0(0°) \cdot \begin{bmatrix} I_{L1\_220} \\ I_{L2\_220} \\ I_{L3\_220} \end{bmatrix} \quad (5.4)$$

Table 13: Rating plate data in auto-transformer operating mode

OLTC Position	400kV Side		220kV Side		10.5kV Side	
	U[V]	I[A]	U[V]	I[A]	U[V]	I[A]
1	462 000	499.9			14 310	5 244.1
2	455 100	507.4			13 890	5 404.9
3	448 700	514.8			13 490	5 565.6
4	442 500	521.9			13 110	5 726.3
5	436 800	528.8			12 750	5 887.1
6	431 300	535.5			12 410	6 047.8
7	426 100	542.0			12 090	6 208.5
8	421 200	548.3			11 780	6 369.3
9	416 500	554.5			11 490	6 530.0
10	412 100	560.5			11 220	6 690.7
11	407 800	566.3			10 950	6 851.4
12	403 900	571.8			10 700	7 012.3
13a	400 000	577.4			10 460	7 173.1
13b	400 000	577.4	231 000	999.7	10 460	7 173.1
13c	400 000	577.4			10 460	7 173.1
14	396 300	582.8			10 230	7 333.8
15	392 800	588.0			10 010	7 494.5
16	389 400	593.1			9 800	7 655.3
17	386 100	598.1			9 600	7 816.0
18	383 000	603.0			9 410	7 976.7
19	380 000	607.8			9 220	8 137.5
20	377 100	612.4			9 040	8 298.2
21	374 300	617.0			8 870	8 458.9
22	371 600	621.4			8 710	8 619.6
23	369 100	625.7			8 550	8 780.4
24	366 600	630.0			8 390	8 941.1
25	364 200	634.1			8 250	9 101.8

In this particular installation the existing Main-1 differential relay is using the traditional approach for differential current calculation, where y/d connected interposing CTs are used on star-connected power transformer

windings. Thus, this relay is calculating differential currents for OLTC position 19 as given in the following equation:

$$\begin{bmatrix} Id\_L1 \\ Id\_L2 \\ Id\_L3 \end{bmatrix} = \frac{1}{607.8} \cdot M0(-150°) \cdot \begin{bmatrix} I_{L1\_400} \\ I_{L2\_400} \\ I_{L3\_400} \end{bmatrix} + \frac{1}{999.7} \cdot M0(-150°) \cdot \begin{bmatrix} I_{L1\_220} \\ I_{L2\_220} \\ I_{L3\_220} \end{bmatrix} \tag{5.5}$$

Note that for such a solution simply the third winding (i.e. tertiary delta winding) is taken as reference winding for phase angle compensation. This is another possible solution to calculate differential currents for this auto-transformer, but with some drawbacks as explained in Section 5.2.

In the PST operating mode the phase angle shift is introduced between the no-load voltages from the two sides, as shown in Figure 10. Column one in Table 14 represents the available OLTC positions, in this case 25. Column three defines the base current for the transformer 400kV side. The 220kV side base current is constant for all positions and has a fixed value of 999.7A. Finally column eight in Table 14 shows how the no-load phase angle shift varies across the PST for different OLTC positions.

Note that the phase angle shift on the PST rating plate is given with a positive value when the 220kV side no-load voltage leads the 400kV side no-load voltage [35] (i.e. advanced mode of operation). Therefore if the phase shift from Table 14 is associated with the 220kV side (i.e. the 400kV side taken as reference side with zero degree phase shift) the angle values from the rating plate must be taken with a minus sign. Due to the existence of a tertiary delta winding the zero sequence currents must be eliminated, thus M0 matrices shall be used on both PST sides. The equation for the PST mode of operation for OLTC position 19 is presented here:

$$\begin{bmatrix} Id\_L1 \\ Id\_L2 \\ Id\_L3 \end{bmatrix} = \frac{1}{563.3} \cdot M0(0°) \cdot \begin{bmatrix} I_{L1\_400} \\ I_{L2\_400} \\ I_{L3\_400} \end{bmatrix} + \frac{1}{999.7} \cdot M0(-3.11°) \cdot \begin{bmatrix} I_{L1\_220} \\ I_{L2\_220} \\ I_{L3\_220} \end{bmatrix} \tag{5.6}$$

Even in the PST operating mode the traditional approach for transformer differential current calculation can be used, where y/d connected interposing CTs are used on star-connected power transformer windings.

In that case the relay can calculate the differential currents for OLTC position 19 as given in the following equation:

$$\begin{bmatrix} Id\_L1 \\ Id\_L2 \\ Id\_L3 \end{bmatrix} = \frac{1}{563.3} \cdot M0(-150°) \cdot \begin{bmatrix} I_{L1\_400} \\ I_{L2\_400} \\ I_{L3\_400} \end{bmatrix} + \frac{1}{999.7} \cdot M0(-153.11°) \cdot \begin{bmatrix} I_{L1\_220} \\ I_{L2\_220} \\ I_{L3\_220} \end{bmatrix} \tag{5.7}$$

Table 14: Rating plate data in PST operating mode

OLTC Position	400kV Side		220kV Side		10.5kV Side		Angle
	U[V]	I[A]	U[V]	I[A]	U[V]	I[A]	Θ[deg]
1	375 100	615.7			9 030	8 307.2	-4.48
2	377 200	612.2			9 150	8 201.4	-4.19
3	379 400	608.8			9 270	8 097.3	-3.89
4	381 500	605.4			9 390	7 995.1	-3.57
5	383 600	602.2			9 510	7 895.0	-3.24
6	385 800	598.7			9 630	7 796.8	-2.89
7	387 900	595.4			9 750	7 700.6	-2.52
8	390 000	592.2			9 870	7 606.8	-2.14
9	392 000	589.1			9 990	7 515.1	-1.75
10	394 100	586.0			10 110	7 426.0	-1.33
11	396 100	583.0			10 230	7 339.0	-0.91
12	398 100	580.2			10 350	7 254.7	-0.46
13a	400 000	577.4			10 460	7 173.1	0.00
13b	400 000	577.4	231 000	999.7	10 460	7 173.1	0.00
13c	400 000	577.4			10 460	7 173.1	0.00
14	401 900	574.7			10 580	7 093.9	0.48
15	403 700	572.1			10 690	7 017.7	0.97
16	405 400	569.7			10 810	6 944.5	1.48
17	407 000	567.4			10 920	6 874.1	2.01
18	408 600	565.3			11 030	6 806.8	2.55
19	410 000	563.3			11 130	6 742.7	3.11
20	411 300	561.5			11 230	6 681.9	3.69
21	412 500	559.8			11 330	6 624.4	4.28
22	413 600	558.4			11 420	6 570.2	4.88
23	414 500	557.1			11 510	6 519.6	5.49
24	415 300	556.1			11 600	6 472.7	6.12
25	416 000	555.2			11 670	6 429.4	6.76

Chapter 6

Evaluation of the Method with Disturbance Recording Files

The new method for calculation of the differential currents has been evaluated on a number of disturbance recording (DR) files captured in the field in pre-existing PST installations.

6.1 PST in Žerjavinec Substation, Croatia

This 400MVA, 400/220kV PST has been in full commercial operation in Žerjavinec Substation since July 2004. Since then numerous disturbance records have been captured by existing numerical differential relays during external faults and normal through-load conditions. These records have been used to check the stability of the new differential protection method. The current recordings presented below were captured by a numerical differential relay with a sampling rate of twenty samples per power system cycle. More information about this PST can be found in Section 2.3 and Section 5.8.

An overview of the relevant part of the Croatian power grid and locations of the four presented external faults are shown in Figure 31.

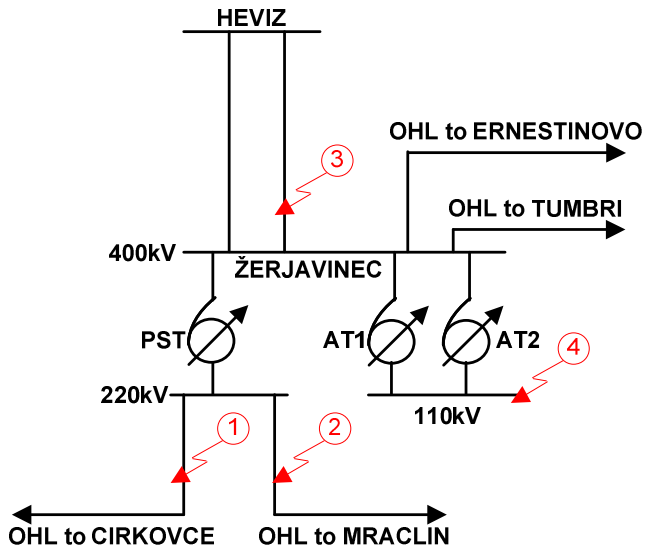

Figure 31: Location of external faults around Žerjavinec Substation.

Table 15 provides a summary of the presented DR files.

Table 15: Summary of the presented DR files

	Type of captured DR file				
	Ext. Fault #1	Ext. Fault #2	Ext. Fault #3	Ext. Fault #4	Through-Load
Type of Fault	L3-Ground	L1-Ground	L2-Ground	L2L3-Ground	NA
Fault Position	Cirkovce OHL	Mraclin OHL	Heviz 1 OHL	110kV Busbar	NA
OLTC Position	25	25	18	13	1
Θ	6,76°	6,76°	2,55°	0°	-4,48°
I_{b400}	555,2A	555,2A	565,3A	577,4A	615,7A
I_{b220}	999.7A	999.7A	999.7A	999.7A	999.7A

The recorded currents were imported into a MATLAB® (MATLAB is a trade mark registered by The MathWorks; additional information can be found at www.mathworks.com) model and the following figures show the result of the calculation with the new differential protection method.

In the following five figures, for every presented DR file from this PST installation, the following waveforms are given:

- 400kV current waveforms;
- 220kV current waveforms;
- differential currents as seen by the numerical differential relay (equation (5.4)), which compensates for the current magnitude variations but is not able to compensate for the phase angle shift variations (i.e. it can only provide the magnitude compensation for different OLTC positions);
- differential currents in accordance with the new method (i.e. equation (5.6)); and
- phase angle difference between the positive and negative sequence current components from the two PST sides.

Note that on these figures there is a significant difference between y-axis scales used on sub-figures showing the RMS values of the differential currents calculated in accordance with the new method (e.g. 0-2%) and the differential currents as seen by the existing differential relay using equation (5.4) (e.g. 0-50%).

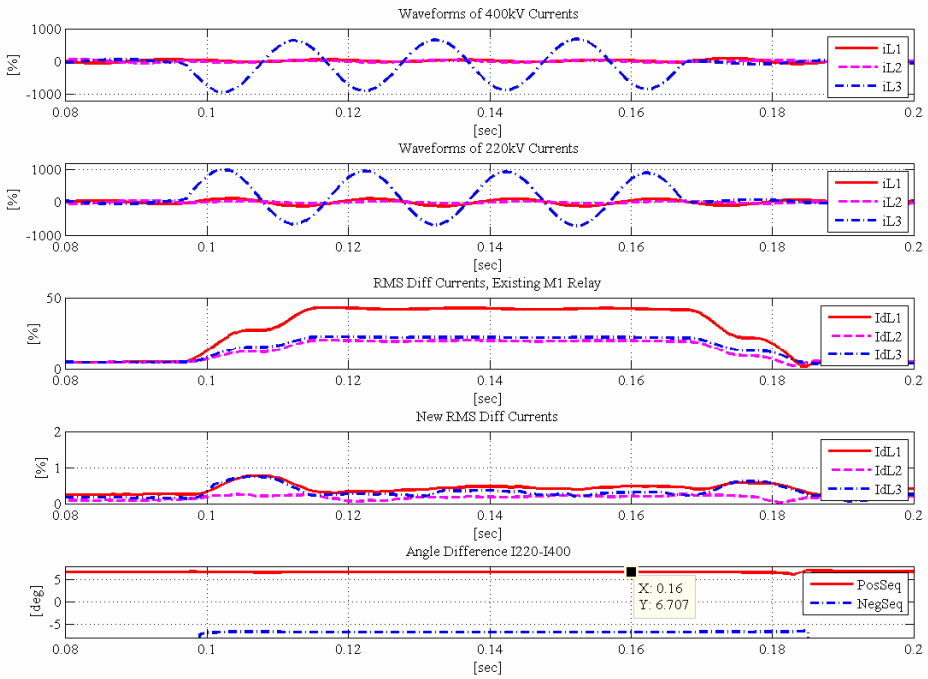

Figure 32: External Fault #1, OHL Cirkovce, OLTC is on position 25.

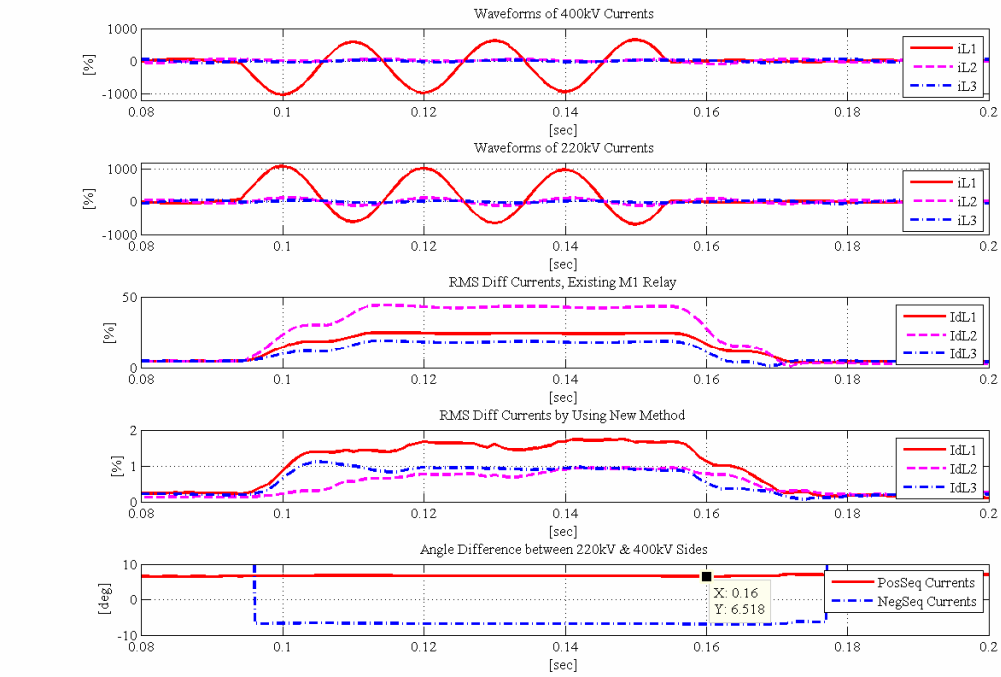

Figure 33: External Fault #2, OHL Mraclin, OLTC is on position 25.

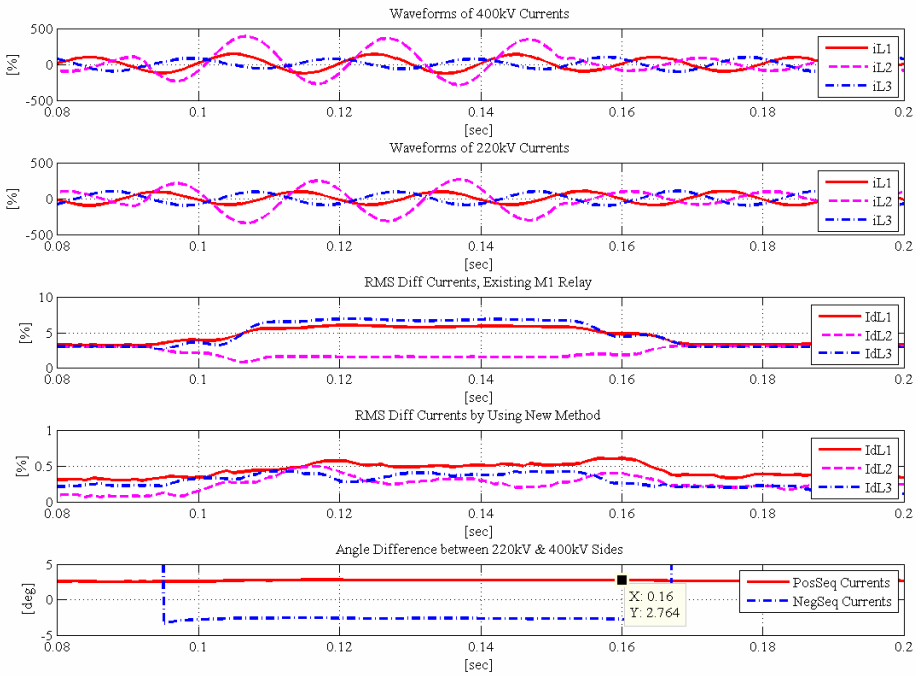

Figure 34: External Fault #3, OHL Heviz 1, OLTC is on position 18.

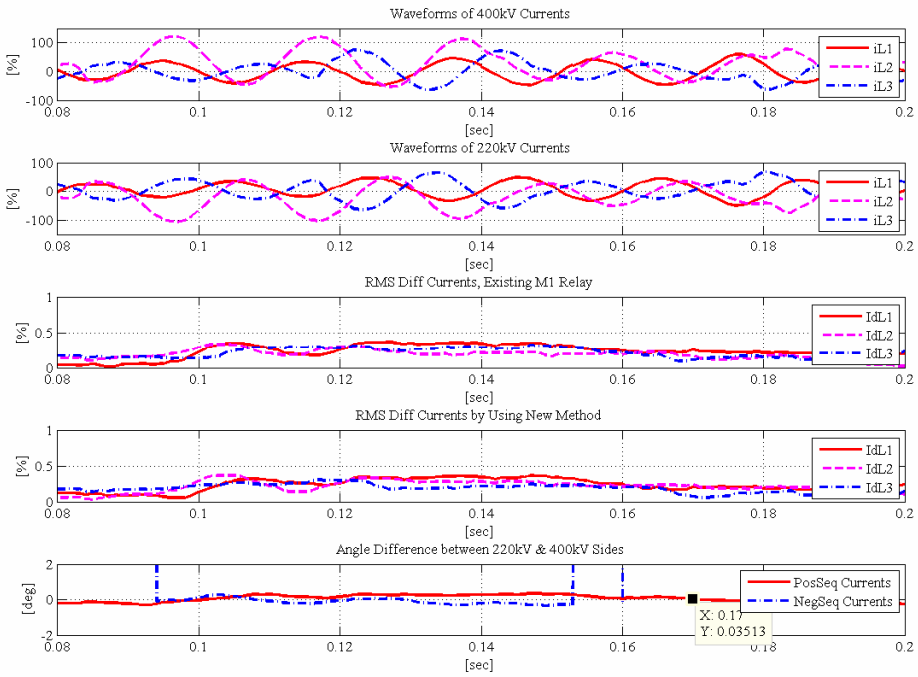

Figure 35: External Fault #4, 110kV Busbar, OLTC is on position 13.

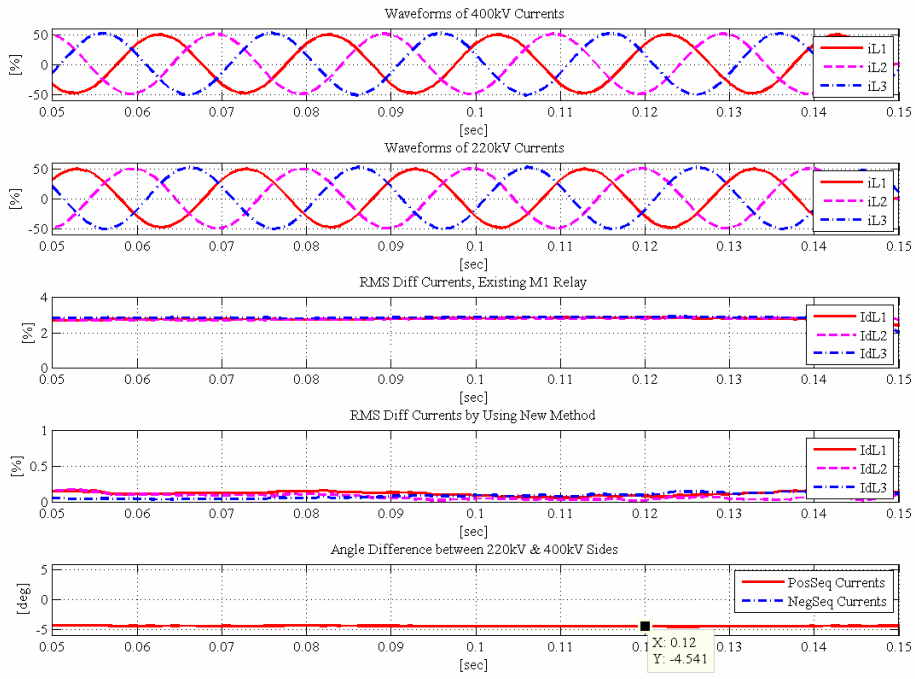

Figure 36: Normal through-load condition, OLTC is on position 1.

The DR files have also been captured at the moment of the OLTC position change in the PST operating mode. The following two figures provide information about the behaviour of the new differential protection method under such operating conditions. For both presented DR files, the following waveforms are given:

- 400kV current waveforms;
- 220kV current waveforms;
- differential currents in accordance with the new method (i.e. by using equation in accordance with (5.6)); and
- phase angle difference between the positive and negative sequence current components from the two PST sides.

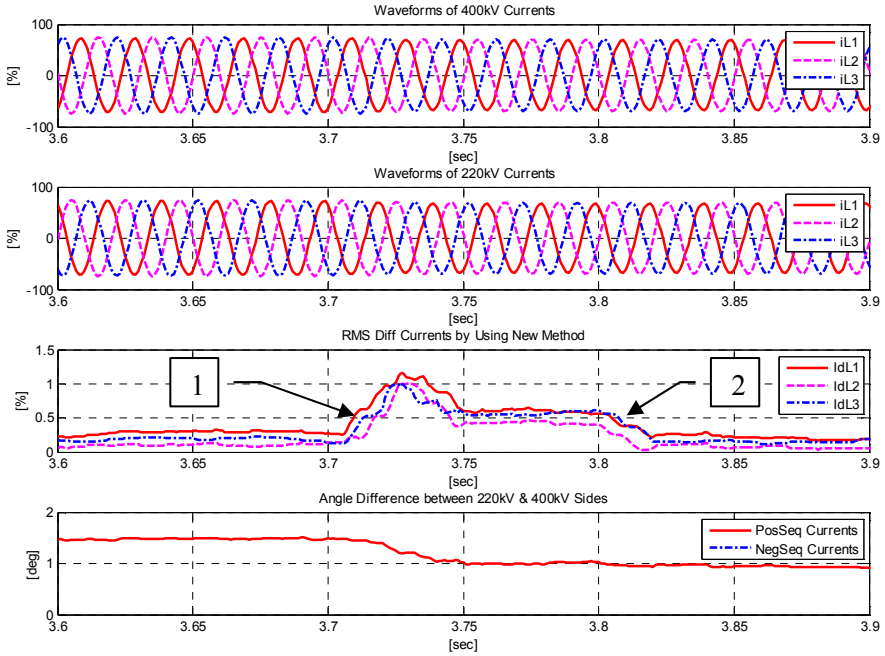

Figure 37: OLTC tapping from position 16 to position 15.

Where:

- Number 1 indicates the instant of OLTC mechanism tapping from position 16 to position 15.
- Number 2 indicates the instant when the new differential method changes internal compensation to the values which correspond to the new OLTC position 15.

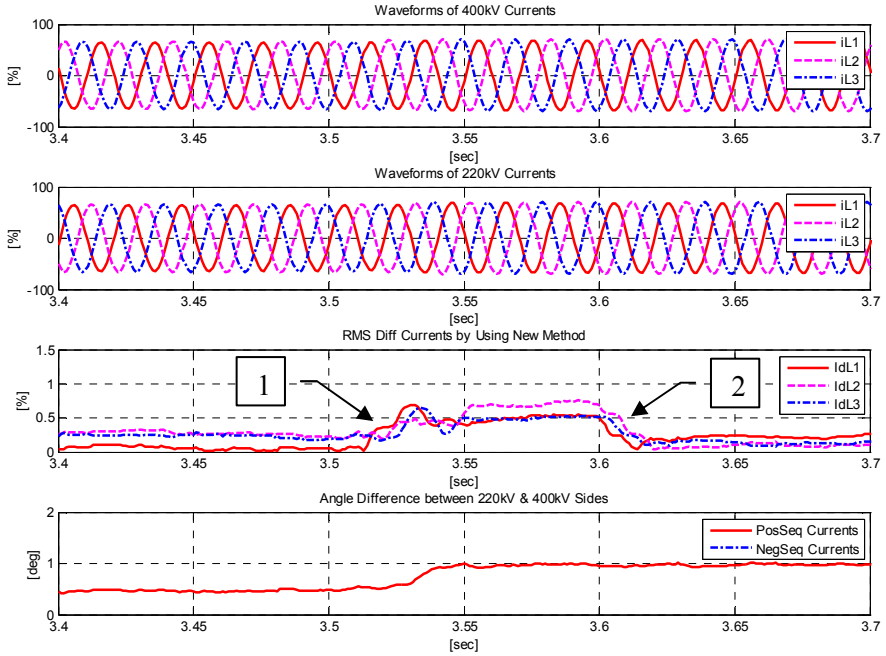

Figure 38: OLTC tapping from position 14 to position 15.

Where:

- Number 1 indicates the instant of OLTC mechanism tapping from position 14 to position 15.
- Number 2 indicates the instant when the new differential method changes internal compensation to the values which correspond to the new OLTC position 15.

From all presented DR files it can be concluded that the new differential protection method is stable for such special PST construction.

6.2 PST Installed in Europe

In this section the DR files recorded on two identical PSTs positioned at the beginning of two parallel 380kV overhead lines (OHL) in Europe are presented. The transformers are of asymmetrical type, dual-core design. The captured incident involved two simultaneous single-phase to ground faults. On OHL #1 it was a phase L2 to ground fault and on OHL #2 it was a phase L1 to ground fault. Existing protection schemes on both PSTs maloperated during this incident. The first scheme maloperated because of the Buchholz relay operation caused by the PST tank vibrations and the second scheme maloperated because of the operation of the existing differential protection relay. The rated quantities for these two identical PSTs are listed below:

- Rated power: 1630MVA;
- Rated voltages: 400/400kV;
- Frequency: 50Hz;
- Angle variation: 0º - 18º (at no-load)

More information about this PST can be found in Section 5.6. The OLTC was in position 30 when the faults occurred. Thus, from Figure 29 all necessary information about the compensation values can be extracted. The base current for this type of transformer is different on the two PST sides and for this tap position their values are I_{Base_S}= 2353A and I_{Base_L}= 2257A. The PST no-load phase angle shift was 16.4º. For the exact equation see (5.1).

The presented recordings were made by two existing numerical differential relays having sampling rates of twelve samples per power system cycle. The S- and L-side currents recorded by the relay were run in the MATLAB model and the following figures show the result of the calculation from the new differential protection method.
In the following two figures, for every presented DR file from this installation, the following waveforms are given:

- S-side and L-side current waveforms;
- instantaneous differential currents waveforms calculated in accordance with the new method;
- RMS differential currents calculated in accordance with the new method; and

- phase angle difference between the positive and negative sequence current components from the two PST sides.

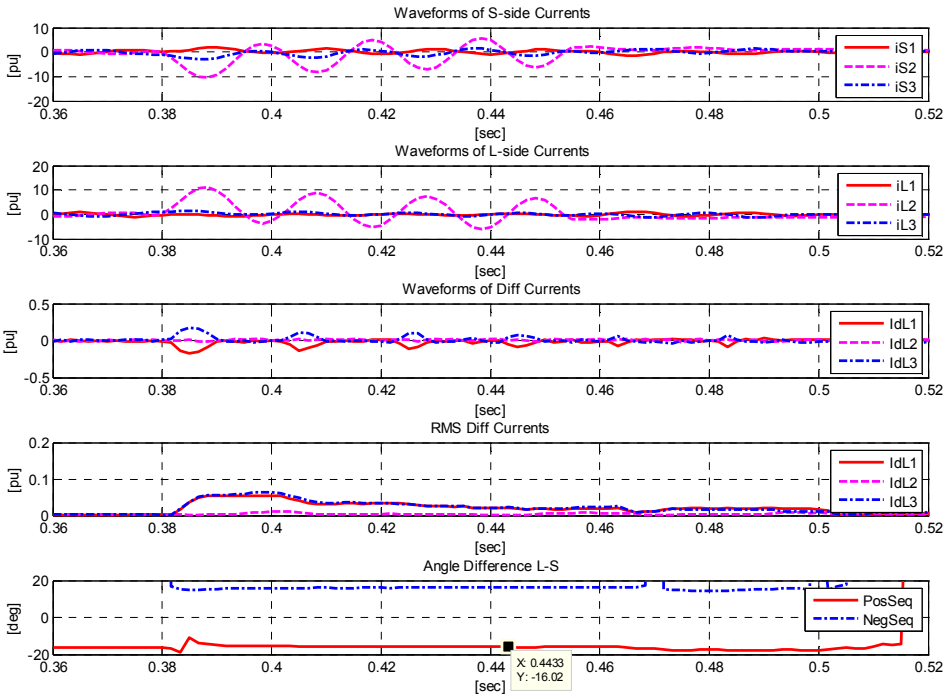

Figure 39: Evaluation of DR file for the first PST.

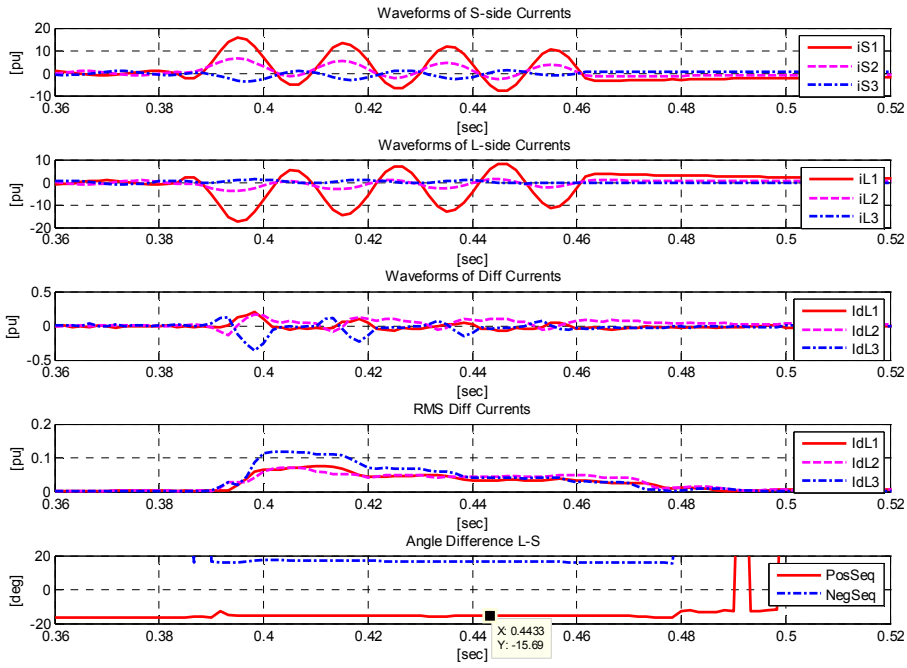

Figure 40: Evaluation of DR file for the second PST.

The two figures show that for this severe external fault the differential current amplitude, calculated by using the new method, remains within 0.15pu (15%), while the bias current is bigger than 6pu (600%). That clearly indicates that the new differential relays will remain stable during this special external fault (see Figure 12).

6.3 PST Installed in South America

In this section the differential current calculation will be made for a PST in South America during an external fault. The transformer is of symmetrical type, dual-core design. The rated quantities of the PST are listed below:

- Rated power: 400MVA;
- Rated voltages: 138/138kV;
- Frequency: 60Hz;
- Angle variation: ±21.66º (at no-load);
- Main CT ratio: 2000/1A; and
- Main CTs are connected in delta on both PST sides.

The PST has two protection schemes, as recommended by [37]. In the Main-1 protection scheme the current transformers are star connected, while in the Main-2 protection scheme the S- and L-side CTs are delta connected. The PST transformer Main-1 protection scheme is shown in Figure 41, and the Main-2 protection scheme is shown in Figure 42. Note that in both figures protection device designations in accordance with IEEE C37.2-1996 standard have been used.

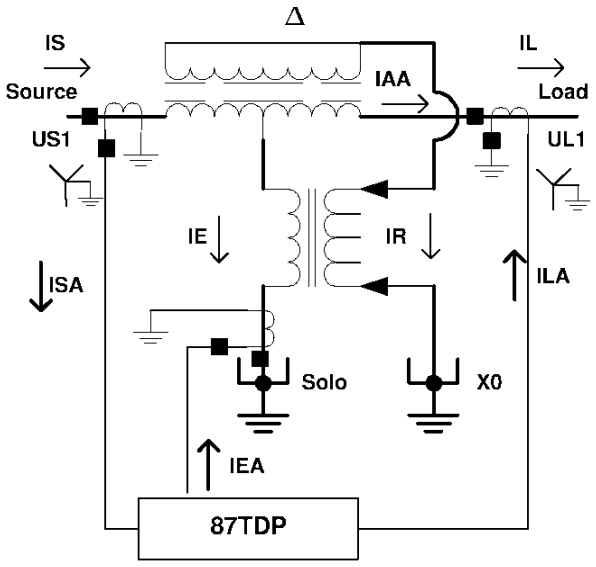

Figure 41: Main-1 protection scheme of the transformer.

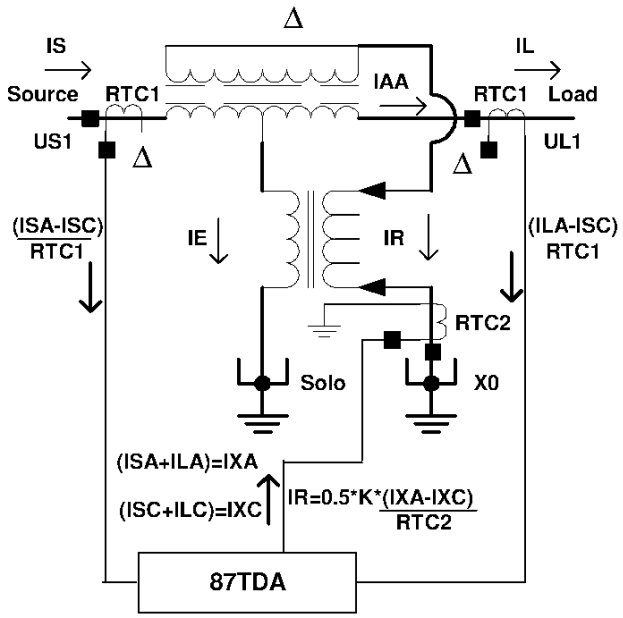

Figure 42: Main-2 protection scheme of the transformer.

The transformer is of a symmetrical type, dual-core design. The base current for this type of transformer is equal for the source and load side. The currents measured in the relay are in secondary amperes, so in the calculation of the base current the current transformer ratio must be included as well as the fact that the main CT's are delta connected. This is compensated in the algorithm of the new universal differential protection by multiplying the base secondary current by $\sqrt{3}$.

$$I_b = \frac{400\text{MVA}}{\sqrt{3}\times 138\text{kV}} \times \frac{1}{2000} \times \sqrt{3} = 1.449\text{A}$$

The main CTs are externally connected in delta on both sides of the transformer, meaning that they do not change the phase angle shift between S- and L-side CT secondary currents. The external fault occurred while the PST phase angle shift was at 5.47^{o}.

The current recording presented was made by a numerical Main 2 differential relay with twelve samples per power system cycle. The differential relay maloperated during this external fault.

The S- and L-side currents recorded by the relay were run in the MATLAB model and Figure 43 shows the result of the calculations made by the new differential protection method.

In this figure the following waveforms are given:

- S-side and L-side current waveforms;
- instantaneous differential currents waveforms calculated in accordance with the new method;
- RMS differential currents calculated in accordance with the new method; and
- phase angle difference between the positive and negative sequence current components from the two PST sides.

The figure shows that the new RMS differential currents remain within 0.025pu (2.5%), indicating that the differential relay using the new method would remain stable during this external fault.

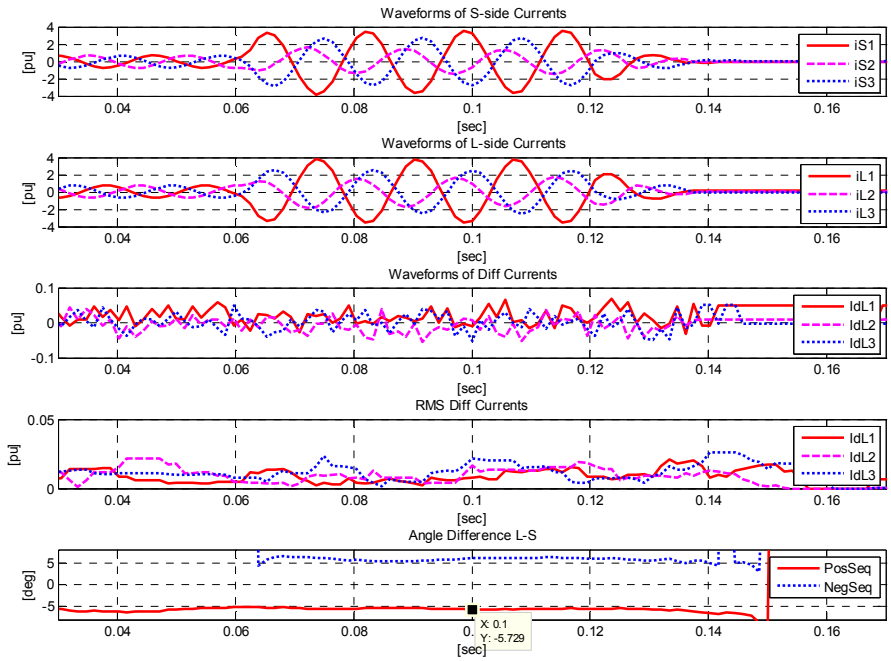

Figure 43: Evaluation of DR file from the PST installed in South America.

6.4 PST Installed in North America

In this section the differential current calculation will be made for a PST in North America during different operating conditions. The transformer is of symmetrical type, single-core design. In order to limit the through going short circuit currents one three-phase series reactor is installed within the PST tank. The ratings of the PST are listed below:

- Rated power: 450MVA;
- Rated voltages: 138/138kV;
- Frequency: 60Hz;
- Angle variation: ±58.0º (at no-load); and,
- Number of OLTC steps: 33 (i.e. ±16).

More information about this PST can be found in Section 5.7. The base current for this transformer is 1883A primary and is equal for the source and the load side. The recordings were captured by an existing PST numerical differential protection relay at a sampling rate of 20 samples per power system cycle.
In the following three figures, for every presented DR file from this PST installation, the following waveforms are given:

- S-side and L-side current waveforms;
- instantaneous differential currents waveforms calculated in accordance with the new method; and
- RMS differential currents calculated in accordance with the new method.

Energizing of the PST Together with a 138kV Cable

This PST is connected in series with a 138kV cable on the S-side. This causes the energizing currents to have special wave shapes. Note that manufacturer recommendations required that this PST is always energized with 0^o phase shift (i.e. tap position 17). The recorded S- and L-side currents were run in the MATLAB model and the results of the calculations are presented in Figure 44.
The individual phase inrush currents are obviously rich in harmonics but the calculated differential current waveforms have properties of "classical power transformer inrush currents". Thus, the traditional methods (i.e. second harmonic blocking or waveform blocking) can be used to restrain the differential protection during inrush conditions.

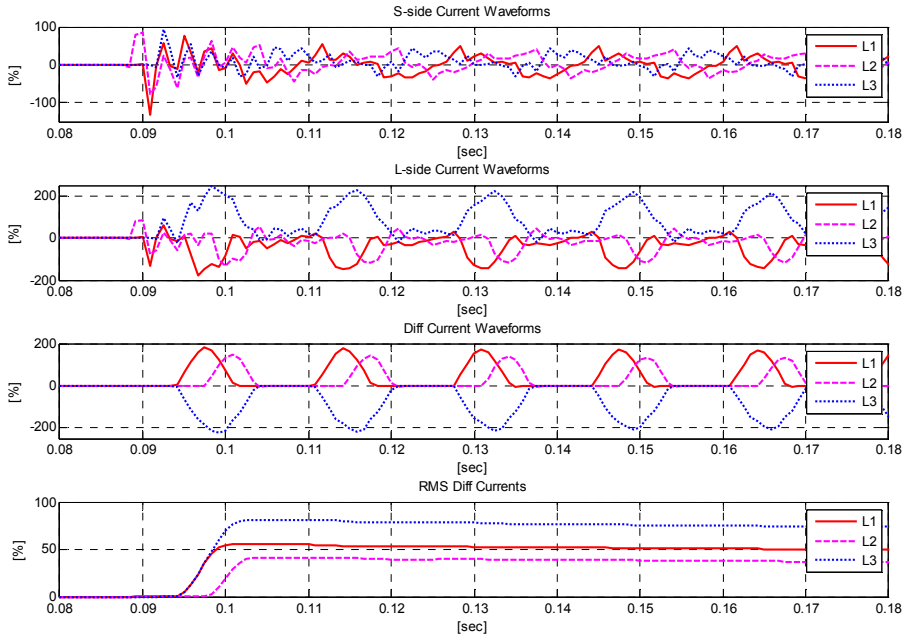

Figure 44: Energizing of the PST and a cable.

Off-rated Frequency

This PST was involved in the USA blackout on 2003-08-14. During the final stages of this blackout a recording was captured, which shows that the PST was overloaded and that the frequency of the captured current waveform was much lower than the 60Hz what is the rated power system frequency. From the captured current waveforms, by using the current zero-crossings, the frequency of the current signal can be estimated to be around 53.5Hz. Consequently it can be concluded that the frequency of the voltage signal was even lower in some parts of the surrounding network. Note that during this disturbance the OLTC was in the mid-position (i.e. 0^{o} phase shift). The recorded S- and L-side currents were run in the MATLAB model and results of the calculations are presented in Figure 45.

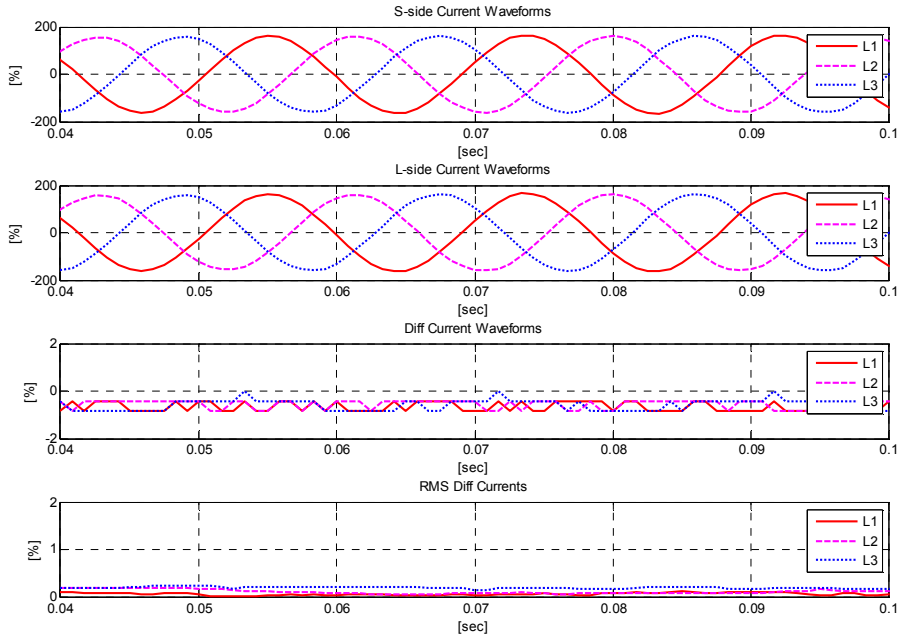

Figure 45: Off-nominal frequency through load condition.

The calculated differential current waveforms demonstrate that the new differential protection method was not influenced by the off-rated-frequency condition. It is as well interesting to note that the IEC standards typically suggest the operation range of the protection relays shall be within ±5Hz from the rated power system frequency.

Through Load Condition

Finally, the through load condition for a 4° phase angle shift (the PST in advanced operating mode) is shown in Figure 46.

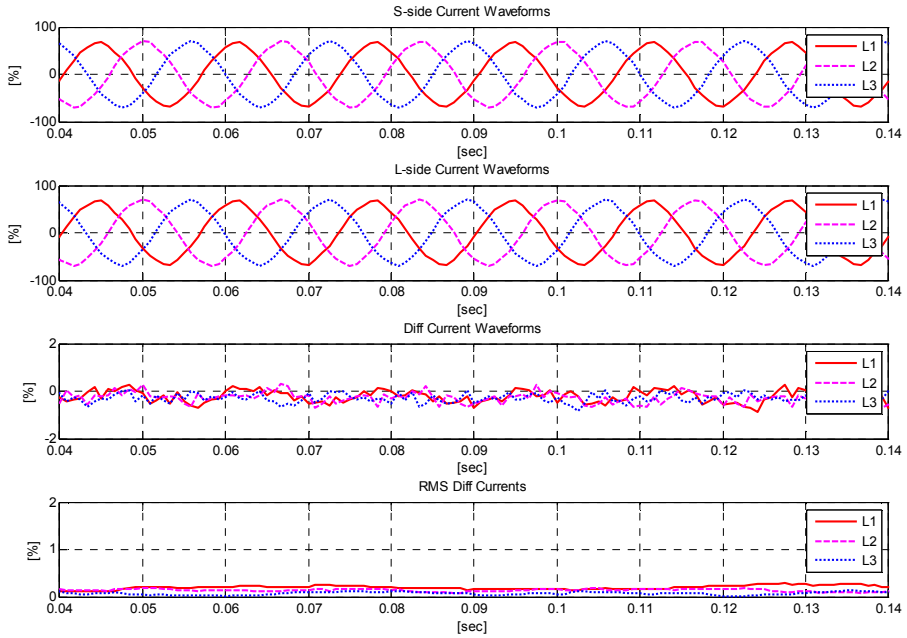

Figure 46: Through load condition for a 4° phase angle shift for the PST in advance operating mode.

The new differential protection method also performs well in this case.

Chapter 7

Evaluation of the Method with Simulation Files

Simulation of a symmetrical, dual-core PST (see Section 2.3) will be presented based on data from an actual PST installation in Europe.

7.1 Setting up the Simulation

The simulation was preformed with the Real-Time Digital Simulator, RTDS® (RTDS is a trade mark registered by RTDS Technologies; additional information can be found at www.rtds.com). A single line diagram (SLD) of the simulated network, together with the PST rated data, is shown in Figure 47. Note that a path parallel with the PST is included in the simulation model, but is not shown in Figure 47.

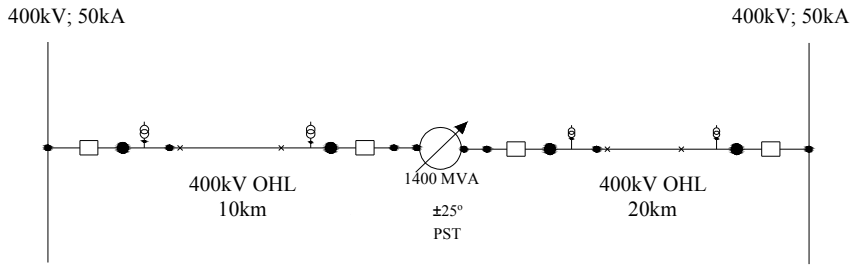

Figure 47: SLD for the simulated power system.

PST Data

The simulated PST is of symmetric type, dual-core design. Due to its size it consists of six single-phase transformers. Each single-phase transformer is located in its own tank. The tanks are interconnected with oil ducts.
The main PST data used for the simulation is shown below:

- Rated power: 1400MVA;
- Rated voltages: 400/400kV;
- Angle variation: $\pm 25^{o}$ (at no-load).

Each PST phase was simulated as two separate single-phase transformers.

The data applied for the series transformers included:

- series unit primary winding with a rated voltage of 100kV (i.e. 50kV for each of the two split windings);
- delta connected, secondary winding of the series unit with rated voltage of 138.6kV;
- rated power of one phase series transformer 609.10MVA;
- leakage reactance of the transformer set to 0.3pu; and,
- no load losses of 0.000106pu.

The data applied for the excitation transformers included:

- exciter unit primary winding with a rated voltage of 225kV and a fixed number of turns;
- exciter unit secondary winding with a rated voltage of 80kV and a variable number of turns (0% - 100%);
- rated power of one phase excitation transformer 594.7MVA;
- leakage reactance of the transformer set to 0.6pu; and,
- no load losses of 0.0093pu.

A detailed SLD of the PST is shown in Figure 49.

Overhead Line Data

The simulated PST was connected to the rest of the system via two quite short 400kV overhead lines. The line on the source side of the transformer was 10km long, and on the load side of the transformer the line was 20km long. Both of the lines can be heavily loaded up to 2100MVA in real life.

In the simulation case the lines were simulated with a T – line model. The loading of the lines in the simulation was higher, due to the fact that the transformer was simulated for overload conditions. The parameters entered for the first line are shown in Figure 48. The parameters for the second line are the same with only exclusion for the length of the line.

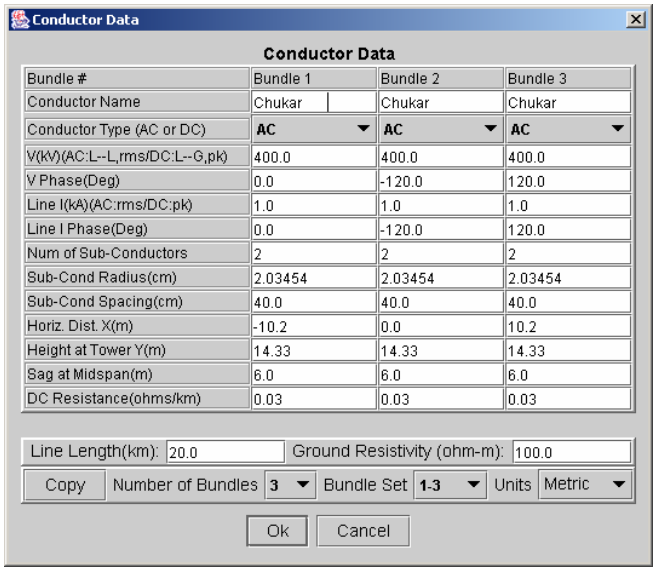

Figure 48: 400kV OHL data.

Sources and Loads

Two sources are used in the simulation; the first source feeds the first line on the source side of the PST, and the second source is located at the end of the second line on the load side of the PST. Both sources are 400kV with an initial phase shift of 0^{o}. The source impedance type was R/L, with the positive sequence impedance set to 8Ω and the zero sequence impedance set to 16Ω. Each source is connected to a bus, loaded with a resistive load of 1200Ω/phase.

Parallel Path

In order to demonstrate the influence of the phase shift of the PST a parallel path had to be introduced in the circuit connecting the two buses (i.e. in parallel with the PST and two 400kV OHLs). The parallel line is simulated with a PI section model.

7.2 Simulated Faults

Once the simulation case was built and compiled, the simulation could be started. The main goal of the simulation was to obtain current waveforms on both sides of the transformer during a fault (external or internal) for different phase shift angles between the transformer ends. The current measurement was performed on circuit breakers on both sides of the transformer. In this simulation case the current transformers were not simulated, so the influence of the CT saturation during a fault could not be obtained.

The external faults (F1 and F2) are simulated on the source and load bus. The internal faults (F3 and F4) are simulated on the series transformer as well as on the regulating (i.e. boosting) transformer. The simulated fault points are shown in Figure 49. For each fault point four different fault types are simulated: L1–L2–L3, L1–L2, L2–L3–Ground and L3–Ground. Once the currents for each fault are obtained the next step involved calculation of the differential currents. The calculations were made with the MATLAB model of the new differential current measurement technique explained in Section 4.5. The sampling rate of 400 samples per power system cycle was used in output files from the simulator.

The first group of faults was simulated for a 25^{o} no-load phase angle shift in the advanced operating mode. This is the highest phase angle shift that could be obtained for this particular PST. All above mentioned fault types in all four fault location points are simulated.

The second group of faults is simulated for a 15^{o} no-load phase angle shift in the advanced operating mode. All above mentioned fault types in all four fault location points are simulated.

The third group of faults is simulated for a 2.5^{o} no-load phase angle shift in the advanced operating mode. All above mentioned fault types in all four fault location points are simulated. For this phase shift angle it can be shown that the new differential protection may not be sensitive enough for an internal single-phase to ground fault at location F3, as described in the following section.

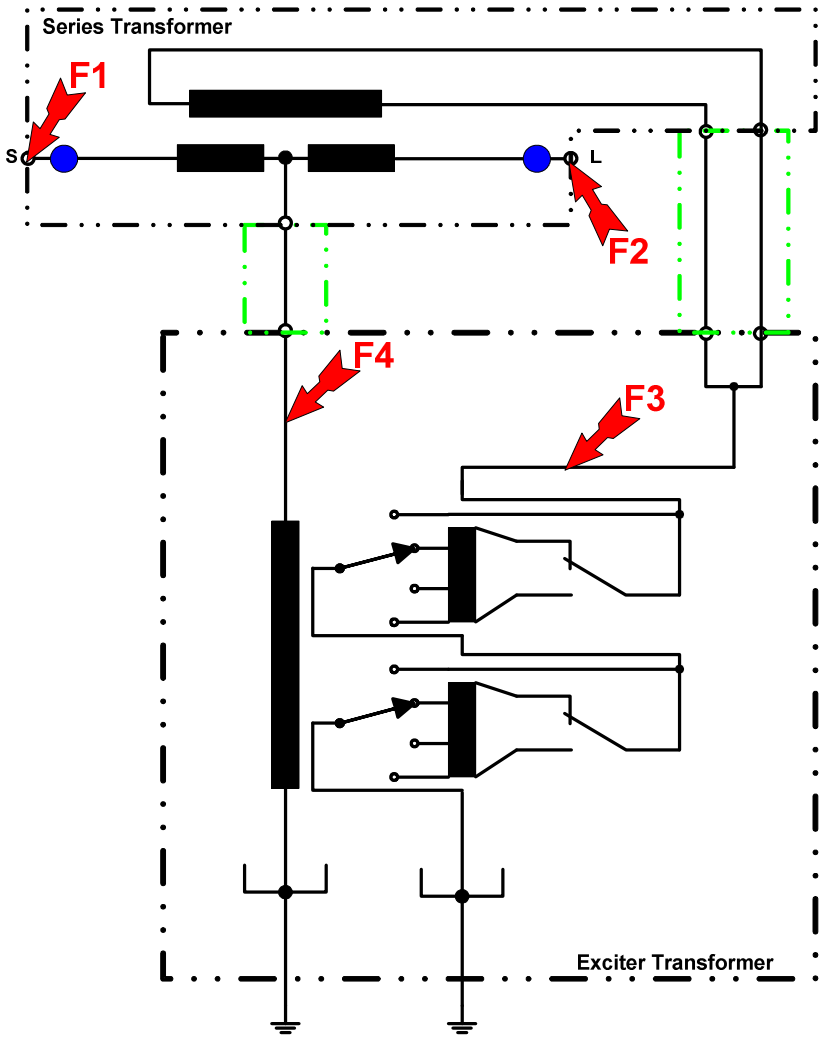

Figure 49: SLD for the simulated PST and simulated fault locations.

Selected results are presented in the following figures.

External Faults on the Source Bus (fault point F1) for a 25° Phase Shift in the Advanced Operating Mode

External L1-L2 fault at F1, Θ=25°

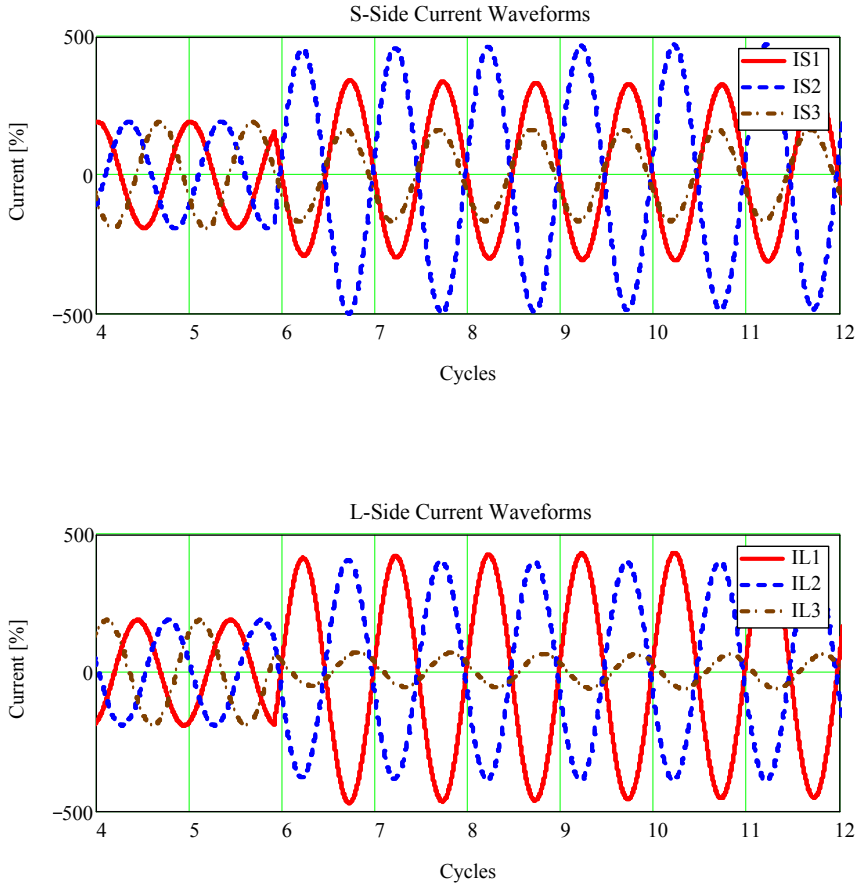

Figure 50: Individual phase currents during this ph-ph external fault

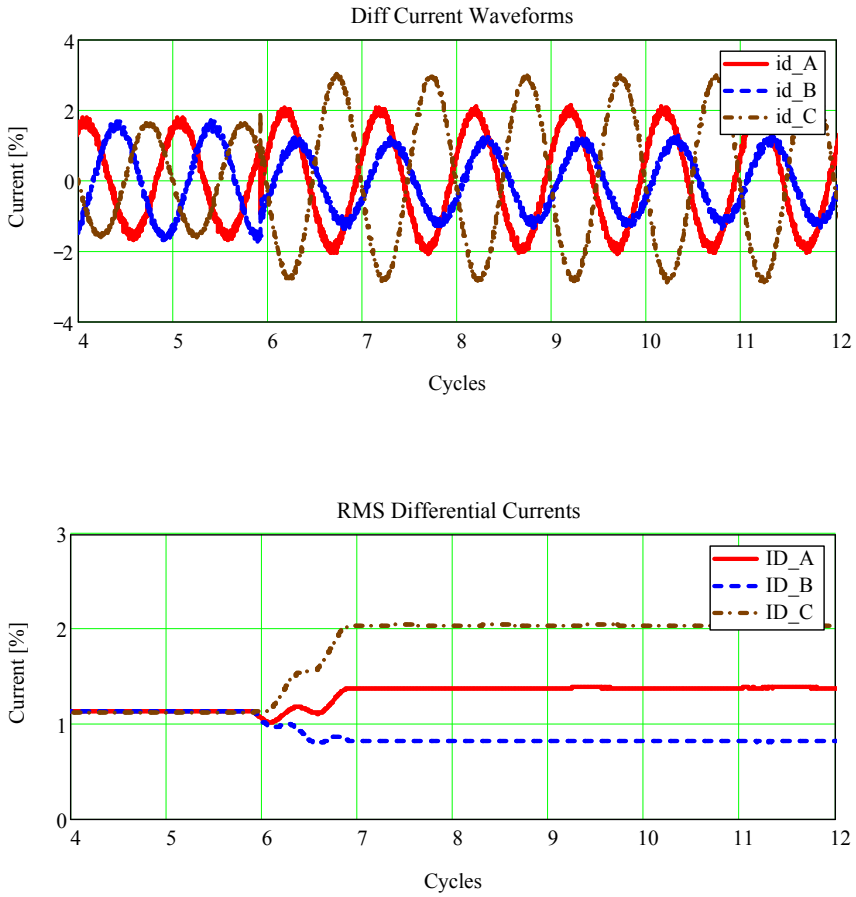

Figure 51: Differential currents during this ph-ph external fault

The above waveforms show that the RMS differential currents remain within approximately 0.02pu (2%), indicating that the differential relay using the new method would remain fully stable during this external fault.

External L1-L2-L3 fault at F1, Θ=25°

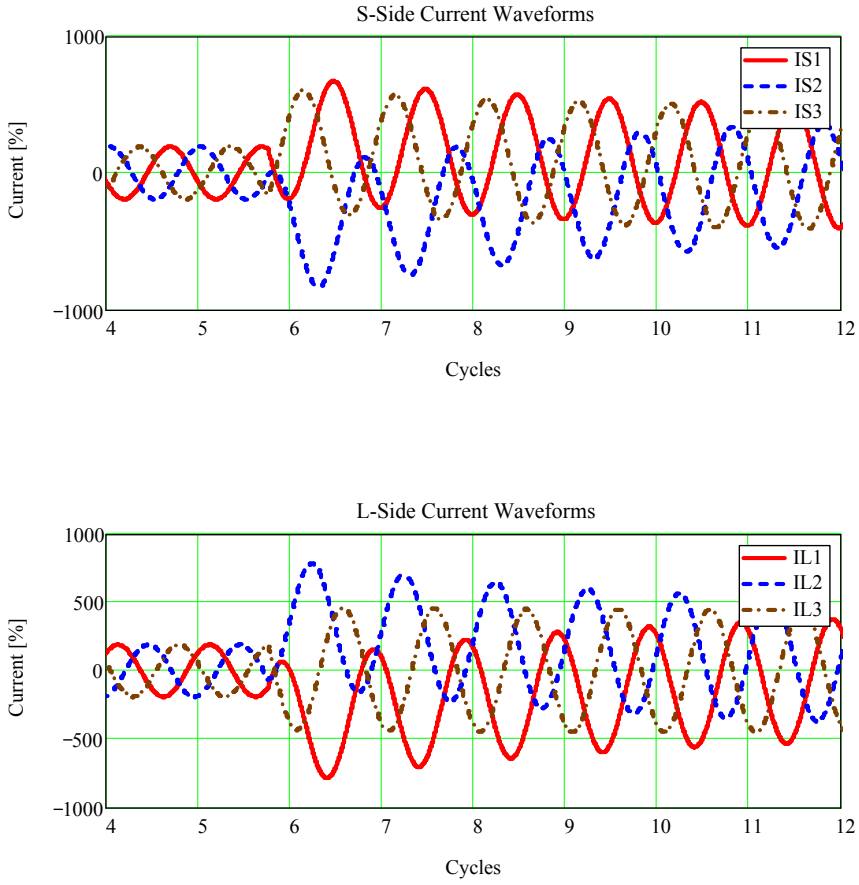

Figure 52: Individual phase currents during this external three-phase fault

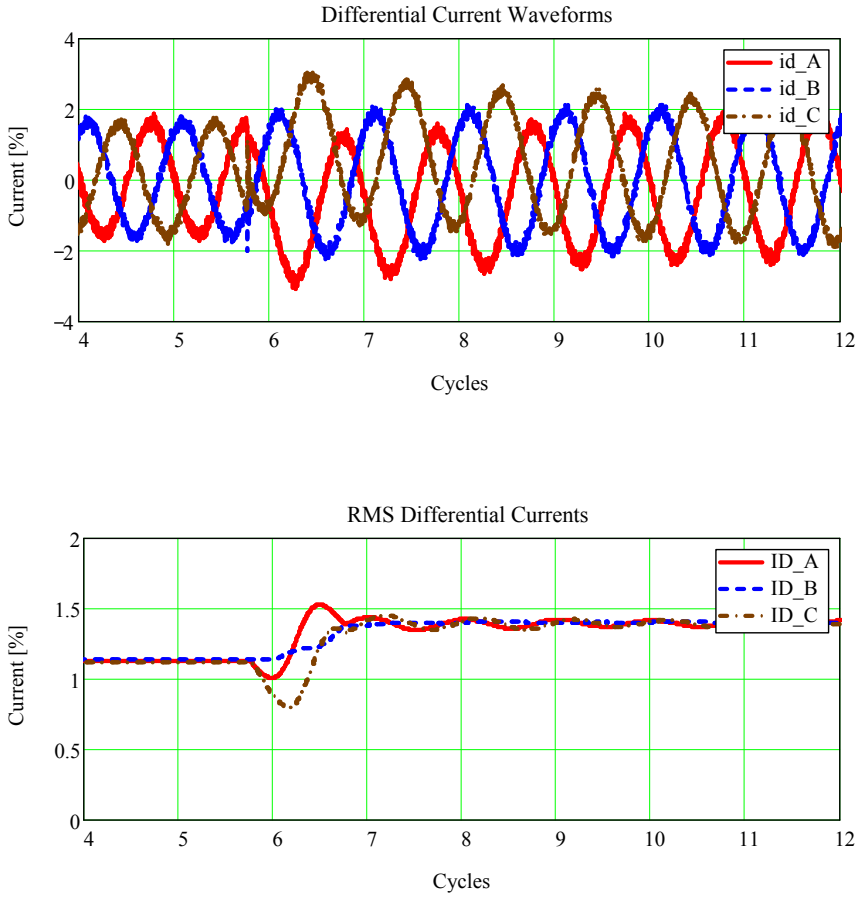

Figure 53: Differential currents during this external three-phase fault

The above waveforms show that the RMS differential currents remain within 0.015pu (1.5%), indicating that the differential relay using the new method would remain fully stable during this external fault.

External L2-L3-Ground fault at F1, Θ=25°

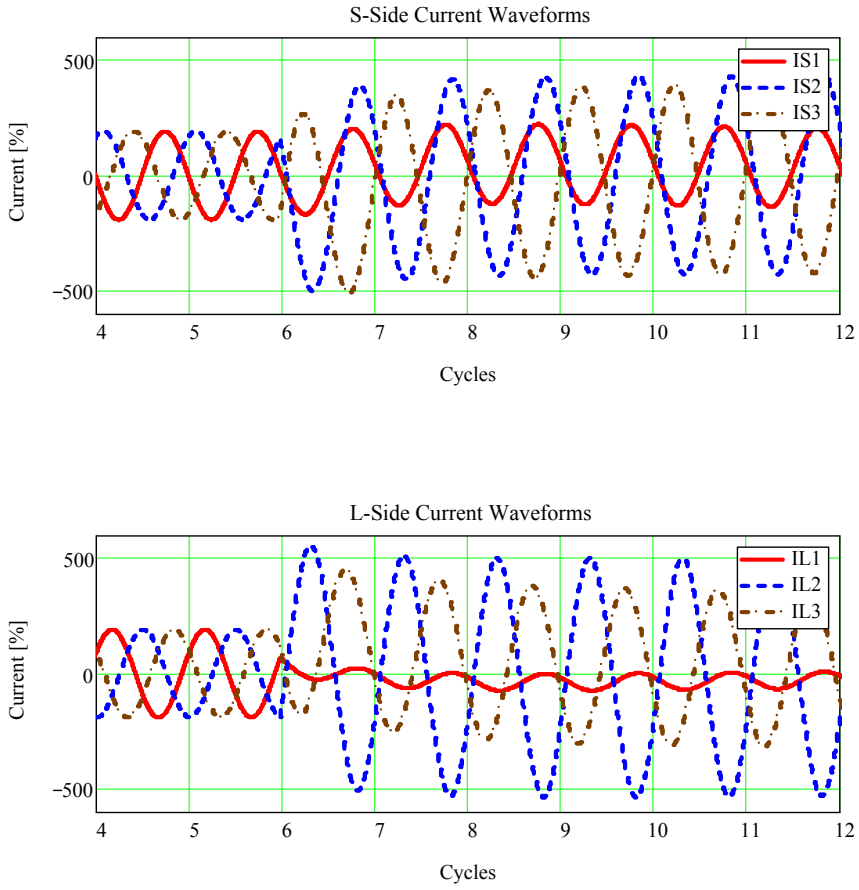

Figure 54: Individual phase currents during this external fault

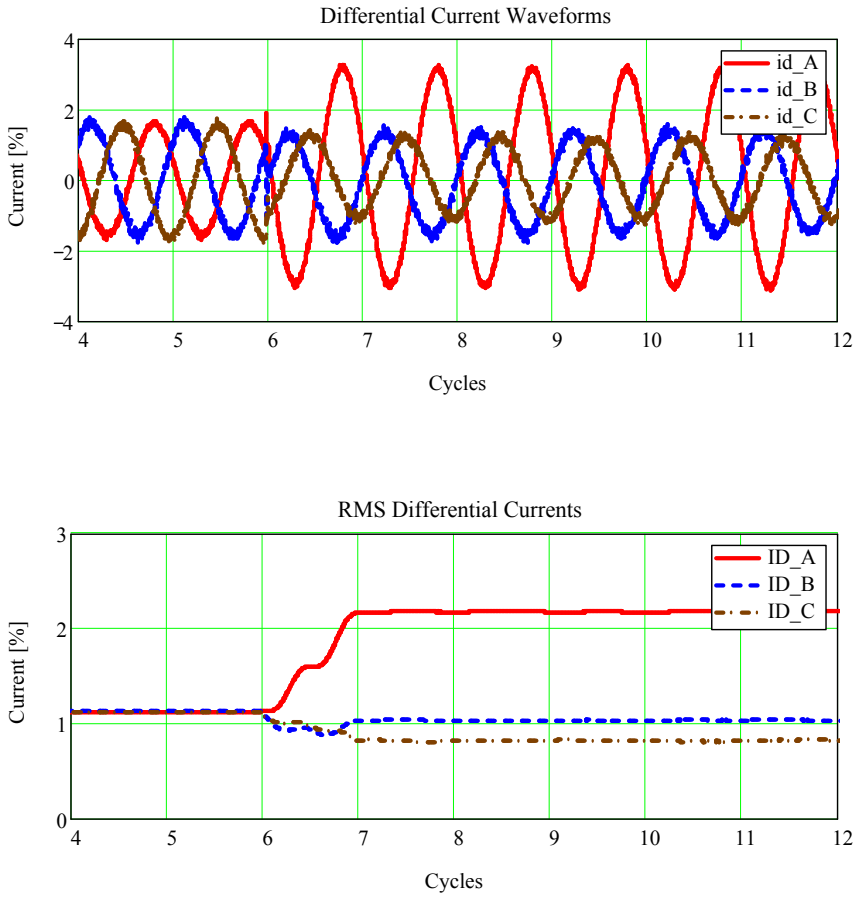

Figure 55: Differential currents during this external fault

The above waveforms show that the RMS differential currents remain within 0.025pu (2.5%), indicating that the differential relay using the new method would remain fully stable during this external fault.

External L3-Ground fault at F1, Θ=25°

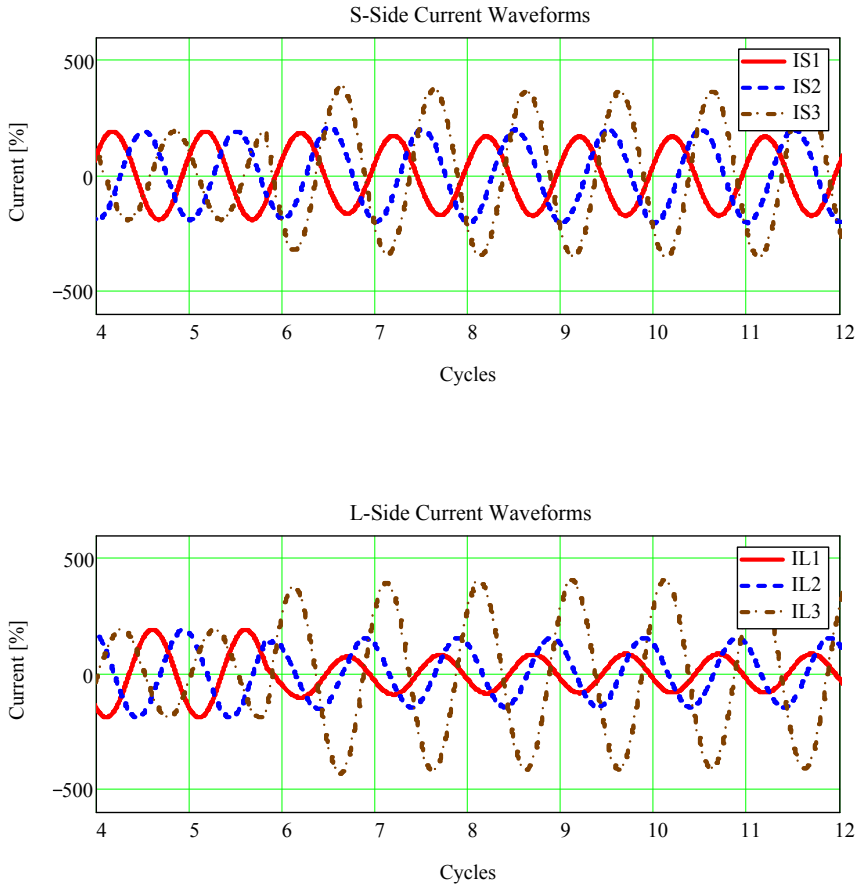

Figure 56: Individual phase currents during this external fault

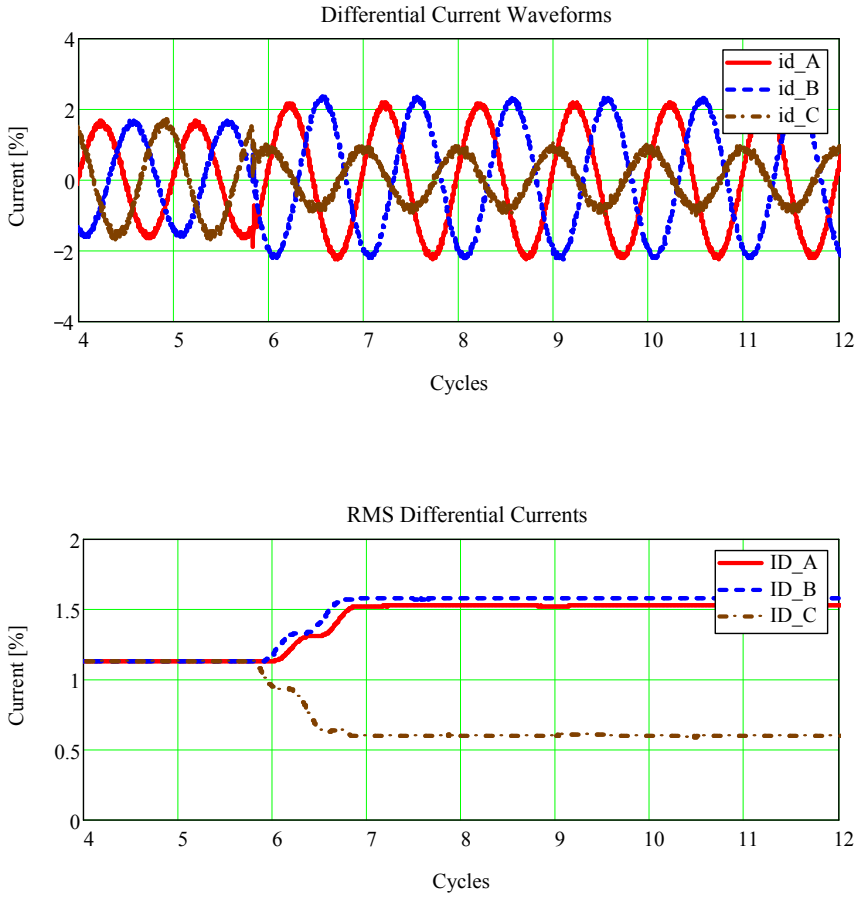

Figure 57: Differential currents during this external fault

The above waveforms show that the RMS differential currents remain within 0.017pu (1.7%), indicating that the differential relay using the new method would remain fully stable during this external fault.

Internal faults on the Secondary Side of the Excitation Transformer (fault point F3) for a 25° Phase Shift in the Advanced Operating Mode

Internal L1-L2 fault at F3, Θ=25°

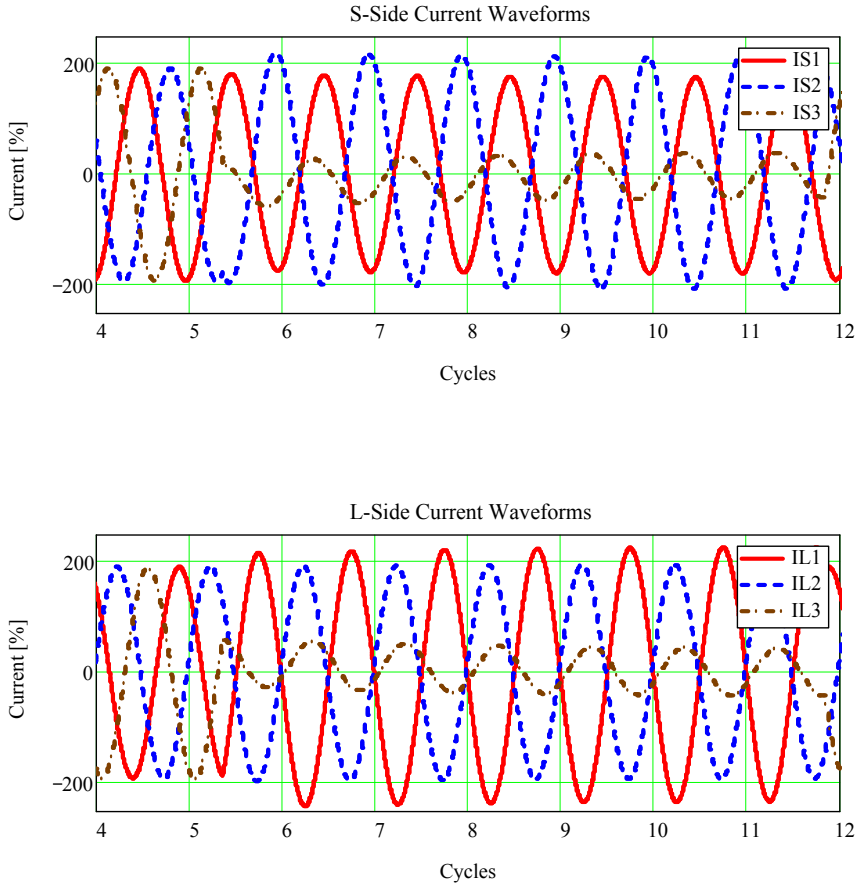

Figure 58: Individual phase currents during this internal fault

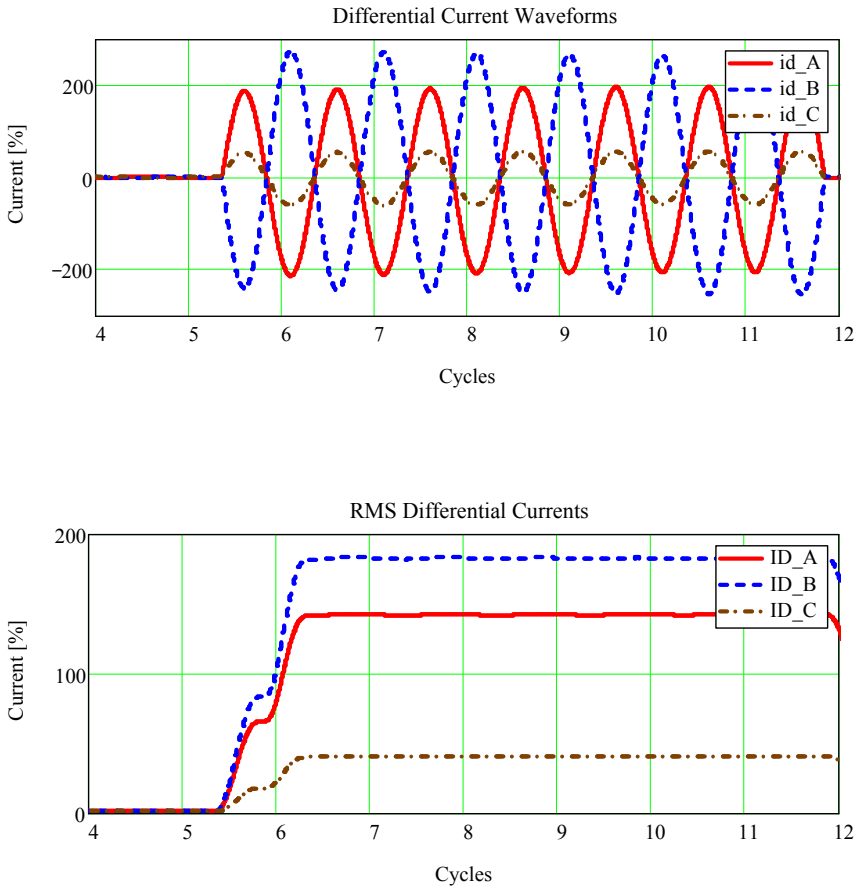

Figure 59: Differential currents during this internal fault

The above waveforms show that the RMS differential currents are big during the internal fault (183%), indicating that the differential relay using the new method would operate for this internal fault.

Internal L2-L3-Ground fault at F3, Θ=25°

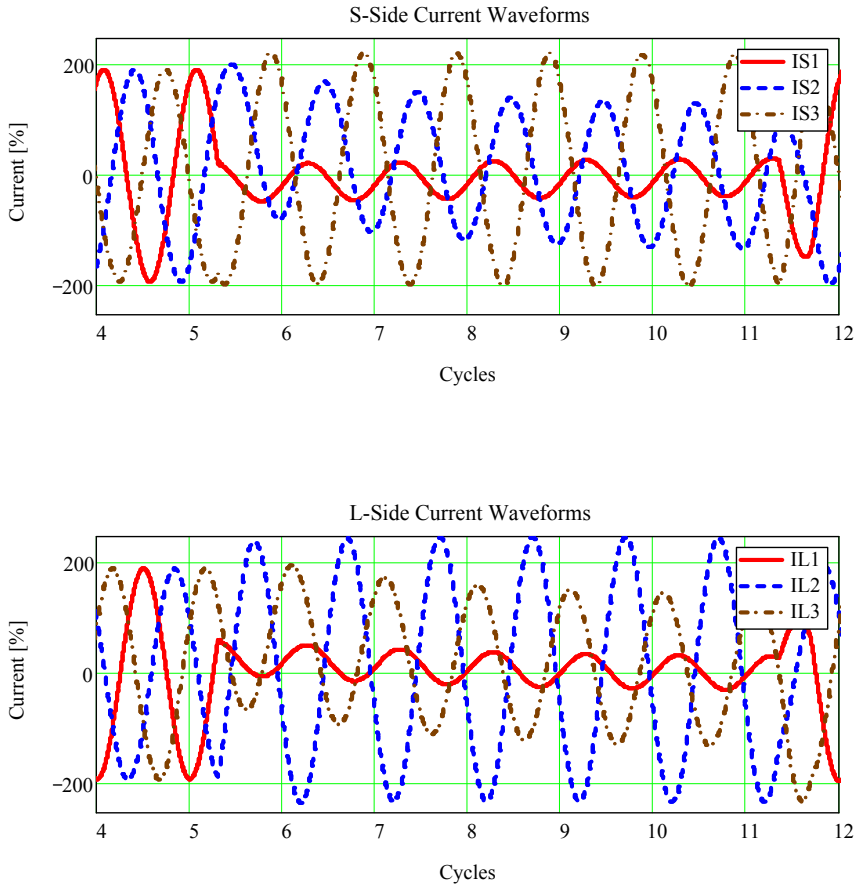

Figure 60: Individual phase currents during this internal fault

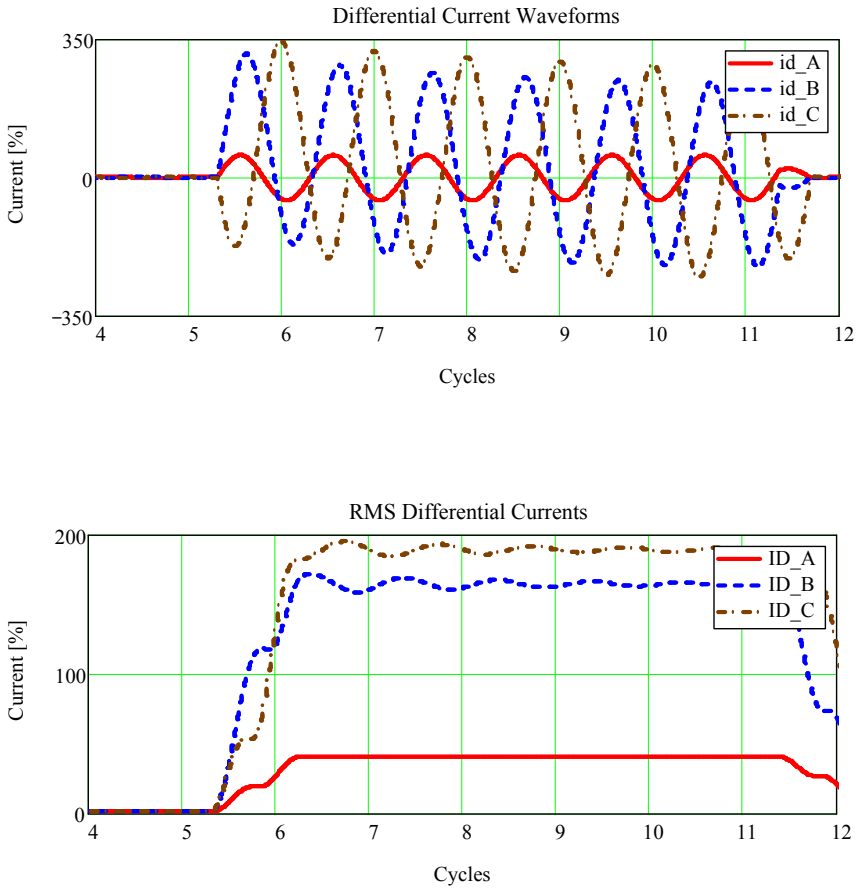

Figure 61: Differential currents during this internal fault

The above waveforms show that the RMS differential currents are big during the internal fault (190%), indicating that the differential relay using the new method would operate for this internal fault.

Internal L3-Ground fault at F3, Θ=25°

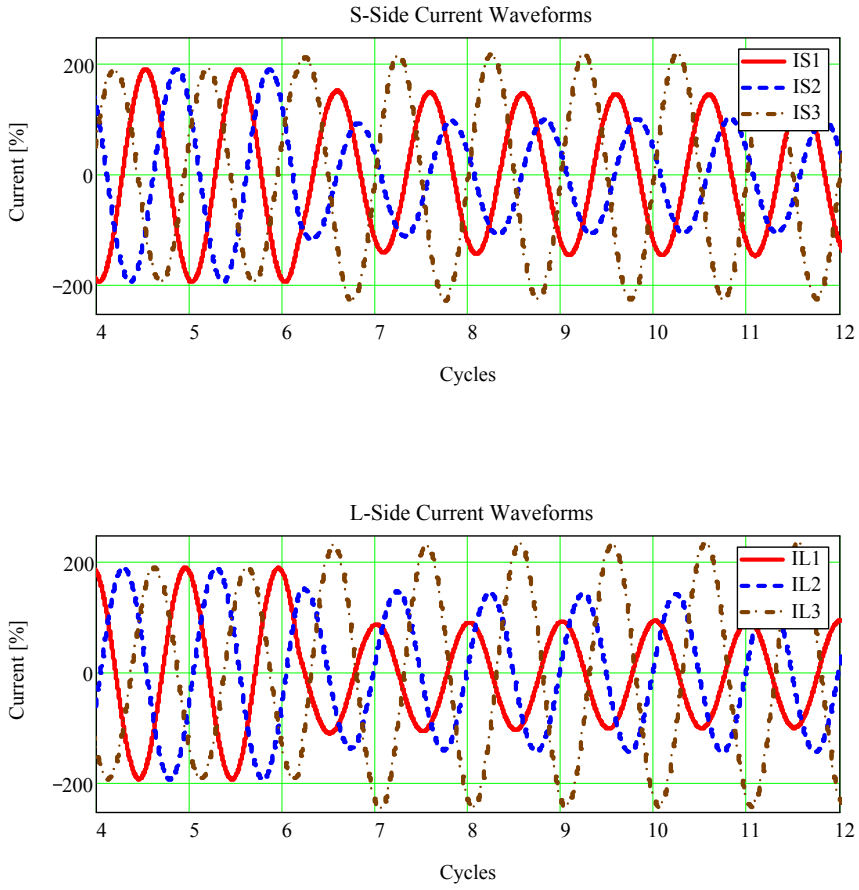

Figure 62: Individual phase currents during this internal fault

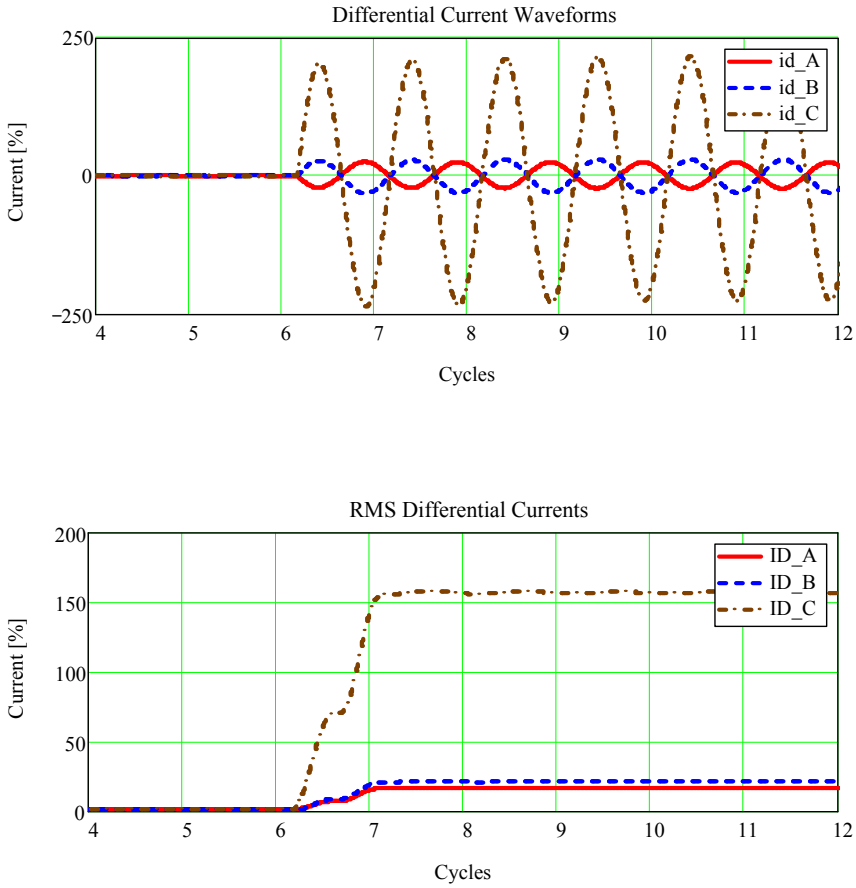

Figure 63: Differential currents during this internal fault

The above waveforms show that the RMS differential currents are big during the internal fault (160%), indicating that the differential relay using the new method would operate for this internal fault.

Internal Faults on the Secondary Side of the Excitation Transformer (fault point F3) for a 2.5° Phase Shift in the Advanced Operating Mode

Internal L3-Ground fault at F3, Θ=2.5°

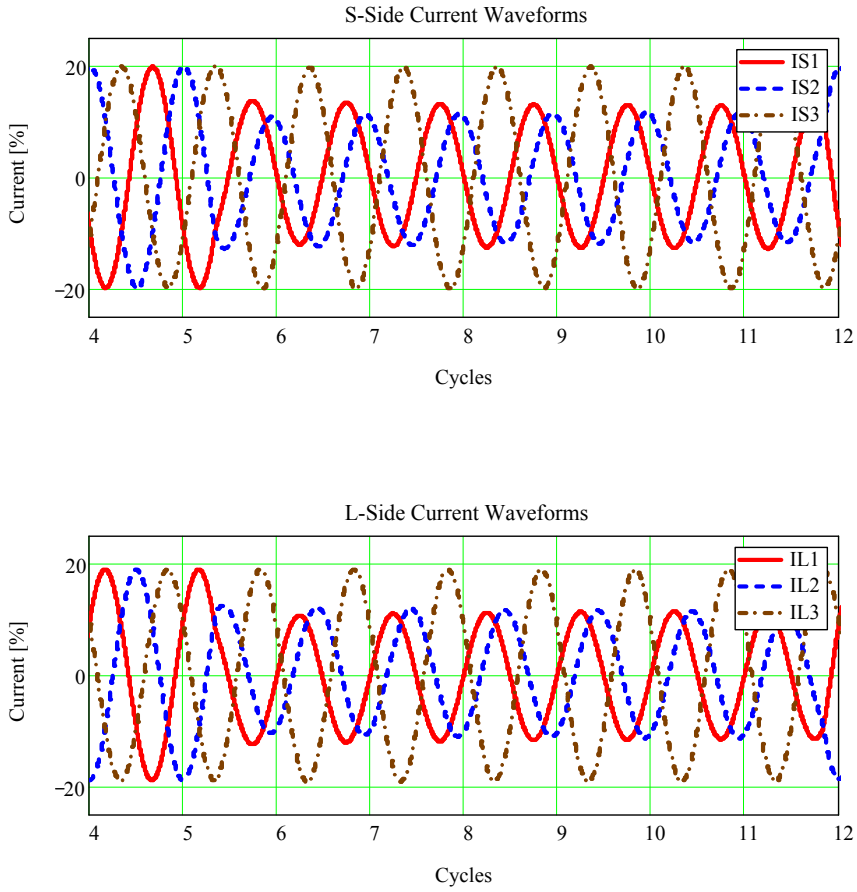

Figure 64: Individual phase currents during this internal fault

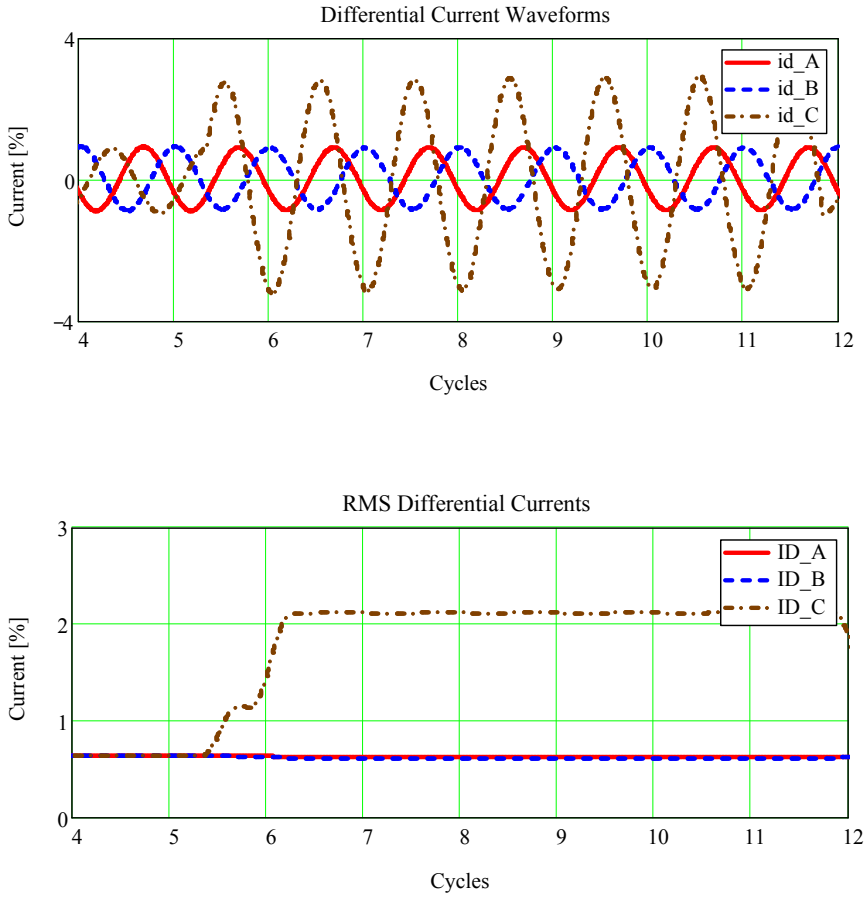

Figure 65: Differential currents during this internal fault

It can be seen from the above waveforms that for the internal earth-fault on the secondary side of the excitation transformer for a very small no-load phase angle shift, the differential current magnitudes are smaller than 2.5%. The main reason is the small number of active turns on the secondary side of the excitation transformer. Thus, additional protection relays like excitation transformer secondary side neutral point earth-fault protection shall be used to detect and clear such faults. For an alternative solution refer to Chapter 11.

Internal Faults on the Primary Side of the Excitation Transformer (fault point F4) for a 2.5° Phase Shift in the Advanced Operating Mode

Internal L3-Ground fault at F4, Θ=2.5°

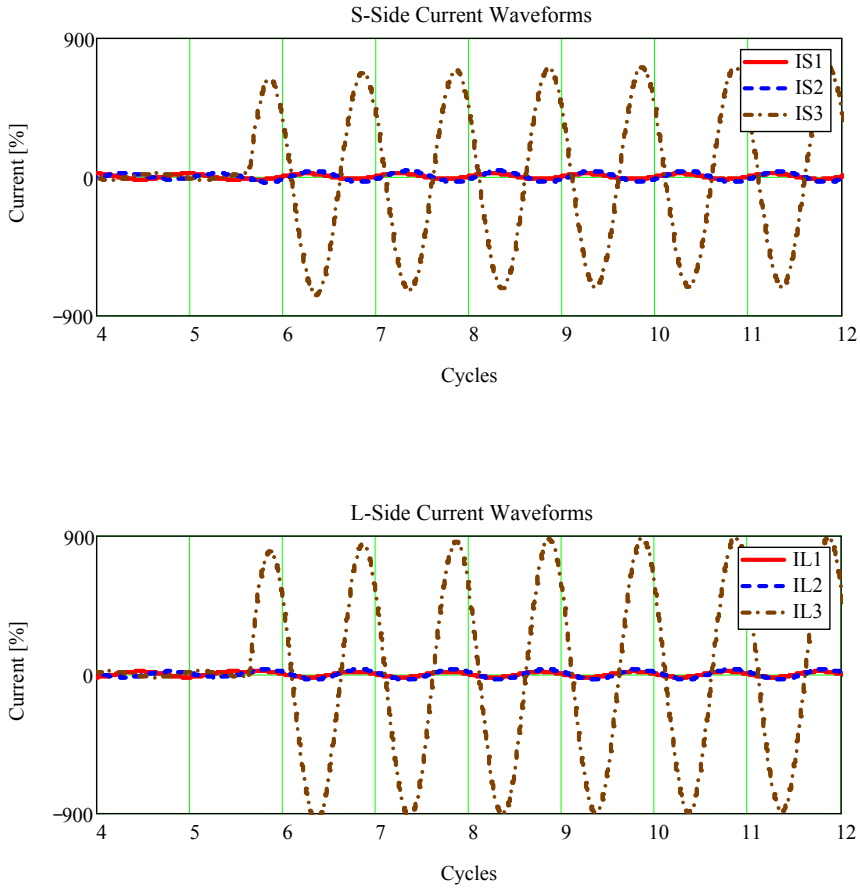

Figure 66: Individual phase currents during this internal fault

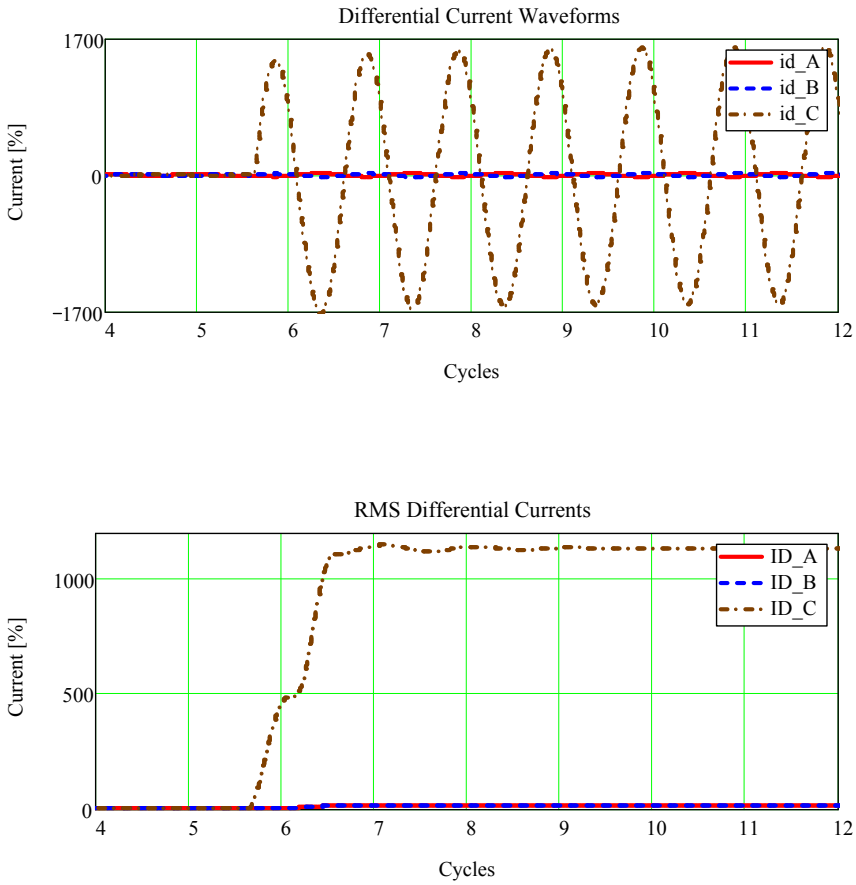

Figure 67: Differential currents during this internal fault

The above waveforms show that the RMS differential currents are quite big during this internal fault (11.5pu), indicating that the differential relay using the new method would operate for this internal fault.

External Faults on the L Side Bus (fault point F2) for a 2.5° Phase Shift in the Advanced Operating Mode

External L3-Ground fault at F2, Θ=2.5°

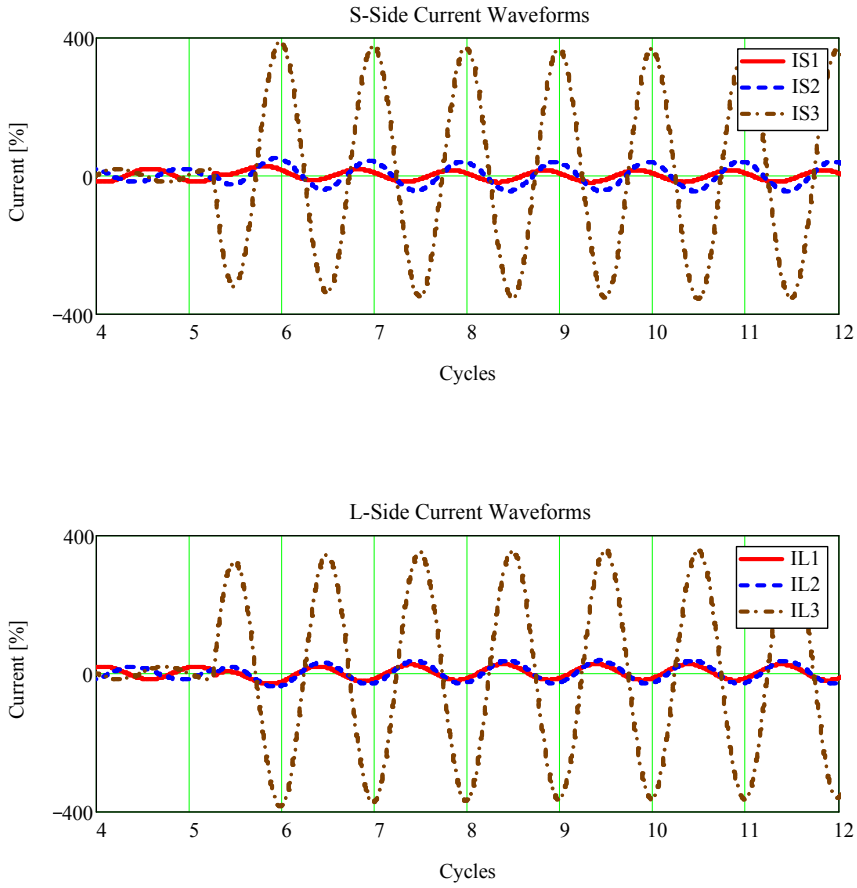

Figure 68: Individual phase currents during this external fault

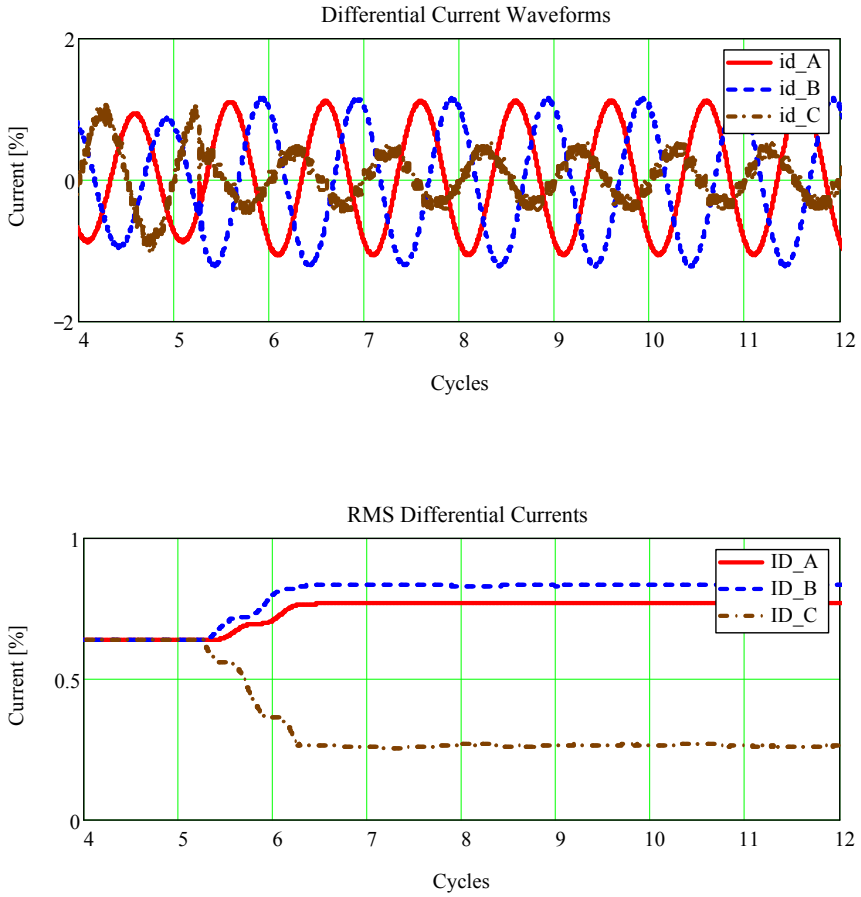

Figure 69: Differential currents during this external fault

The above waveforms show that the RMS differential currents remain within 0.01pu (1.0%), indicating that the differential relay using the new method would remain fully stable during this external fault.

Chapter 8

Implementation Possibilities

In this chapter, implementation possibilities for the presented differential protection method will be discussed.

8.1 Mixed Solution (Analogue + Numerical)

In the previous part of this document the following items were discussed:

- special converter transformers (Figure 2);
- problems which arise when standard numerical differential protection is applied for differential protection of such special converter transformers (Section 3.2); and,
- properties of M and M0 matrix transformations (Section 4.7).

If these three elements are combined it is possible to design improved differential protection for special converter transformers by using a mixture of analogue and numerical techniques.

If one is able to provide rotation, in the appropriate direction, of the three-phase currents externally to compensate for the additional, non-standard phase angle shift Ψ, the net transformer connection as seen by the numerical differential relay reverts back to the standard power transformer vector group. This allows for protection of the converter transformer as if it did not have special "HV winding extensions". The standard numerical transformer differential relay software features can then be used in the usual way to provide differential protection for this special converter transformer, as if it were of a standard vector group design (e.g. Dy11d0 for the special converter transformer shown in Figure 2a).

Rotation of Three-Phase Currents by Angle Ψ, by Using Analogue Technique

Busbar protection summation type design has been used by different relay manufacturers for decades. The auxiliary summation CT used for this type of design has three primary windings and one secondary winding. It was found out that by using a set of three identical auxiliary summation CTs one can provide external rotation by angle Ψ without changing the main CT secondary current magnitude (e.g. with an overall ratio 1/1A or 5/5A). The necessary connections, for the external rotation of the three-phase currents by angle Ψ in the anticlockwise direction are shown in Figure 70. In the left-hand side of Figure 70, wiring comes from the main CT and wiring from the right-hand side of Figure 70 shall be connected to the numerical differential relay.

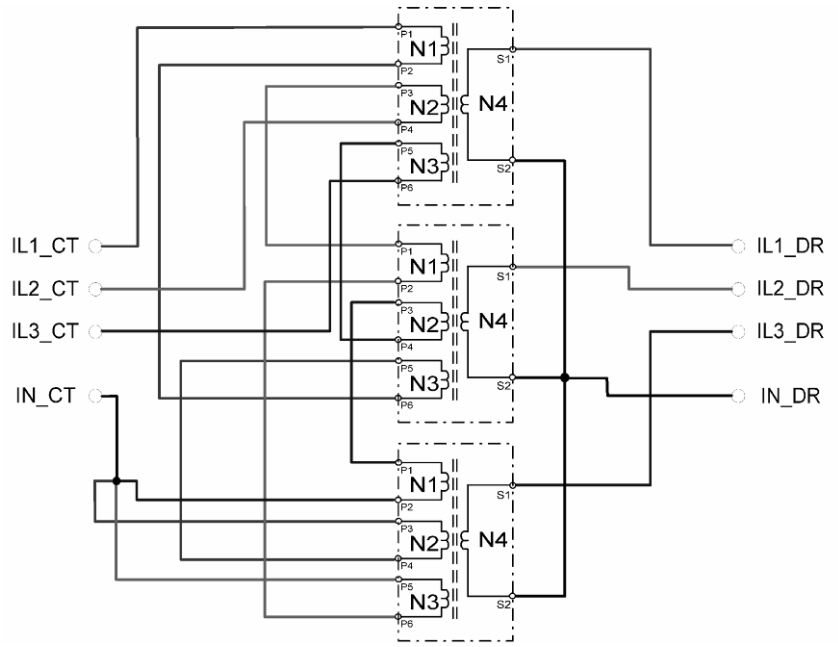

Figure 70: Auxiliary CT set connections for anticlockwise (i.e. positive) rotation by angle Ψ.

By using ampere-turn balancing, the following equation can be written for the auxiliary summation CT connections shown in Figure 70.

$$\begin{bmatrix} IL1\_DR \\ IL2\_DR \\ IL3\_DR \end{bmatrix} = \frac{1}{N4} \cdot \begin{bmatrix} N1 & -N2 & -N3 \\ -N3 & N1 & -N2 \\ -N2 & -N3 & N1 \end{bmatrix} \cdot \begin{bmatrix} IL1\_CT \\ IL2\_CT \\ IL3\_CT \end{bmatrix} \tag{8.1}$$

where:

- IL1_CT is the main CT secondary current in phase L1;
- IL1_DR is the phase L1 current, rotated by angle Θ in an anticlockwise direction, which shall be connected to the differential relay; and,
- N1, N2, N3 and N4 are turn numbers of the four windings within each auxiliary summation CT.

Obviously if one can choose the auxiliary summation CT turn numbers in such a way that:

$$\frac{1}{N4} \cdot \begin{bmatrix} N1 & -N2 & -N3 \\ -N3 & N1 & -N2 \\ -N2 & -N3 & N1 \end{bmatrix} = M0(\Psi) \tag{8.2}$$

the connections shown in Figure 70 will provide the necessary rotation of the three-phase currents by angle Ψ in an anticlockwise (i.e. positive) direction without changing the main CT secondary current magnitude (e.g. with overall ratio 1/1A or 5/5A). Sometimes, within the same application, the rotation in clockwise direction by angle Ψ is needed as well. By using the properties of the M0 matrix transformation, it can be shown that the same auxiliary summation CT set can be used, but it shall be connected as shown in Figure 71. Thus, the connection shown in Figure 71 will provide the necessary rotation of the three-phase currents by angle Ψ in a clockwise (i.e. negative) direction.

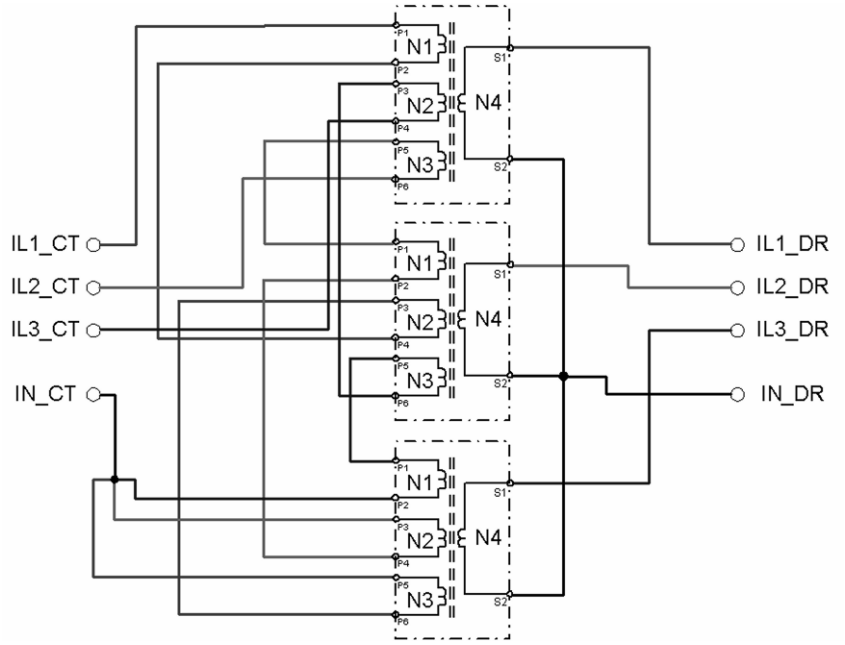

Figure 71: Auxiliary CT set connections for clockwise (i.e. negative) rotation by angle Ψ.

Table 16 gives example of possible design solutions regarding the turn numbers within auxiliary summation CTs for the most typical, additional phase angle shifts Ψ from converter transformers used in practice.

Table 16: Auxiliary summation CT design details

Design Phase Angle Shift Ψ	Auxiliary Summation CT Turn Numbers				Auxiliary Summation CT Performance	
	N1	N2	N3	N4	Achieved Overall Ratio	Achieved Rotation Angle
±7.5°	26	16	10	39	1/1.009	±7.59°
±15°	26	19	7	40	1/1.009	±14.92°

Small CT secondary current magnitude errors of less than 1% and small phase angle errors of approximately 0.1^o caused by imperfection in the auxiliary summation CT design will not cause any significant false differential current in practical installations.
Note that auxiliary summation CTs are designed to remove the zero sequence current from the protected power transformer side where they are connected. Thus, the zero sequence currents will not be available within the differential relay from that power transformer side.

Differential Protection Solution for a Transformer with $\Psi=15^o$

The overall differential protection solution and all relevant data for this transformer application (including power transformer vector diagram) are shown in Figure 72. Review of the power transformer vector diagram shows that the LV side no-load voltages shall be rotated by 15^o in an anticlockwise direction in order to be in phase with the HV side no-load voltages. Thus, the same rotation shall be provided for the LV side currents for the differential protection when the HV side is selected as the reference winding. To do that, one set of auxiliary summation CTs that provide current rotation by 15^o in anticlockwise direction are required. This auxiliary CT set is used in order to put the transformer overall phase shift, as seen by the differential relay, back to the standard Yy0 vector group. The main CT secondary current magnitudes are not altered at all on the LV side. The numerical differential relay software features can then be used in the usual way to compensate for this special converter transformer, as if it were a standard two-winding transformer with vector group Yy0. All other relevant application data such as main CT ratios and power transformer rated power, rated currents and rated voltages shall be used as they are in the actual installation to derive the differential relay settings.

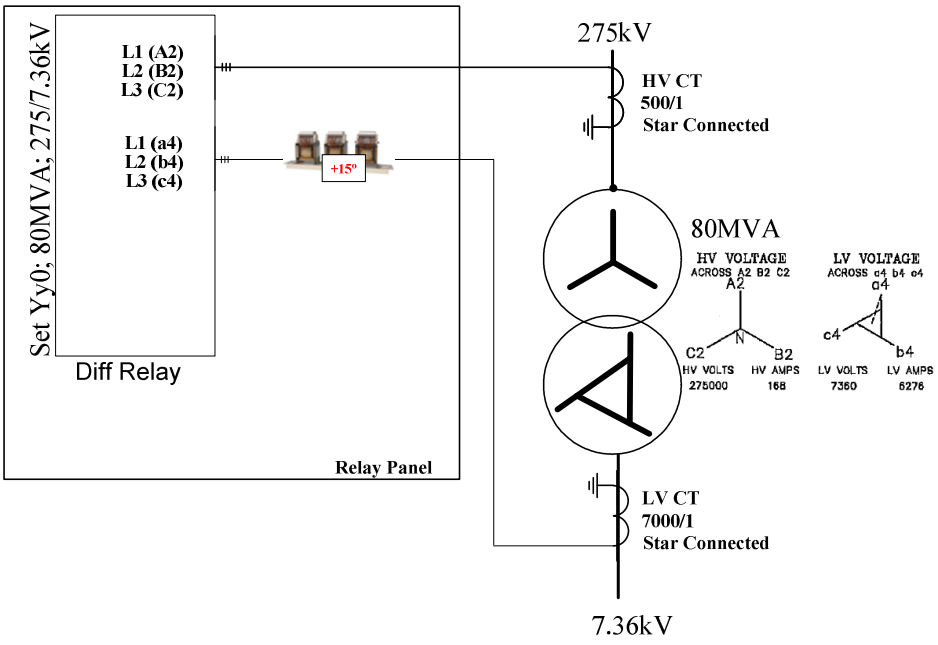

Figure 72: Differential protection solution for a transformer with 15° phase shift.

Differential Protection Solution for a 24-pulse Converter Transformer

This converter transformer is quite special because within the same transformer tank, two three-phase transformers, of similar design as shown in Figure 3, are put together. The first internal transformer has vector group Zy11¾d10¾. The second internal transformer has vector group Zy0¼d11¼. Such an arrangement gives an equivalent five-winding power transformer with a 15° phase angle shift between LV windings of the same connection type. The power transformer construction details and corresponding phasor diagram for positive sequence no-load voltages are shown in Figure 73.

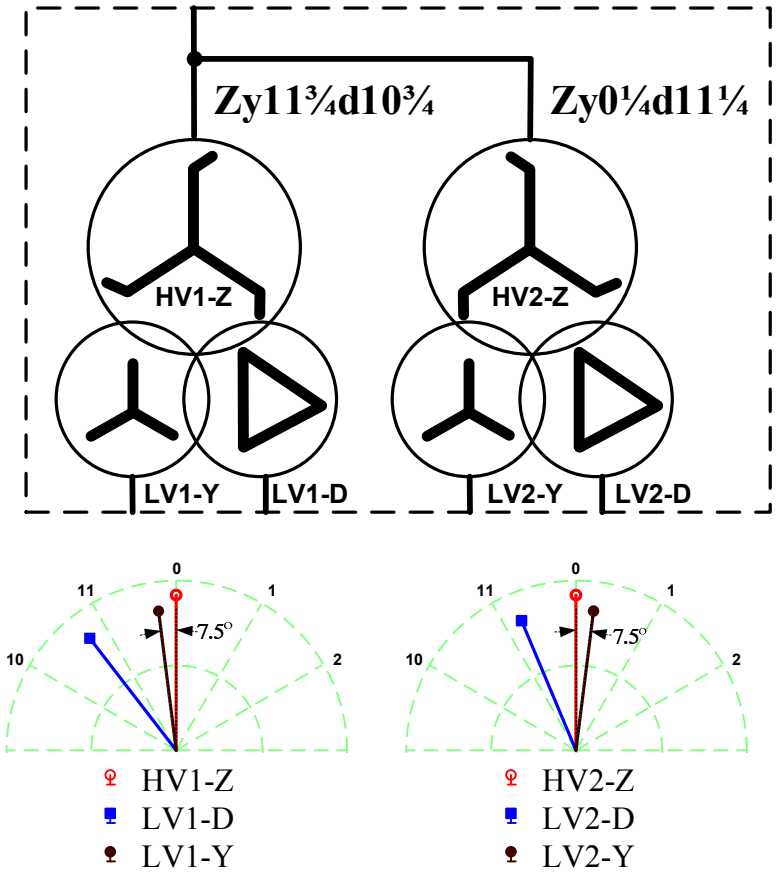

Figure 73: 24-pulse converter transformer with positive sequence phasor diagram.

From the transformer phasor diagram it can be seen that:

- LV1-Y and LV1-D sides shall be rotated by 7.5° in a clockwise direction; and
- LV2-Y and LV2-D sides shall be rotated by 7.5° in an anticlockwise direction,

in order to put the 24-pulse converter transformer overall phase shift, as seen by the differential relay, back to the standard Yy0d11y0d11 vector group.

For such transformers, four sets of auxiliary summation CTs that provide current rotation by 7.5^{o} are required. Two sets, connected for current rotation in a clockwise direction shall be applied on the two LV sides of the first internal transformer. Two sets, connected for current rotation in an anticlockwise direction shall be applied on the two LV sides of the second internal transformer. These auxiliary CTs are used in order to put the 24-pulse converter transformer overall phase shift, as seen by the differential relay, back to the standard Yy0d11y0d11 vector group. Note that all twelve pieces of auxiliary summation CTs used for this application are exactly the same. The main CT secondary current magnitudes are not altered on any of the four LV sides. Hence, the numerical differential relay software features can now be used in the usual way to compensate for this special converter transformer, as if it were a standard five-winding transformer with vector group Yy0d11y0d11. All other relevant application data like main CT ratios and 24-pulse converter transformer windings rated power, rated currents and rated voltages shall be used as they are stated on respective equipment rating plates to derive the differential relay settings. The overall differential protection solution is shown in Figure 74. Note that in this figure, protection device designations in accordance with IEEE C37.2-1996 standard have been used.

Summary about Mixed Solution

Standard numerical power transformer differential relays can be used to provide differential protection for the special converter transformers with non-standard, but fixed, phase angle shift. The only pre-request is that the external auxiliary CTs are used to compensate for the additional phase angle shift Ψ, typically caused by special arrangements of the converter transformer HV winding. Once this compensation is done externally, the numerical differential relay shall be set and applied as if the special converter transformer was designed with the standard vector group connection.

Using the presented solution, the differential relay is ideally balanced during all through load conditions and for all types of external faults. Hence, no false differential current will be measured by the differential relay. This will enable the end user to set the minimum differential protection pickup to a quite sensitive level (e.g. 15-20%), ensuring sensitive protection for low-level transformer internal faults such as interturn faults. The approach presented is not dependent on the particular

special converter transformer construction details, and by using the described principle, it is possible to provide differential protection for any three-phase power transformer with non-standard, but fixed phase angle shift, which can not be directly covered by the setting facilities of the numerical transformer differential protection relays.

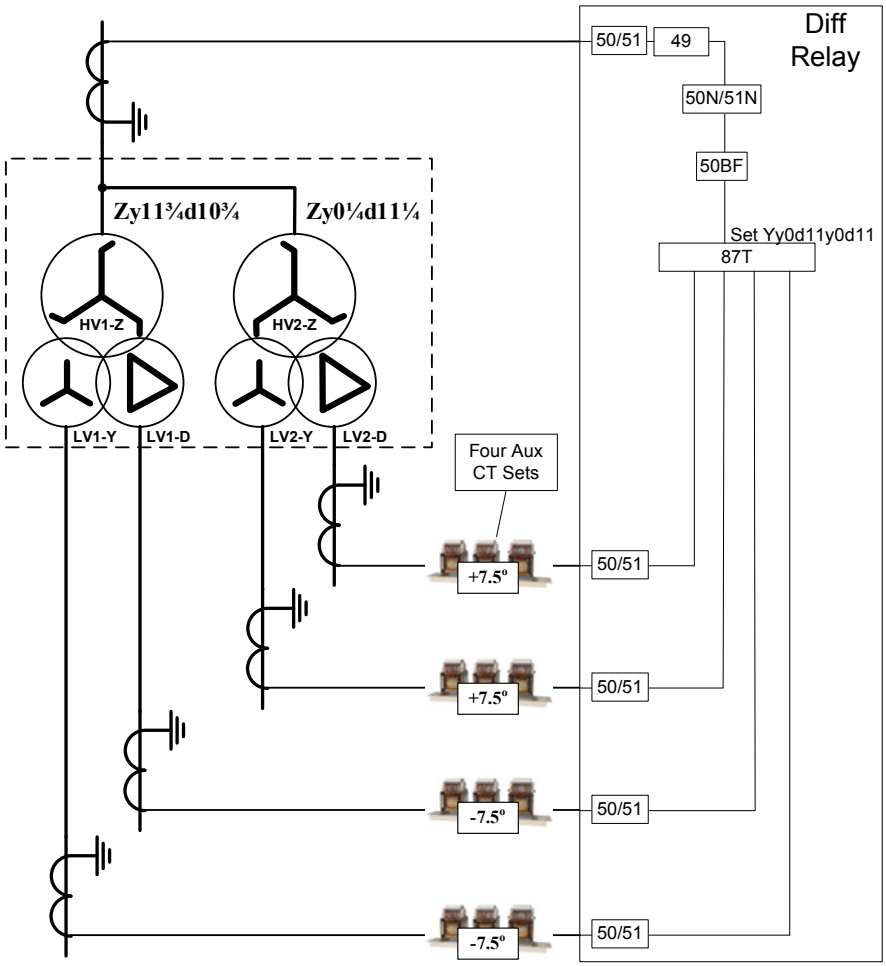

Figure 74: Overall protection solution for 24-pulse converter transformer.

8.2 Fully Numerical Implementation

The first possibility for numerical implementation would be to mimic the mixed solution presented in the previous section. The only difference from the mixed solution would be that the functionality of the summation interposing CTs is implemented in the relay software for processing the analogue input values, while the traditional transformer differential function is still used inside of the numerical relay in order to execute the differential protection algorithm.

The second possibility for numerical implementation would be to perform all compensation within the differential protection function itself. One such possible solution for a PST application is shown in Figure 75, and a corresponding flow chart is given in Figure 76.

The following abbreviations are used in Figure 75:

- DFF = “Digital Fourier Filter”;
- A/D = “Analogue to digital converter”;
- Max = “Maximum of”;
- BCD = “Binary Coded Decimal”; a group of five or six binary signals, coded in a special way, in order to monitor the OLTC position; and
- mA = “milli-Ampere”; a low level current signal (e.g. 4-20mA) used in practice as an alternative solution for monitoring of the OLTC position.

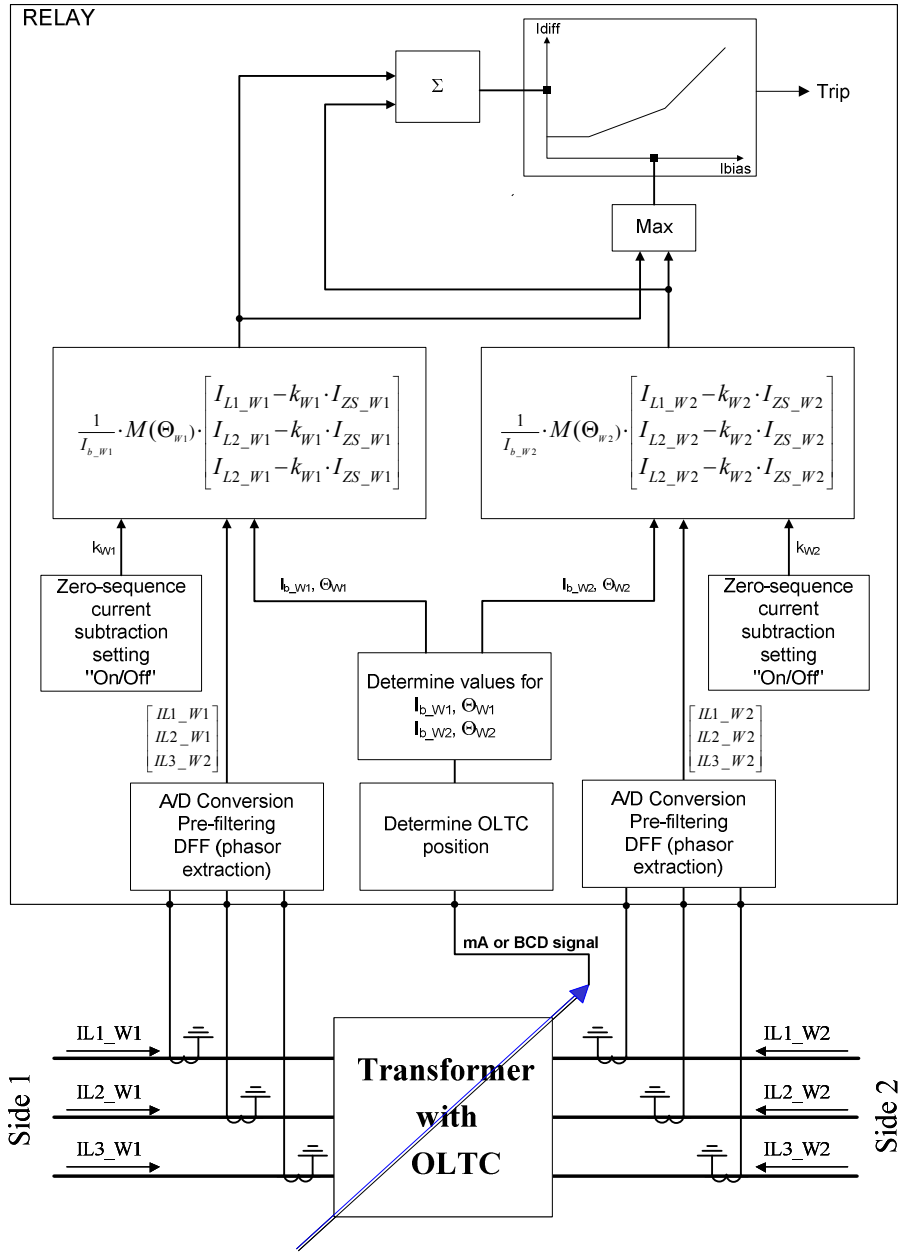

Figure 75: Fully numerical implementation for PST differential protection.

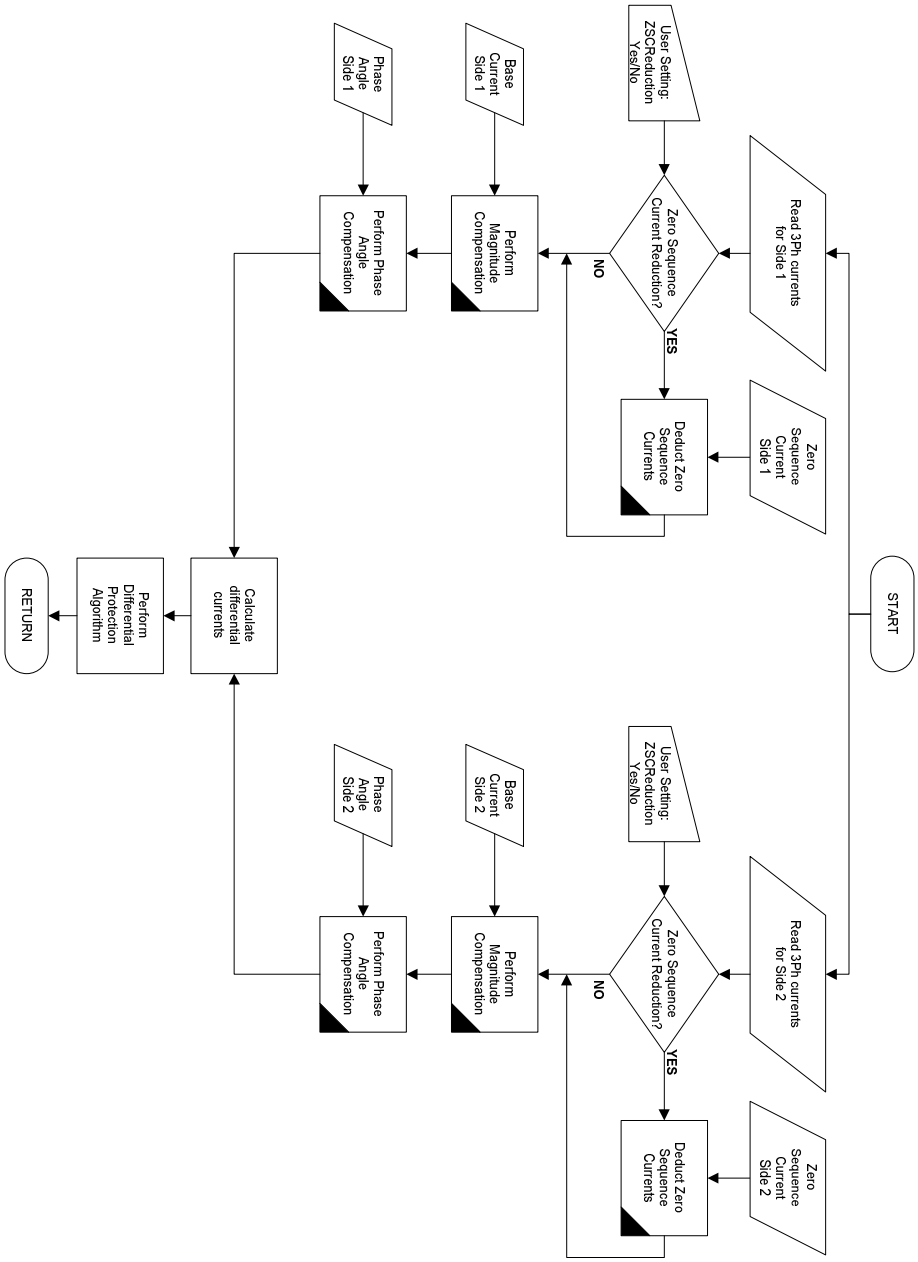

Figure 76: Flow chart for complete numerical implementation of the PST differential protection.

Chapter 9

Transient Magnetizing Currents

As stated in Section 2.4 any abrupt change of the power transformer terminal voltage will result in a transient current into the power transformer. This transient current is generally termed inrush current and is typically caused by:

- initial energization of the power transformer (initial inrush);
- voltage recovery after the clearing of an external, heavy short circuit in the surrounding power system (recovery inrush);
- energization of another, parallel power transformer (sympathetic inrush); or,
- out-of–phase synchronization of a generator-transformer block with the rest of the power system.

Initial inrush is a form of over-current that occurs during the energization of a transformer and is a large transient current which is caused by part cycle saturation of the magnetic core of the transformer. For power transformers, the magnitude of the initial inrush current has a typical value of two to five times the rated load current. By use of some additional devices (e.g. pre-insertion resistors or point on wave switching relays) the magnitude of the inrush current can be reduced. However, the influence of such devices will not be considered in this thesis.
The inrush current slowly decreases from the initial peak value by the effect of oscillation damping due to the winding and magnetizing resistances of the transformer, as well as the impedance of the system it is connected to, until it finally reaches the normal exciting current value. This process typically takes several minutes and as a result, the inrush current could be mistaken for a short circuit current and the transformer

can be erroneously taken out of service by the overcurrent, earth-fault or differential relays.
Special transformers have similar properties regarding inrush current as standard three-phase power transformers. Actual field recordings of inrush currents into a phase-shifting transformer are shown in the following two figures. Note that PSTs are typically energized at an OLTC position which corresponds to 0^{o} phase angle shift.

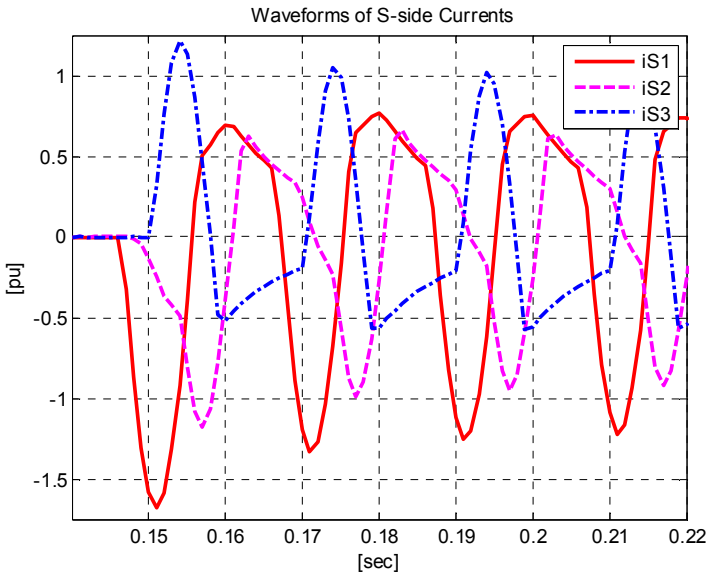

Figure 77: Recorded initial inrush into 600MVA, 232kV, 50Hz, dual-core, symmetrical PST.

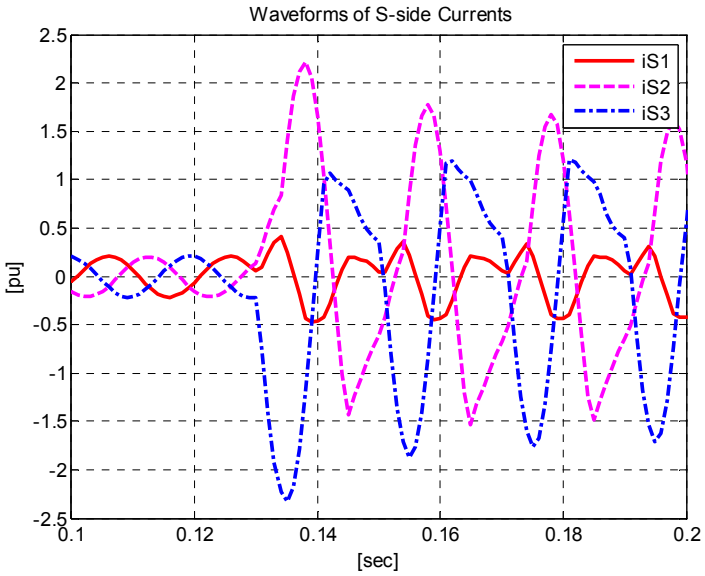

Figure 78: Recorded sympathetic inrush into 600MVA, 232kV, 50Hz, dual-core, symmetrical PST.

9.1 Inrush Current Calculation

The simplified equation often used to calculate the peak value of the first cycle of the inrush current is given in [61] as follows:

$$I_{pk} = \frac{\sqrt{2}\times U}{\sqrt{(\omega\times L)^2 + R^2}} \times \left(\frac{2\times B_N + B_R - B_S}{B_N}\right) \tag{9.1}$$

where:

- I_{pk} = Peak inrush current in [Primary Amperes];
- U = Applied voltage in [Volts];
- L = Air core inductance of the energized winding in [Henry];
- R = Total DC resistance of the transformer windings in [Ohms];
- B_R = Remanent flux density of the transformer core in [Tesla];

- B_S = Saturation flux density of the core material in [Tesla]; and,
- B_N = Normal rated flux density of the transformer core in [Tesla].

In reality, equation (9.1) will not give sufficient accuracy, since a number of transformer and system parameters exist that effect the magnitude of the inrush current significantly, are not included in the calculation. The above equation neglects the following important transformer and system parameters which can have as much as 60% impact [61] on the magnitudes of the inrush current:

- inductance of the air-core circuit adjusted for the transient nature of the inrush current phenomenon;
- impedance and short circuit capacity of the system; and
- core geometry and winding configurations and connections (e.g., 1- vs. 3-phase; Y- vs. Delta winding connections; Grounded vs. non grounded Y connections; etc.).

9.2 Effect of Transformer Design Parameters on the 2nd Harmonic Component of the Inrush Current

The design of power transformers has changed slightly over time [61], and at the same time, more modern materials have been used. These factors will influence the power transformer inrush current and consequently the differential protection design.

Effect of Design Flux Density

The inrush current peak increases as the design induction level increases. This is caused by core saturation for a greater part of the voltage cycle. For the same reason, the minimum percentage of the 2nd harmonic / peak inrush current ratio decreases with the induction. Modern transformers generally operate at higher flux density values with the increased use of higher grain oriented steels. This results in modern transformers having higher inrush currents due to the higher rated design induction value but lower minimum percentage of 2nd harmonic / peak inrush current ratio [61]. A typical example for a 36MVA, three-phase transformer is given in Figure 79.

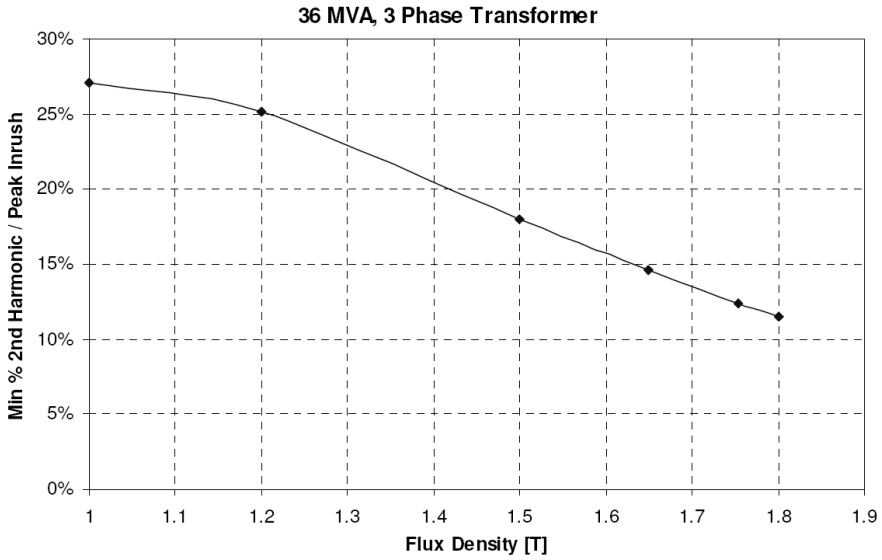

Figure 79: Typical 2nd harmonic / peak inrush current ratio [61].

Effect of Core Material

A new feature of modern transformers is the use of highly grain oriented and domain – refined electrical steel type materials that have a higher value of saturation flux density, a larger linear portion of the magnetization curve, and a lower remanent flux density compared to regular grain oriented type materials.

Thus, these higher grain orientation materials are associated with higher minimum percentage of 2^{nd} harmonic / peak inrush current ratios. For the same flux density, the new, modern materials have an appreciably greater minimum percentage of 2^{nd} harmonic / peak inrush current ratio than Regular Grain Oriented (RGO) material [61].

Effect of Core Joint Type

Until a decade or two ago, a non step-lap (e.g. conventional) type joint was commonly used in transformer cores, however modern transformers use a step-lap type joint, as shown in Figure 80 (from [9]). Because of the high

reluctance of the core joints, the remanent flux density levels of a transformer core are significantly lower than the flux density level of the core material itself. As the conventional joint has a greater reluctance than a step-lap joint, it follows that a core with the step-lap joint would have a much lower minimum percentage of 2nd harmonic / peak current ratio than those of a core with a conventional joint [61].

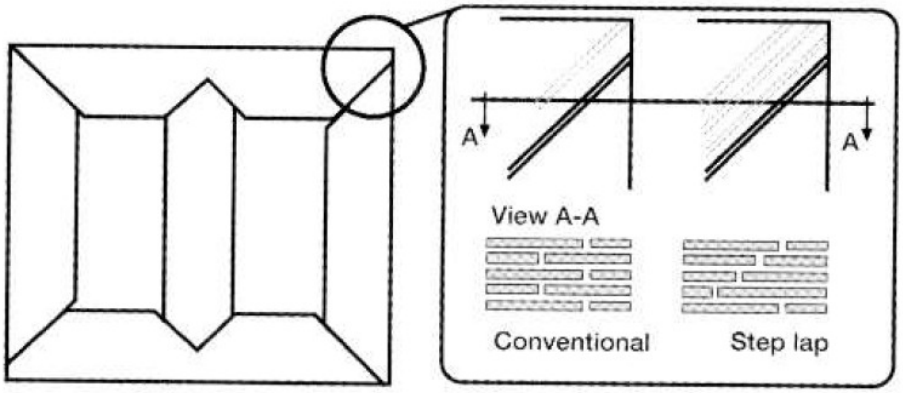

Figure 80: Three-leg magnetic core with conventional or step lap joint [9].

Effect of Winding Connection Type

In a three–phase power transformer, the connection of the primary and secondary windings and the grounding of any star connected winding will dictate the distribution of the inrush current generated in one winding to the other phases and line currents. For instance the line current of a star connected primary winding will see the full winding inrush current, while the line current for a delta connected primary winding will be reduced since the inrush current can enter the other phases.

The percentage of the second harmonic will not be affected by the winding connection or number of phases [61]. It is only a function of the rated flux density, core material parameters (saturation flux density, the remanent flux density) and lap joints.

9.3 Effects on Transformer Differential Protection

Knowledge about transformer inrush currents significantly influences the design of protection relays. The main impact of the inrush current is the increased risk of unwanted operation for instantaneous overcurrent, earth-fault and transformer differential protection elements within the relay. The transformer differential function must be blocked to prevent unwanted operation in the case of inrush currents.

Inrush Detection by Harmonic Analysis of Instantaneous Differential Currents

The most commonly used method involves the detection of the 2nd harmonic content of the inrush currents which is used to block the differential function [11], [12], [17] and [32]. Typically, when the ratio of the second harmonic current component with respect to the fundamental current component exceeds a preset level (e.g. 15%), the transformer differential protection in that phase is blocked.
The instantaneous differential currents are calculated by using equation (4.30), with the only difference being that the currents used in the equation are instantaneous values (i.e. samples) from all transformer sides. Note that it is quite important to measure the second harmonic content in the instantaneous differential current and not in the individual winding phase currents. The main reasons are:

- the possibility of high harmonic current content in the individual winding phase currents, especially in industrial applications;
- the content of the fundamental current component is typically much bigger in the individual winding phase currents than in the respective differential currents during sympathetic and recovery inrush; and,
- the lack of distinct correlation between phases within differential protection and individual winding phase currents.

Practice has shown that although using the second harmonic blocking approach may prevent false tripping during inrush conditions, it may sometimes increase fault clearance time for heavy internal faults followed by CT saturation. On the positive side, the second harmonic restrain/blocking approach will increase the security of the differential relay for a heavy external fault with CT saturation.

Inrush Detection by Waveform Analysis of Instantaneous Differential Currents

The waveform blocking criterion is a good complement to the harmonic analysis. The waveform blocking is a pattern recognition algorithm that searches for intervals within each fundamental power system cycle with low magnitude of the inrush current. In the inrush current waveform there is a period of time, within each power system cycle, during which very low magnetizing currents flow. Thus, an inrush condition can be identified when a low rate of change of the instantaneous differential current exists for at least a quarter of the fundamental power system cycle, as shown in Figure 44. This figure is as well excellent example why it is mandatory to perform such analysis in the instantaneous differential current waveforms and not in the individual phase current waveforms. This criterion can be mathematically expressed for phase L1 as:

$$\left|\frac{\partial i_{Diff\_L1}}{\partial t}\right| \approx \left|\frac{\Delta i_{Diff\_L1}}{\Delta t}\right| \leq C1 \tag{9.2}$$

where, i_{Diff_L1} is the instantaneous differential current in Phase L1, t is a time and C1 is a constant, fixed in the relay algorithm.

Cross-blocking Between Phases

The basic definition of cross-blocking is that one of the three-phases can block the operation (i.e. tripping) of the other two phases of the differential protection due to the properties of the instantaneous differential current in that phase (i.e. waveform analysis or 2nd harmonic content). This principle increases the security of the differential protection during power transformer energizing.

9.4 Internal Faults Followed by CT Saturation

A primary fault current typically does not contain any 2nd harmonic component. However, in the case of DC saturation of the CTs, the secondary fault current will temporarily contain a 2nd harmonic. For heavy internal transformer faults followed by CT saturation, the distorted CT secondary current may contain a quite high level of the second harmonic. As a consequence, delayed operation of the restrained differential protection might occur.

Inrush Detection by Adaptive Techniques

The term "Adaptive Relaying" has been defined in [8]. The combination of the 2nd harmonic and waveform analysis methods, allows the relay designer to optimize the detection of inrush currents while avoiding some of the potential drawbacks. One possible way, with good field experience [11], is to combine these methods as follows:

- employ both the 2nd harmonic and the waveform criteria to detect the initial inrush condition;
- one minute after power transformer energizing, the 2nd harmonic criterion can be disabled in order to avoid long clearance times for heavy internal faults and the waveform criterion alone can take care of the sympathetic and recovery inrush scenarios; and,
- temporarily enable the 2nd harmonic criterion for six seconds when a heavy external fault has been detected, to gain additional security for external faults.

The behaviour of the differential protection under such operating conditions was tested. First the differential protection relay was setup in the traditional way, with a second harmonic blocking level set at 15% and always active. This resulted in slow operation of the differential relay for an internal fault followed by CT saturation as shown in Figure 81.

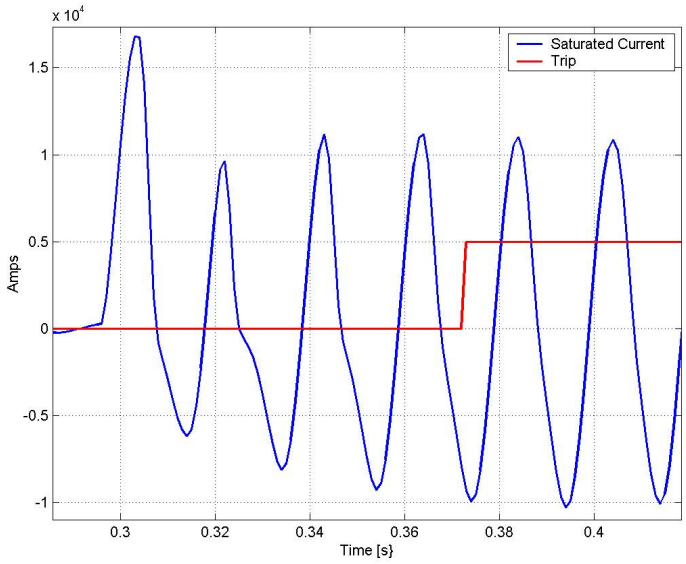

Figure 81: Slow differential protection operation due to traditional use of 2nd harmonic blocking.

After this test, the differential relay was set to adaptively use the second harmonic. No other setting parameter was changed. Then the operation of the differential function for internal faults was not effected at all by the presence of the second harmonic due to distorted CT secondary current, as shown in Figure 82. These tests show that modern numerical differential protection relays can adaptively use the second harmonic blocking criteria. The protection system can utilize the 2nd harmonic criterion as a restrain quantity during inrush conditions, but disregard its delaying influence during internal faults. This feature ensures much faster operation of the differential function for internal faults followed by CT saturation.

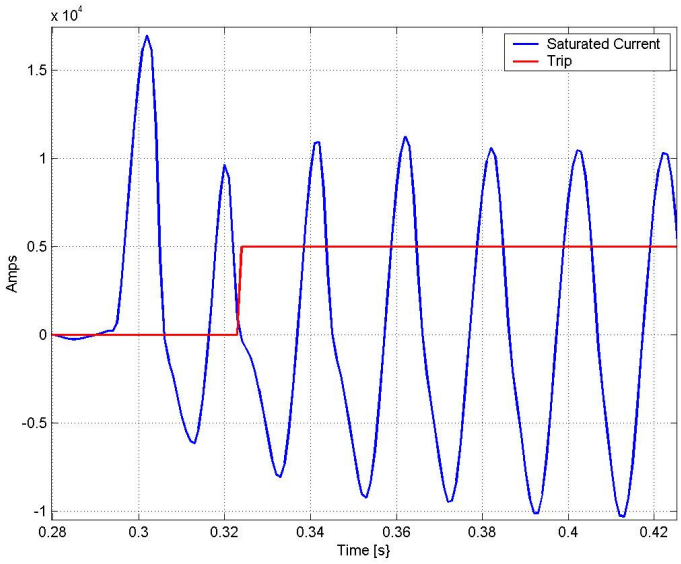

Figure 82: Fast differential protection operation with adaptive 2nd harmonic blocking.

9.5 Energizing of a Faulty Transformer

When a faulty transformer is energized the fault current might contain a high percentage of second harmonic. As a consequence, delayed operation of the restrained differential protection might occur. Modern numerical differential protection [12] might incorporate adaptive features in order to ensure faster operation for such faults. Some other solutions for the same problem have been proposed in the literature [16] and [47]. Two recorded field cases of energizing a faulty transformer will be presented.

Field Case #1

This field case was captured on a three-winding power transformer with the following rating data 25MVA; 115/38.5/6.6kV; Yy0d11; 50Hz, in accordance with IEC terminology [58]. The transformer suffered an internal turn-to-turn fault within the 35kV winding in phase L2, as shown

in Figure 108. After correct tripping by the differential protection the operator tried to energize again the faulty transformer. The DR file was captured during this transformer energizing attempt by the existing differential relay having a sampling rate of 20 samples per power system cycle. In Figure 83 the following waveforms, either extracted or calculated from this DR file, are presented:

- 110kV current waveforms;
- instantaneous differential current waveforms; and,
- RMS values of the differential currents.

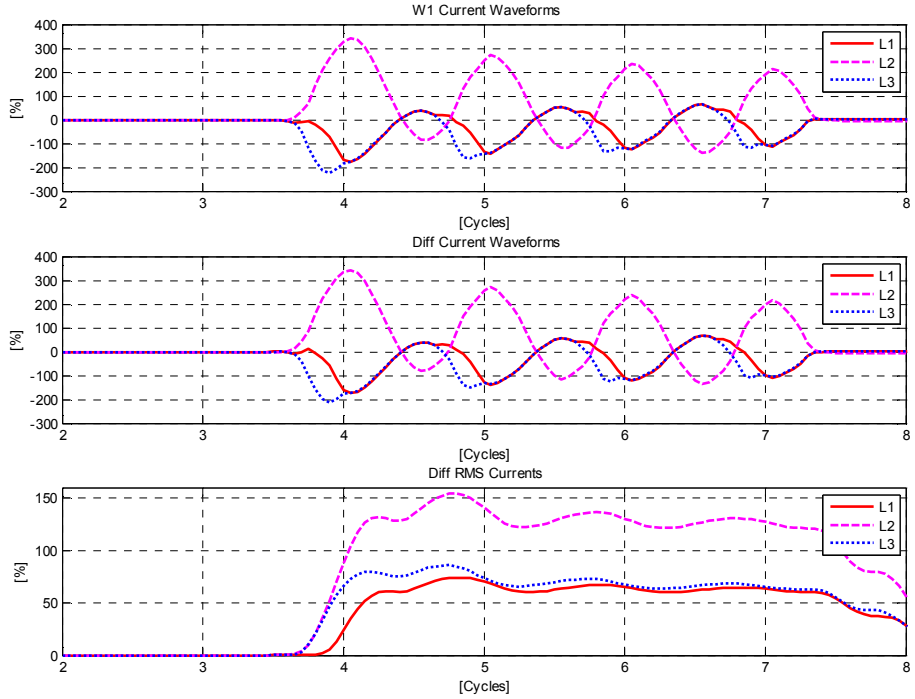

Figure 83: Captured DR file during energizing of a faulty 25MVA transformer.

Note that the 110kV winding currents do not have typical inrush waveforms. For example, typical current gaps, as shown previously are no longer present. This characteristic can be used within numerical differential protection to speed up the relay operation.

Field Case #2

This field case was captured on a three-winding power transformer with the following rating data 20MVA, 110±13*1,15%/21/10,5kV, YNyn0(d5), 50Hz. Note that the transformer tertiary winding is not loaded and it is used as a delta-connected equalizer winding. The 110kV winding neutral point is directly grounded while the 20kV winding neutral point is grounded via a 40Ω resistor. The transformer suffered an internal fault in the 110kV winding in phase L2, as shown in Figure 111. After correct tripping by the differential protection relay the operator tried again to energize the faulty transformer. The DR file was captured during this transformer energizing attempt by the existing differential relay having a sampling rate of 20 samples per power system cycle. In Figure 84 the following waveforms, either extracted or calculated from this DR file, are presented:

- 110kV current waveforms;
- instantaneous differential current waveforms; and,
- RMS values of the differential currents.

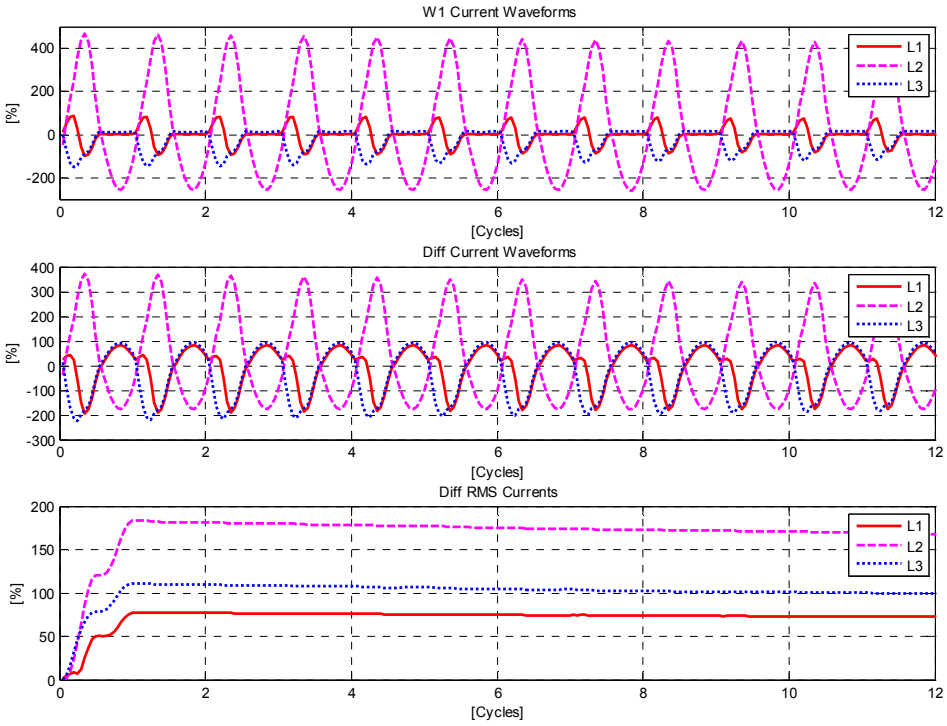

Figure 84: Captured DR file during energizing of a faulty 20MVA transformer.

Note that the 110kV, phase L2 winding current has a close to sinusoidal waveform while the other two phases have typical inrush current waveforms. Current waveforms generated by such operating conditions can cause delayed operation of the transformer differential protection. Using adaptive features within numerical differential relays [12] makes it possible to speed-up the operation of traditional differential protection for such cases.

Chapter 10

Differential or Directional Protection

Directional protection monitors the phase angle difference between two phasors in order to determine whether protection operation should occur or not. A similar concept of α- and β- plane for the differential protection was introduced in [5], however it was only defined for protected objects with two ends and mainly used for line/feeder differential protection. In its basic form these two planes define the phase angle relationship between the currents from two sides of a protected object, which makes a directional principle inherent to the differential protection scheme. Recently an α-plane based concept was used for the design of a numerical line differential protection [26], [27] and [28].

10.1 Generalized Directional Principle for Differential Protection

The directional principle is also inherent to equation (4.32). In order to be better understood, the directional principle equation (4.32) can be re-written in the following form:

$$\begin{bmatrix} Id\_L1 \\ Id\_L2 \\ Id\_L3 \end{bmatrix} = \begin{bmatrix} DCC\_L1_{W1} \\ DCC\_L2_{W1} \\ DCC\_L3_{W1} \end{bmatrix} + \sum_{i=2}^{n} \begin{bmatrix} DCC\_L1_{Wi} \\ DCC\_L2_{Wi} \\ DCC\_L3_{Wi} \end{bmatrix} \tag{10.1}$$

On the right-hand side of equation (10.1) we have two terms, which offer the possibility to represent an n-winding transformer with an equivalent two-winding transformer. The first term is the differential current contribution from the winding one side, as defined in equation (4.31). The second term represents the differential current contribution from the equivalent second winding. If we now assume that magnitude and phase angle corrections are ideally performed, the total differential current shall be equal to zero for all symmetrical or non-symmetrical through-load conditions including external faults. Thus, if we assume that the all three differential currents are approximately zero the following formula can be written:

$$\begin{bmatrix} DCC\_L1_{W1} \\ DCC\_L2_{W1} \\ DCC\_L3_{W1} \end{bmatrix} \approx -\sum_{i=2}^{n} \begin{bmatrix} DCC\_L1_{Wi} \\ DCC\_L2_{Wi} \\ DCC\_L3_{Wi} \end{bmatrix} \tag{10.2}$$

Note that this formula is only valid during all through-load conditions (i.e. not during internal faults). Consequently for every one of the three-phases the resultant phasors from the left and right hand side of formula (10.2) should have equal magnitude and shall be in phase (i.e. with phase angle shift of 0^o between them). Theoretically, any phase angle other than 0^o between these two phasors would mean the existence of a differential current and consequently the presence of an internal fault. In the case of an ideal internal fault, these two phasors would be 180^o out of phase. If this directional rule is applied, the differential protection is converted to a directional comparison protection by the simple analysis of the phase angle shift between the two phase-wise phasors defined in formula (10.2).
Note the minus sign on the right hand side of formula (10.2). In practice, this minus sign means that the CT reference direction, shown in Figure 14, is reversed for the equivalent second winding. This inversion ensures the zero degree phase angle shift between the two phasors during all through-load conditions.

It is possible to re-write equation (10.1) in the following way:

$$-\sum_{i=2}^{n}\begin{bmatrix} DCC\_L1_{Wi} \\ DCC\_L2_{Wi} \\ DCC\_L3_{Wi} \end{bmatrix} = \begin{bmatrix} DCC\_L1_{W1} \\ DCC\_L2_{W1} \\ DCC\_L3_{W1} \end{bmatrix} - \begin{bmatrix} Id\_L1 \\ Id\_L2 \\ Id\_L3 \end{bmatrix} \tag{10.3}$$

If (10.3) is now inserted into (10.2) the following formula is obtained:

$$\begin{bmatrix} DCC\_L1_{W1} \\ DCC\_L2_{W1} \\ DCC\_L3_{W1} \end{bmatrix} \approx \begin{bmatrix} DCC\_L1_{W1} \\ DCC\_L2_{W1} \\ DCC\_L3_{W1} \end{bmatrix} - \begin{bmatrix} Id\_L1 \\ Id\_L2 \\ Id\_L3 \end{bmatrix} \tag{10.4}$$

Note that this formula is only valid during all through-load and external fault conditions when all three differential currents are approximately zero (i.e. not valid during internal faults). Now the directional comparison can be performed on two phase-wise phasors obtained from the left and the right hand side of the formula (10.4). From a mathematical point of view formulas (10.4) and (10.2) are equivalent. However, in practice it is much easier to implement formula (10.4) within a numerical differential relay. At the same time formula (10.4) can be easily applied on any protected power transformer side by simply exchanging the differential current contribution from the winding one side with the differential current contribution from the winding side were formula (10.4) shall be applied.
For power transformer differential protection, the negative-sequence current component based differential currents are calculated by using equation (4.34). Thus the directional comparison criterion obtained from formula (10.4) for phase-wise differential currents can be applied in a similar manner for negative sequence current components and it is given in the following formula:

$$DCCNS\_L1_{W1} \approx DCCNS\_L1_{W1} - IdNS \tag{10.5}$$

This formula is only valid during all through-load conditions (i.e. not during internal faults). Note that a similar formula can be constructed for the positive sequence current components as well.

10.2 Negative Sequence Based Internal/External Fault Discriminator

The use of negative sequence quantities for transformer protection has been proposed in the literature [30], [46]. The existence of a relatively high negative-sequence current component is in itself proof of a disturbance on the power system, and possibly of a fault in the protected power transformer. The negative-sequence current components are measurable indications of abnormal conditions, similar to the zero-sequence current components. One advantage of the negative-sequence current component compared to the zero-sequence current component is that it provides coverage for phase-to-phase faults as well, not only for phase-to-earth faults. Theoretically, the negative sequence current component does not exist during symmetrical three-phase faults. However the negative sequence current component appears during the initial stage of such faults, as shown in [39], for a period of time long enough for the numerical differential relay to make a proper directional decision. Further, the transfer of the negative sequence current component through the power transformer is not prevented by Yd or Dy winding connections. The negative sequence current component is always properly transformed to the other side of any power transformer, regardless of its phase angle shift and type of external disturbance. Finally, the negative sequence current component is typically not affected by fully symmetrical through-load currents. The algorithm of the internal/external fault discriminator is based on the theory of symmetrical components. In [21] and [43] it has been stated that the:

- source of the negative-sequence currents is at the point of fault;
- negative-sequence currents distribute through the negative-sequence network; and,
- negative-sequence currents obey the first Kirchhoff's law.

Imagine a power transformer with a turns ratio equal to 1, and a zero degree phase displacement, e.g. a transformer of the connection group Yy0. For an external fault the fictitious negative sequence source will be located outside the differential protection zone at the fault point. Thus the negative sequence current component will enter the healthy power transformer on the fault side, and leave it on the other side, properly transformed. According to the current direction definitions in Figure 14, the negative sequence current components on the respective power

transformer sides will have opposite directions. In other words, the internal/external fault discriminator sees these currents as having a relative phase displacement of exactly 180°, as shown in Figure 85.

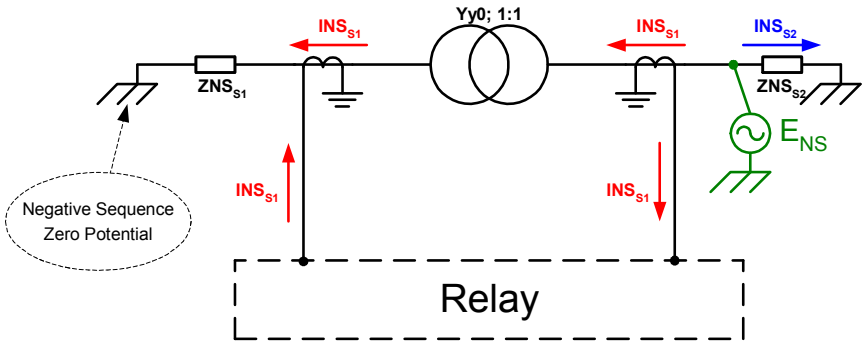

Figure 85: Flow of Negative Sequence Current Components during external fault.

For an internal fault (with the fictitious negative sequence voltage source within the protected power transformer) the negative sequence current components will flow out of the faulty power transformer on both sides. According to the current direction definitions in Figure 14, the negative sequence currents on the respective power transformer sides will have the same direction. In other words, the internal/external fault discriminator sees these currents as having a relative phase displacement of zero electrical degrees, as shown in Figure 86. In reality, for an internal fault, there might be some small phase shift between these two currents due to the possibility of having different negative sequence impedance angles for the source equivalent circuits on the two power transformer sides.

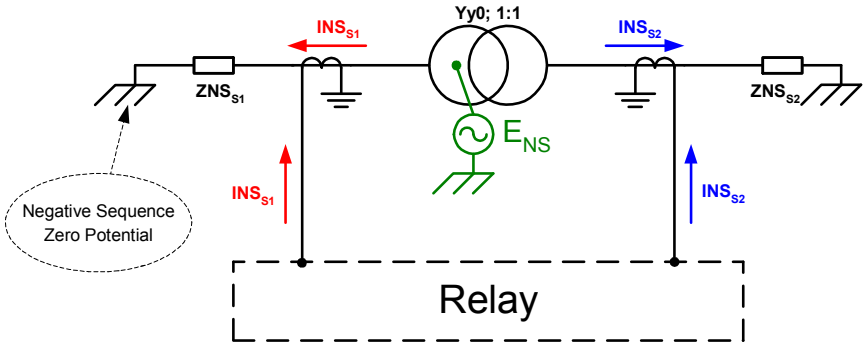

Figure 86: Flow of Negative Sequence Current Components during internal fault.

However, if a power transformer has a non-zero phase displacement, a non-unity turns ratio and a multi-winding arrangement, the internal/external fault discriminator can be instead based on a directional comparison method, as defined by formula (10.5). When this directional comparison method is used, a similar $0^o/180^o$ rule is again valid between the two negative sequence current component phasors defined by formula (10.5). Thus, for any unsymmetrical external fault, the two negative sequence current component phasors defined by formula (10.5) will be in phase regardless of the power transformer turns ratio, phase angle displacement or number of windings, while for any internal fault these two phasors will be approximately 180^o out of phase.

In order to perform the internal/external fault algorithm (e.g. directional comparison), the magnitude of the two negative sequence phasors must be high enough. Both negative sequence phasor magnitudes must exceed a certain minimum limit before the directional comparison is permitted. On the other hand, in order to obtain a good sensitivity of the internal/external fault discriminator, the value of this minimum limit must not be too high. In the algorithm this limit is made settable in the range from 1% to 20% of the differential protection base, with a nominal value of 4%. If either of the negative sequence current component phasors to be compared is too small (less than the pre-set minimum limit), no directional comparison is made in order to avoid the possibility of an incorrect decision. This magnitude check will also guarantee the stability of the algorithm when the power transformer is energized.
Once both negative sequence current component phasors exceed the pre-set minimum limit the directional comparison is performed. An internal fault is declared if the phase angle between the two phasors is between 120 and 240 degrees. This is done in order to ensure proper operation of the phase angle comparator during external faults followed by CT saturation.

The internal/external fault discriminator is actually a very powerful and reliable method. It detects even minor faults, with high sensitivity and speed, and at the same time discriminates with a high degree of dependability between internal and external faults. Thus it can be added as the second criterion for the operation of the traditional power transformer differential relay. If the operating point of the differential relay is above the traditional operating characteristic and simultaneously the internal/external fault discriminator confirms that the fault is internal, the

trip signal can be issued immediately without any additional time delay typically needed to check for second and fifth current components as described in Section 9.4. Thus, extremely fast tripping is achieved for most internal faults.

Note that the internal/external fault discriminator has the following shortcomings:

- it requires that the protected transformer is loaded (i.e. connected to the rest of the power system on at least two sides); and,
- it doesn't provide clear indication about the faulty phase.

10.3 Evaluation of the Directional Comparison Principle by Using Records of Actual Faults

The performance of the internal/external fault discriminator and phase-wise directional comparison principle will be evaluated by using recordings of actual faults captured in the field.

Field Case #1

This field case was captured on a three-winding transformer with the following rating data 16/8/8MVA; 115/6.3/6.3kV; Yd5d5; 50Hz. This transformer is protected by a numerical, three-winding differential protection. However, due to special connections, as explained in Section 4.6, the phase shift compensation shall be performed as if the transformer were with the vector group Yd7d7.
In order to calculate the differential currents in accordance with equation (4.30) the base currents and compensation matrixes as shown in Table 17 shall be used.

Table 17: Compensation data for 16/8/8MVA; 115/6.3/6.3kV; Yd7d7 Transformer

	Base Current Ib	Compensation Matrix MX
W1, 115kV	80.3A	$M0(0^{o}) = \frac{1}{3} \cdot \begin{bmatrix} 2 & -1 & -1 \\ -1 & 2 & -1 \\ -1 & -1 & 2 \end{bmatrix}$
W2, 6.3kV	1466.7A	$M(-150^{o}) = \begin{bmatrix} -0.244 & 0.911 & 0.333 \\ 0.333 & -0.244 & 0.911 \\ 0.911 & 0.333 & -0.244 \end{bmatrix}$
W3, 6.3kV	1466.7A	$M(-150^{o}) = \begin{bmatrix} -0.244 & 0.911 & 0.333 \\ 0.333 & -0.244 & 0.911 \\ 0.911 & 0.333 & -0.244 \end{bmatrix}$

The two 6.3kV networks are passive (i.e. without installed generation) and have high-impedance grounded neutral points. The 110kV star point of this transformer is directly grounded. The disturbance file was captured during an external earth-fault in the 110kV network at a sampling rate of 600Hz (i.e. 12 samples per cycle). Note that this is an excellent example of why zero sequence current reduction is absolutely necessary on the 110kV side. Without it, the power transformer differential relay would maloperate for this external fault due to the massive zero sequence current component on the 110kV side, which is not at all present on the other two delta sides.

In Figure 87 the following waveforms, either extracted or calculated from this DR file, are presented:

- W1, W2 and W3 individual phase current waveforms;
- RMS values of the differential currents; and,
- phase angle between the two negative sequence phasors, as defined in formula (10.5).

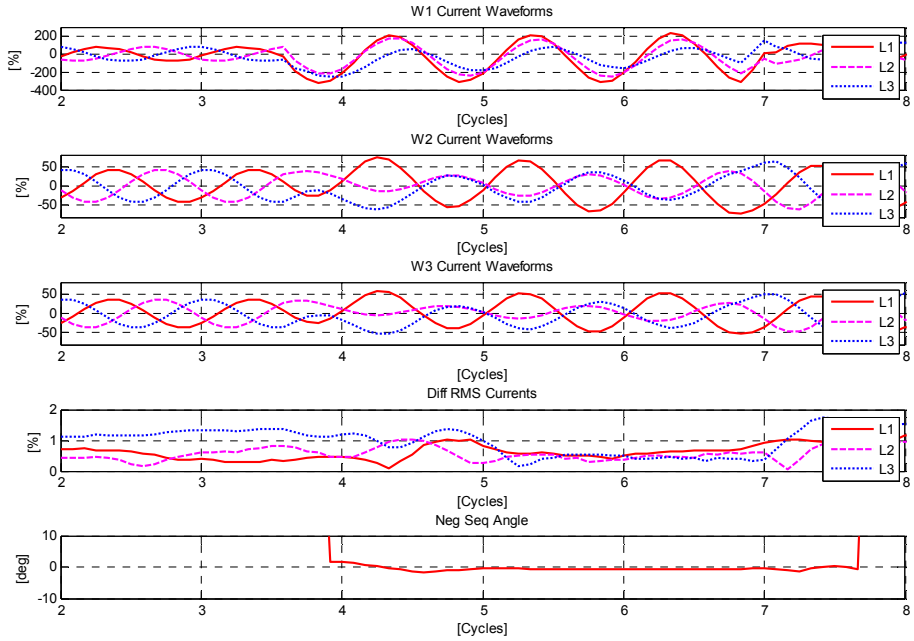

Figure 87: External fault on 110kV side.

Therefore, regardless of the different grounding methods of the two networks, the internal/external fault discriminator will categorize this disturbance as an external fault. In Figure 88 the phasor diagram for the "usual" negative sequence current components from all three sides of the protected transformer are shown at the time instant which corresponds to time 5.5 cycles shown in Figure 87. Note that certain magnitude differences and phase angle shifts do exist between the negative sequence current components from the two delta sides.

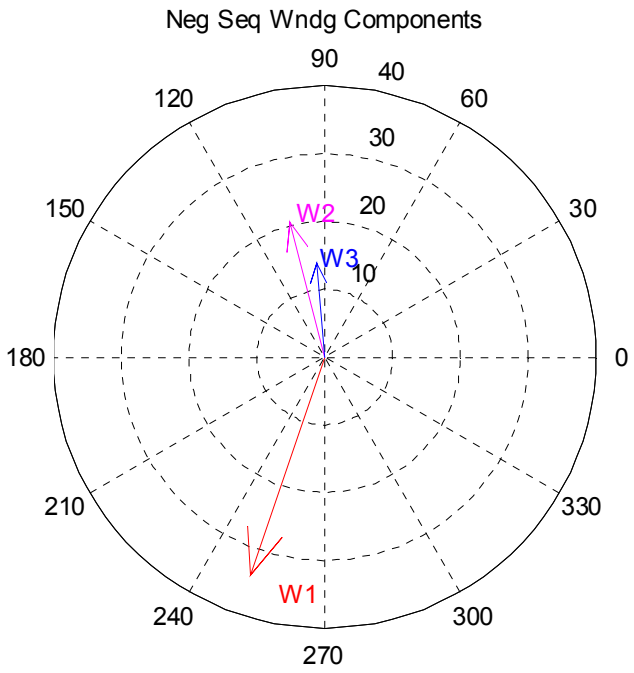

Figure 88: Negative sequence current components at t=5.5 cycles.

Field Case #2

This field case was captured on a symmetrical type, dual-core PST with the following rating data 600MVA; 232kV; ±35^{o} in 57 steps; 50Hz. This PST is protected with the classic IEEE protection scheme [37]. In order to calculate the differential currents in accordance with equation (4.30) the base currents and compensation matrixes as shown in Table 18 shall be used. The fault happened in full retard position (i.e. tap position one). The disturbance file was captured during an external three-phase fault on the L-side of the PST at a sampling rate of 1000Hz (i.e. 20 samples per cycle).
In Figure 89 the following waveforms, either extracted or calculated from this DR file, are presented:

- S- and L-side individual phase current waveforms; and,
- phase angle between the two negative sequence phasors, as defined in formula (10.5).

Table 18: Compensation data for the 600MVA; 232kV; ±35° double-core PST

	Base Current Ib	Compensation Matrix MX
S-side, 232kV	1493A	$M(0^o)=\begin{bmatrix}1 & 0 & 0\\ 0 & 1 & 0\\ 0 & 0 & 1\end{bmatrix}$
L-side, 232kV	1493A	$M(35^o)=\begin{bmatrix}0.879 & -0.271 & 0.391\\ 0.391 & 0.879 & -0.271\\ -0.271 & 0.391 & 0.879\end{bmatrix}$

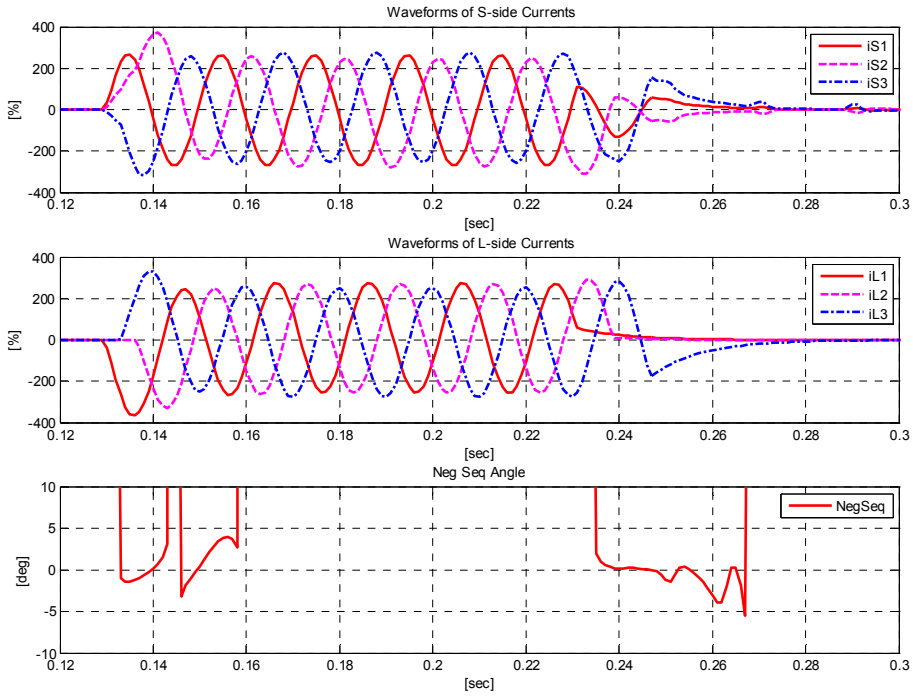

Figure 89: External three-phase fault on the L-side of a 600MVA, 232kV PST.

Note that the internal/external fault discriminator could determine that this fault is external during the first and last cycle of the fault, regardless of the fact that this is a symmetrical three-phase fault.

Field Case #3

This field case was captured on a three-winding transformer with the following rating data 40/40/10MVA; 110/36.75/10.5kV; Yy0d5; 50Hz. Note that this transformer tertiary winding is not loaded and it is used as a delta-connected equalizer winding. This transformer is protected with a numerical, two-winding differential protection. In order to calculate the differential currents in accordance with equation (4.30) the base currents and compensation matrixes as shown in Table 19 shall be used.

Table 19: Compensation data for the 40MVA; 110/36,75/10.5kV transformer

	Base Current Ib	Compensation Matrix MX
W1, 110kV	201A	$M0(0^o) = \frac{1}{3} \cdot \begin{bmatrix} 2 & -1 & -1 \\ -1 & 2 & -1 \\ -1 & -1 & 2 \end{bmatrix}$
W2, 36,75kV	628.4A	$M0(0^o) = \frac{1}{3} \cdot \begin{bmatrix} 2 & -1 & -1 \\ -1 & 2 & -1 \\ -1 & -1 & 2 \end{bmatrix}$

The 35kV network is passive (i.e. without installed generation) and with resistance grounded neutral point. The earth-fault current in the 35kV network is limited to 300A primary. The 110kV star point of this transformer is directly grounded. The disturbance file is captured during an evolving fault at the 35kV busbar, caused by an animal climbing into the busbar. The fault started as L3-to-ground, then it evolved into L2-L3-to-ground and finally it became a three-phase fault. Note that the captured recording starts during the L3-to-ground fault, therefore the pre-fault current waveforms are not available. The sampling rate in the file is 1000Hz (i.e. 20 samples per cycle).

In Figure 90 the following waveforms, either extracted or calculated from this DR file, are presented:

- W1- and W2-side individual phase current waveforms; and,
- RMS differential currents.

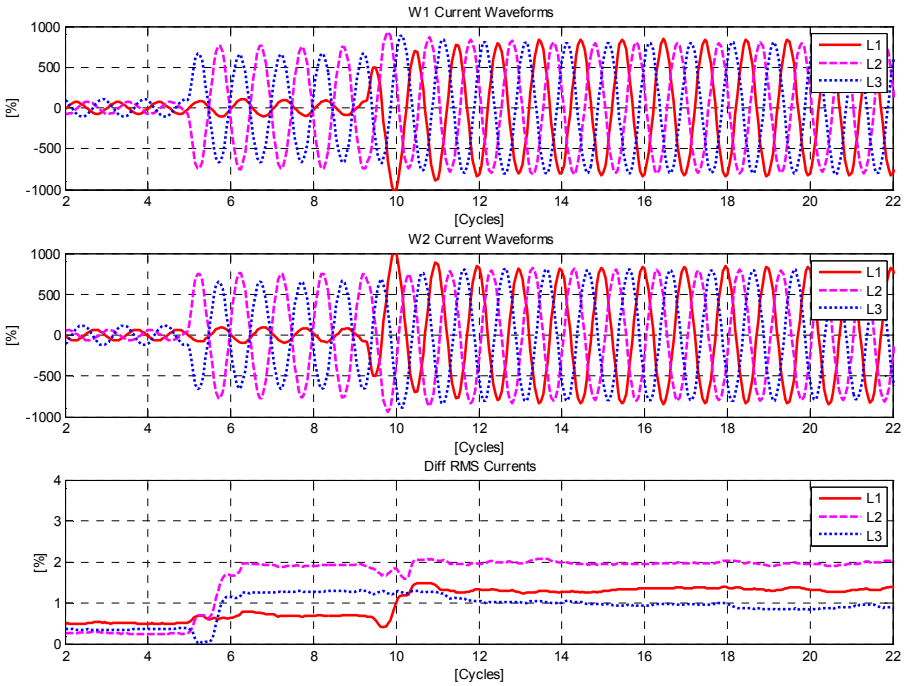

Figure 90: External evolving fault on the 35kV side.

In Figure 91 the following waveforms, calculated from this DR file, are presented:

- phase angle difference between the two negative sequence and the two positive sequence phasors respectively as defined by equation (10.5); and,
- phase angle difference between the phase-wise phasors, as defined in the equation (10.4).

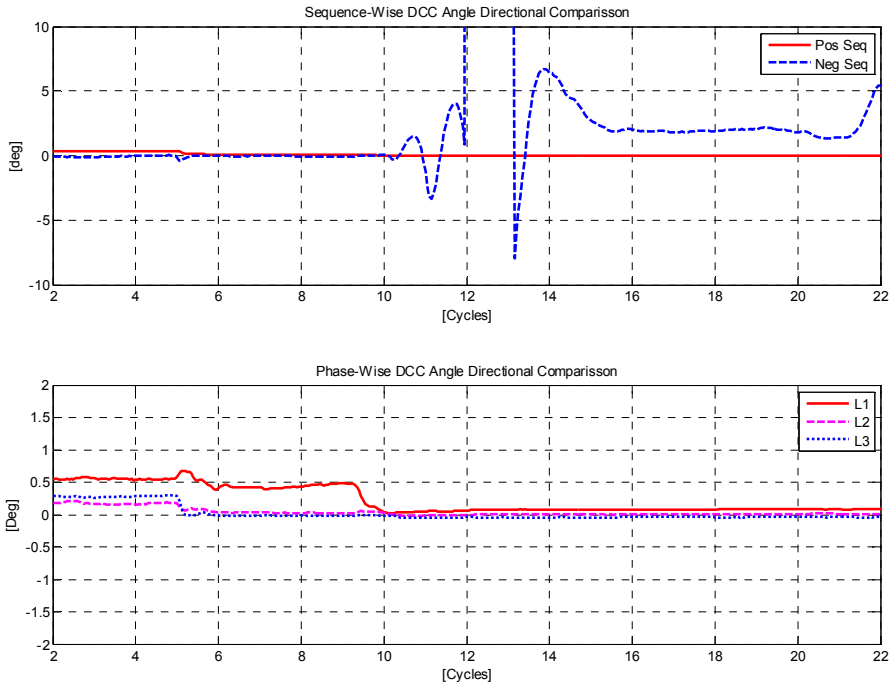

Figure 91: Directional comparison during an external evolving 35kV fault.

Note that the negative sequence based internal/external fault discriminator could determine that this fault is external at the beginning of the fault. However after the fault becomes a three-phase fault, the negative sequence phase angle starts to deviate from the theoretical value of zero degrees. The reason is that negative sequence quantities had quite small magnitudes while the fault was the three-phase fault. Such behaviour of the negative sequence quantities made it difficult to precisely determine the phase angle between them. At the same time positive sequence and phase-wise directional comparisons can securely determine that this fault is external for the entire fault duration.

Field Case #4

This field case was captured on an auto-transformer with the following rating data 160/160/50MVA; 220/126/10.5kV; YNautod11; 50Hz, in accordance with the IEC terminology [58]. It shall be noted that this auto-transformer tertiary winding is not loaded and is used as a delta-connected equalizer winding. The transformer was protected with one two-winding differential relay.

In order to calculate the differential currents for this transformer in accordance with equation (4.30) the base currents and compensation matrixes as shown in Table 20 shall be used.

Table 20: Compensation data for the 160MVA; 220/126/10.5kV auto-transformer

	Base Current Ib	Compensation Matrix MX
W1, 220kV	420A	$M0(0^o) = \frac{1}{3} \cdot \begin{bmatrix} 2 & -1 & -1 \\ -1 & 2 & -1 \\ -1 & -1 & 2 \end{bmatrix}$
W2, 126kV	733A	$M0(0^o) = \frac{1}{3} \cdot \begin{bmatrix} 2 & -1 & -1 \\ -1 & 2 & -1 \\ -1 & -1 & 2 \end{bmatrix}$

The disturbance file was captured by the numerical differential relays and stored directly in secondary amperes. The CT on the 220kV side was 600/1 and on the 126kV side 1000/1. Thus, these ratios must be taken in the account during the analysis of the secondary quantities from the DR file. This external fault was captured during the primary testing of the relay. The fault was intentionally applied for testing purposes as a single-phase L1 fault on the 126kV side. Phases L2 and L3 on 126kV side were left open circuited during the test, after which the transformer 126kV CB was directly closed onto the fault. The sampling rate in the file is 600Hz (i.e. 12 samples per cycle).

In Figure 92 the following waveforms, either extracted or calculated from this DR file, are presented:

- W1- and W2-side individual phase current waveforms;
- RMS values of the differential currents; and,
- phase angle between the two negative sequence phasors, as defined in formula (10.5).

Note that the incomplete circuit on the 126kV side (i.e. open L2 and L3 phases) did not adversely influence the proper operation of the negative sequence based internal/external fault discriminator.

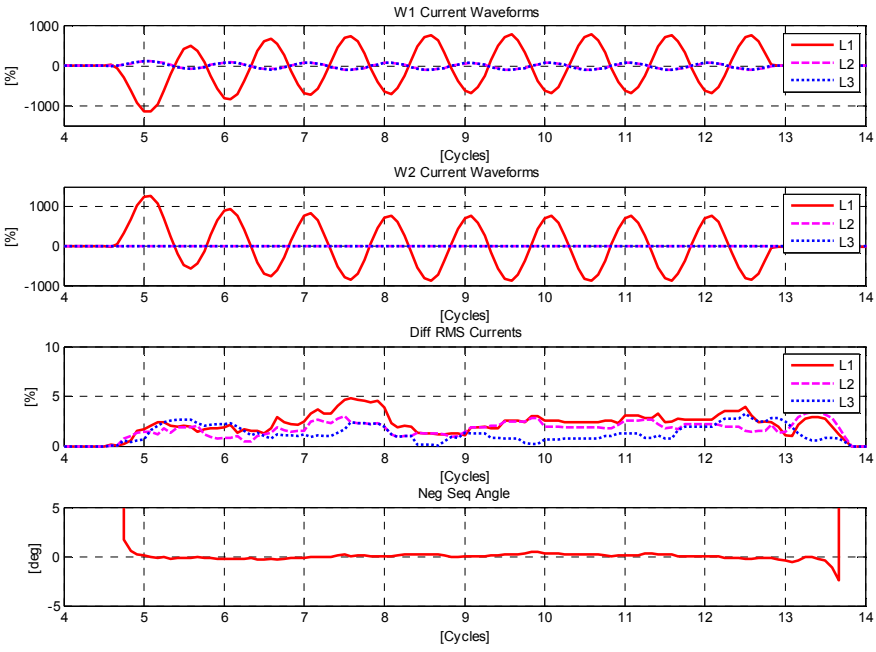

Figure 92: External L1-Ground fault on the 126kV side of a 160MVA auto-transformer.

Field Case #5

This field case is a repeat of the primary test presented above under Field Case #4. The only difference is that an additional resistance was added in the CT secondary circuit in phase L1 on the 126kV side. This was done in order to check the performance of the relay for CT saturation.
In Figure 93 the following waveforms, either extracted or calculated from this DR file, are presented:

- W1- and W2-side individual phase current waveforms; and
- RMS values of the differential currents.

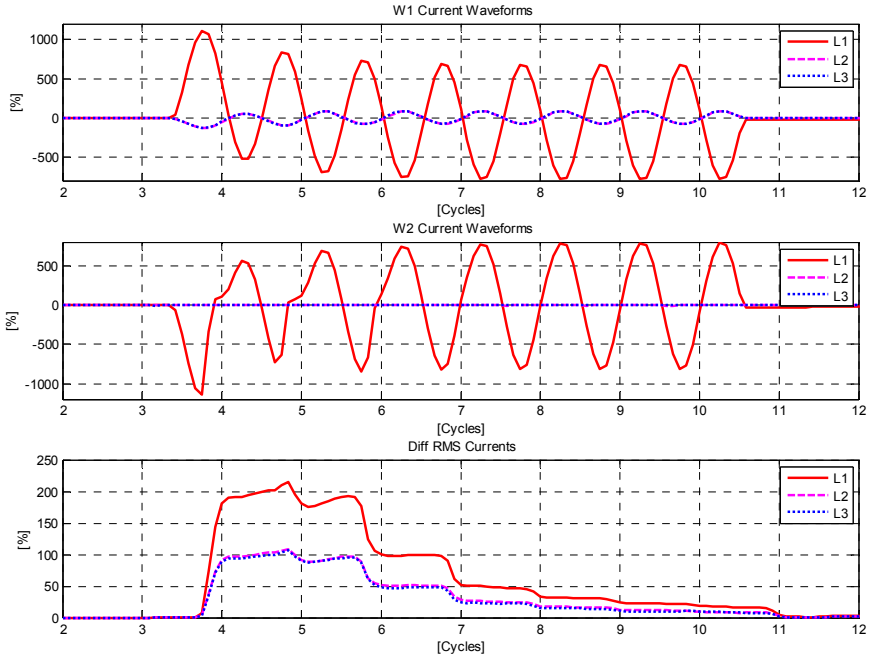

Figure 93: External L1-Ground fault on the 126kV side
of a 160MVA auto-transformer with CT saturation.

In Figure 94 the following waveforms, calculated from this DR file, are presented:

- phase angle difference between the two negative sequence and the two positive sequence phasors respectively as defined by equation (10.5); and,
- phase angle difference between the phase-wise phasors, as defined in equation (10.4).

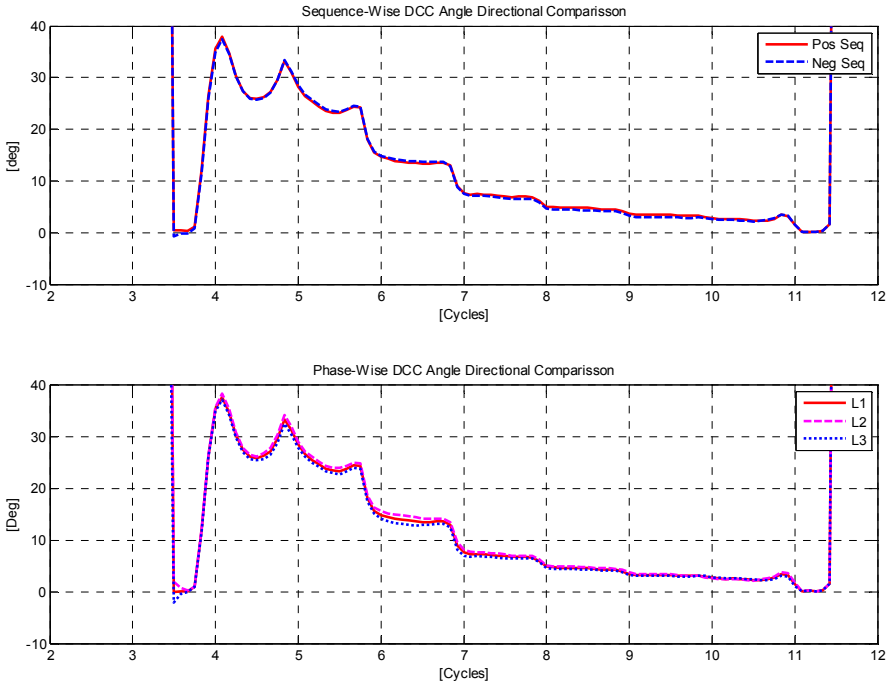

Figure 94: Directional comparison during an external L1-Groung fault.

Note that the CT saturation of the 126kV CT caused an angle deviation from the theoretical 0^o for all directional comparison principles applied in this case. However, this deviation is only temporary while the CT is saturated. Note that before CT saturation the relay could measure this angle equal to zero and thus easily conclude that this fault is external. The transient angle deviation of 40^o is still far away from the theoretical angle for internal fault of 180^o.

Field Case #6

This field case was captured on a three-winding transformer with the following rating data 20/20/10MVA; 110/36.75/10.5kV; Yy0d5; 50Hz. Note that this transformer tertiary winding is not loaded and is used as a delta-connected equalizer winding. This transformer is protected with a numerical, two-winding differential protection. In order to calculate the differential currents in accordance with equation (4.30) the base currents and compensation matrixes as shown in Table 21 shall be used.

Table 21: Compensation data for the 20MVA; 110/36,75/10.5kV transformer

	Base Current Ib	Compensation Matrix MX
W1, 110kV	101A	$M0(0^o) = \frac{1}{3} \cdot \begin{bmatrix} 2 & -1 & -1 \\ -1 & 2 & -1 \\ -1 & -1 & 2 \end{bmatrix}$
W2, 36,75kV	314A	$M0(0^o) = \frac{1}{3} \cdot \begin{bmatrix} 2 & -1 & -1 \\ -1 & 2 & -1 \\ -1 & -1 & 2 \end{bmatrix}$

The 35kV network is passive (i.e. without installed generation) and with a resistance grounded neutral point. The earth-fault current in the 35kV network is limited to 300A primary. The 110kV star point of this transformer is directly grounded. The disturbance file was captured when an operator had erroneously tried to open the disconnector under-load in the 35kV transformer bay. The fault was therefore an external fault for the transformer differential protection, which started as an L1-L2 fault and evolved into a three-phase fault. During this fault the 35kV CTs went into extremely heavy saturation that ultimately caused the maloperation of the existing differential relay. The sampling rate in the file is 1000Hz (i.e. 20 samples per cycle).

In Figure 95 the following waveforms, either extracted or calculated from this DR file, are presented:

- W1- and W2-side individual phase current waveforms; and,
- RMS values of the differential currents.

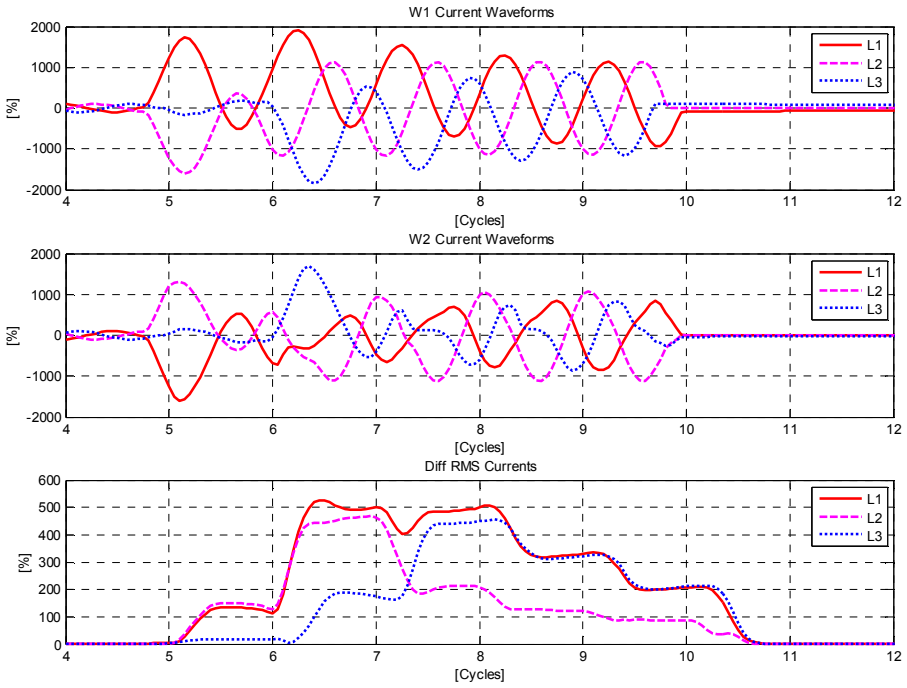

Figure 95: External L1-L2 fault evolving into
a three-phase fault on the 35kV side.

In Figure 96 the following waveforms, calculated from this DR file, are presented:

- phase angle difference between the two negative sequence and the two positive sequence phasors respectively as defined by equation (10.5); and,
- phase angle difference between the phase-wise phasors, as defined in equation (10.4).

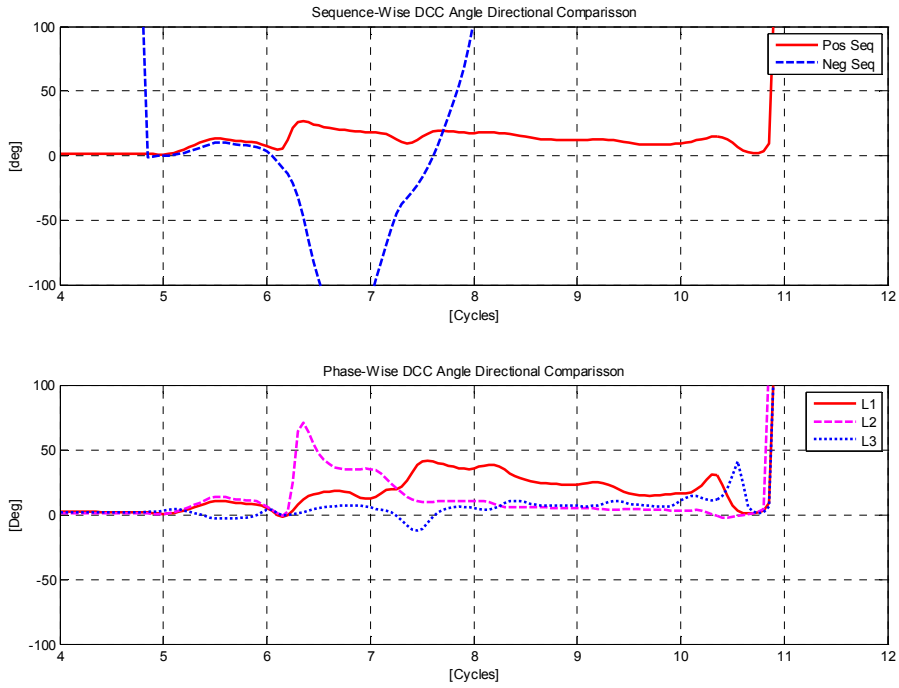

Figure 96: Directional comparison during the external fault on the 35kV.

Note that saturation of the 35kV CTs caused an angle deviation from the theoretical 0^{o} for all directional comparison principles. However, deviation of the negative sequence angle is by far the biggest one due to CT secondary current distortions caused by the evolving three-phase fault. Note that before the CT saturation, the relay could measure this angle equal to zero and thus easily conclude that this fault was external.

Field Case #7

This field case was captured on an auto-transformer with the following rating data 150/150/30MVA; 220/115/10.5kV; YNautod5; 50Hz, in accordance with IEC terminology [58]. It shall be noted that this auto-transformer tertiary winding was not loaded and is used as a delta-connected equalizer winding. This auto-transformer is protected with two numerical, two-winding differential protections from different manufacturers, in accordance with the utility protection philosophy.
In order to calculate the differential currents for this transformer in accordance with equation (4.30), the base currents and compensation matrixes as shown in Table 22 shall be used.

Table 22: Compensation data for the 150MVA; 220/115/10.5kV auto-transformer

	Base Current Ib	Compensation Matrix MX
W1, 220kV	394A	$M0(0^o) = \frac{1}{3} \cdot \begin{bmatrix} 2 & -1 & -1 \\ -1 & 2 & -1 \\ -1 & -1 & 2 \end{bmatrix}$
W2, 115kV	753A	$M0(0^o) = \frac{1}{3} \cdot \begin{bmatrix} 2 & -1 & -1 \\ -1 & 2 & -1 \\ -1 & -1 & 2 \end{bmatrix}$

The disturbance file is captured during an internal phase-to-ground fault, which occurred on the connection between the 110kV phase L2 winding and the 110kV phase L2 bushing within the auto-transformer tank. The sampling rate of the file is 1000Hz (i.e. 20 samples per cycle).

In Figure 97 the following waveforms, either extracted or calculated from this DR file, are presented:

- W1- and W2-side individual phase current waveforms; and,
- RMS values of the differential currents.

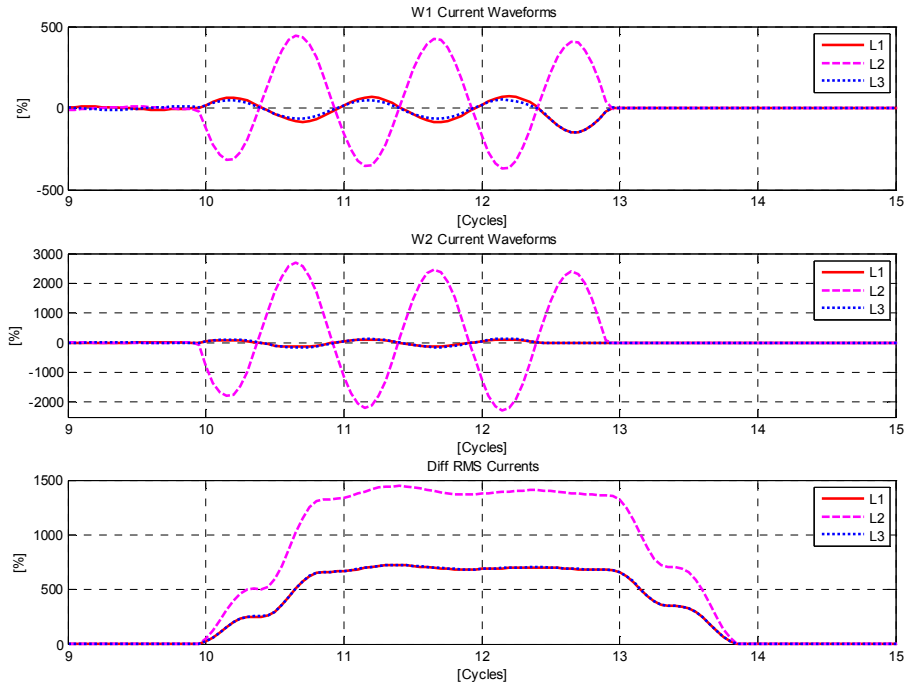

Figure 97: Internal L2-ground fault on the 110kV side of a 150MVA auto-transformer.

In Figure 98 the following waveforms, calculated from this DR file, are presented:

- phase angle difference between the two negative sequence and the two positive sequence phasors respectively as defined by equation (10.5); and,
- phase angle difference between phase-wise phasors, as defined in equation (10.4).

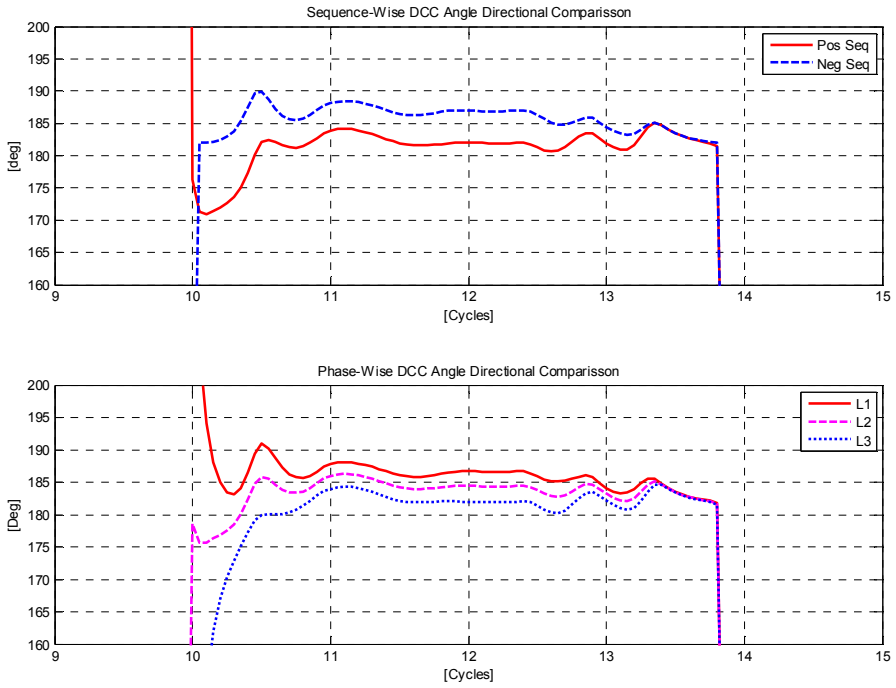

Figure 98: Directional comparison during internal fault.

Note that all directional comparison methods could determine that this fault is internal. But the comparison based on negative sequence quantities could operate in less than half a cycle from the point of fault inception.

Chapter 11

Turn-to-Turn Fault Protection

A study of the records for modern transformer breakdowns that have occurred over a period of years indicates that between 70% and 80% of the total number of transformer failures are eventually traced to internal winding insulation failure [63]. If not quickly cleared, these turn-to-turn faults usually develop into more serious, and costly to repair earth-faults, involving the power transformer iron core. Alternatively, turn-to-turn faults cause arcing within the power transformer tank, making significant damage until tripped by the Buchholtz relay.

These winding faults are mostly a result of the degradation of the insulation system due to thermal, electrical, and mechanical stress, moisture, and other factors. Degradation means reduced insulation quality, which will eventually cause a breakdown in the insulation, leading to adjacent winding turns being shorted (turn-to-turn fault) or to a winding being directly shorted to earth (winding to earth failure). Most often the insulation undergoes a gradual aging process before such a fault happens. Ageing of the insulation reduces both the mechanical and dielectric withstand strength. Under external fault conditions, power transformer windings are temporarily subjected to high radial and compressive forces. As the load increases with system growth, the operating stresses increase. In an ageing transformer the conductor insulation is weakened to the point where it can no longer sustain any additional stress. Under increased stress, for example due to external fault, the insulation between adjacent turns suffers a dielectric failure and a turn-to-turn fault may develop.

A short circuit of a few turns in the power transformer winding (i.e. turn-to-turn fault) will give rise to a heavy fault current in the short-circuited turns. However, changes in the transformer terminal currents will be quite small because of the high ratio of transformation between the whole winding and the short-circuited turns. For that reason, traditional power transformer differential protection has typically not been sensitive enough

to detect such winding turn-to-turn faults before they develop into more serious and costly to repair earth-faults. Such faults can also be detected by Buchholtz (gas operated) relays. However, the detection interval for such low-level faults is in the order of hundreds of milliseconds or even seconds, which often allows the fault to evolve into a more serious one.
Regarding the turn-to-turn fault detection, in the current literature, the most advanced methods are utilizing either wavelet or artificial neural network [3], [18], [40], [50], [53], [55] and [57]. However, in this thesis, methods to improve standard differential protection in order to detect turn-to-turn faults are suggested.

11.1 Basic Turn-to-Turn Fault Theory

Operation of the transformer differential protection is based on Ampere-turn-balance for all coils located on one magnetic core. Let us consider the simplest case of a two winding, single-phase transformer as shown in Figure 99, with its relevant phasor diagram.

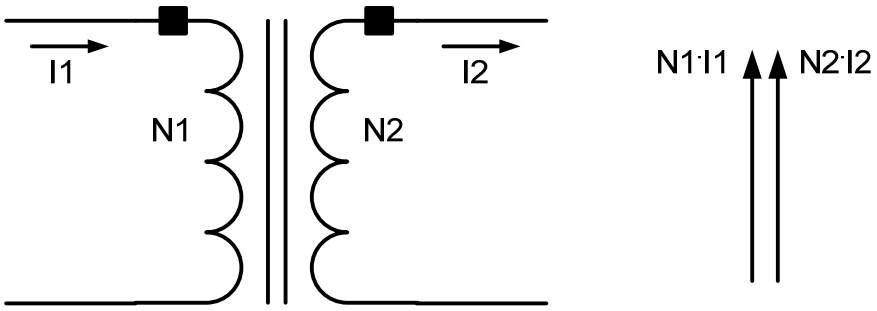

Figure 99: Single-phase, two-winding transformer.

The phasor diagram, shown in Figure 99, neglects the existence of magnetizing current which is necessary to create a magnetic flux in the transformer core. A differential relay would measure currents I1 and I2 scale them appropriately using equation (4.30), and then find a negligible differential current during normal through-load conditions.

Note that power transformers are primarily used to transfer active power between two networks. Thus, it is reasonable to assume that the winding current and voltage are approximately in phase. That means that for power transformers used in a power system, the resultant flux is lagging approximately 90^o behind the current phasors [9].
Let's assume that a turn-to-turn fault has happened in winding two, involving Nx turns, as shown in Figure 100. Note that for practical turn-to-turn faults Nx<<N2.

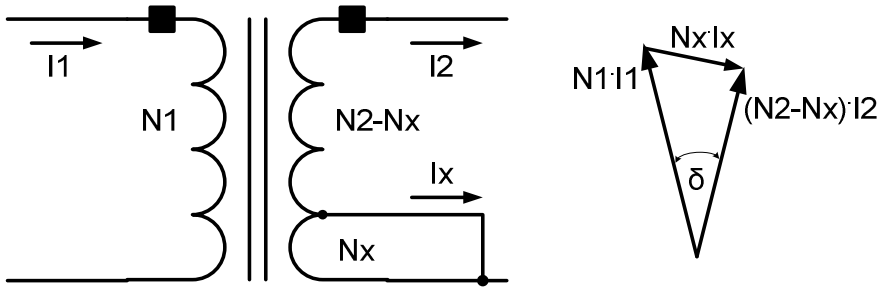

Figure 100: Single-phase, two-winding transformer with an internal turn-to-turn fault.

The induced voltage in the short-circuited turns will cause the additional current component Ix, which is not measured by the differential relay, to circulate through the shorted turns. Because the impedance of the shorted turns is mostly inductive, the current Ix will lag the voltage by approximately 90^o. However, the Ampere-turn-balance principle for all coils located on one magnetic core must still be fulfilled, irrespective of the existence of a turn-to-turn fault. In order to fulfill this requirement, two measured currents will get a certain phase angle shift δ, as shown in Figure 100, but not necessarily any sufficient magnitude increase, in order to compensate for the additional ampere-turn component $Nx \cdot Ix$.

A differential relay will see the component $Nx \cdot Ix$ as a differential current. However, for a turn-to-turn fault, involving just a few turns, the resultant differential current magnitude might be quite small and certainly not within the tripping region of the differential relay operating characteristic.
However, if the differential relay would instead look into the phase angle shift between the two measured currents the turn-to-turn faults can be

detected. Note that the previous explanation for a single-phase, two-winding transformer is still valid in the case of a three-phase power transformer, if the differential relay monitors the phase angle shift between the differential current contributions from different power transformer sides, as explained in Section 10.1.

11.2 Traditional Power Transformer Differential Protection

The problem with classical transformer differential protection is that low-level faults such as turn-to-turn faults can not be detected. The differential relay minimum pickup current in the first section of the relay operate – restraint characteristic is traditionally set to a value between 30% and 40%. When a minor turn-to-turn fault, at fault inception, causes a differential current of 15%, it cannot be detected until it evolves into a more severe fault with bigger differential currents.
However, the opportunity to perform complete magnitude and phase angle shift compensation, as described in Chapter 4, allows for greater sensitivity in the minimum pickup value (e.g. 15%) of the traditional differential protection. This sensitive pickup value enables the traditional differential protection to be more capable in detecting turn-to-turn faults, as illustrated in the examples presented at the end of this chapter.

11.3 Directional Comparison Based on Negative Sequence Current Component

The existence of negative sequence current components during turn-to-turn fault conditions allows the use of the internal/external fault discriminator, described in Section 10.2, for detection of such faults. The sensitive, negative sequence current based turn-to-turn fault protection independently detects low-level faults not detected by the traditional transformer differential protection. The essential part of this sensitive negative sequence protection is the internal/external fault discriminator previously described. In order to be activated, the sensitive protection doesn't require any pickup signal from the power transformer biased differential protection, based on phase currents. If the magnitudes of the

contributions to the negative sequence differential current are above the minimum limit (e.g. 4%), then their relative phase displacement is determined. If the disturbance is characterized as an internal fault, then a separate trip request will be placed. Any decision regarding a final trip request must be confirmed several times in succession in order to cope with possible CT transients, causing a short additional operating time delay. Trustworthy information on whether a fault is internal or external is typically obtained in about ten milliseconds after the fault inception, depending on the magnitudes of the fault currents. For low-level turn-to-turn faults the overall response time of this protection can be in the order of 30 milliseconds. At heavy through-load conditions this feature shall be temporarily blocked, in order to prevent maloperation during secondary CT transients.

This protection principle for turn-to-turn faults has, however, the following drawbacks:

- Requires the presence of relatively high negative sequence current components on at least two sides of the protected power transformer;
- might be desensitized by the presence of unsymmetrical through-load currents; and,
- doesn't provide any indication about the faulty phase.

11.4 Phase-Wise Directional Comparison

As described in Section 10.1, the differential protection can be converted to the directional comparison principle. Thus, if this directional comparison principle is applied in a phase segregated way, a sensitive detection of turn-to-turn faults can be achieved as explained at the end of Section 11.1.
In the case of a turn-to-turn fault in any winding on one magnetic core limb, the phase shift between the two phasors from the same phase as defined by equation (10.4) will not be any more zero degrees. Instead, they will have some other arbitrary phase angle shift, caused by the quite high current in the shorted turns, as shown in Figure 100.

Therefore, by continuously monitoring the phase angle between these two phasors in a phase-wise fashion, sensitive, but simple, protection against turn-to-turn faults can be achieved. In order to avoid maloperation of this algorithm for heavy through-fault currents, it can be disabled when the level of the stabilizing current exceeds the pre-set level (e.g. 170% of the power transformer rating). Captured recordings from the field, show that possible trip levels for this type of detection can be set from 3 to 5 degrees, which will ensure a very sensitive turn-to-turn fault detection.

The following additional checks can also be made:

- check that negative sequence differential current is bigger than a pre-set level (e.g. 4%);
- check that different phase angle shifts exist in all three-phases. If the phase angle shift is exactly the same in all three-phases it is most probably caused by incorrect compensation of the OLTC position in case of a PST. It will typically indicate loss of tap-position compensation in the case of differential protection for a phase-shifting transformer. In such a case a separate alarm can be issued; and,
- check that the highest phase differential current doesn't have excessive second harmonic content.

11.5 Evaluation of the Proposed Turn-to-Turn Fault Detection Principles

The performance of the proposed methods to detect turn-to-turn faults will be evaluated on four actual winding faults captured in the field and one RTDS simulated internal winding fault for a symmetrical, double core PST.

Field Case #1

This field case was captured on an auto-transformer with the following rating data 300/300/100MVA; 400/115/10.5kV; YNautod5; 50Hz, in accordance with IEC terminology [58]. It should be noted that this auto-transformer tertiary winding is not loaded and is used as a delta-connected

equalizer winding. This auto-transformer is protected with two numerical, two-winding differential protections from different manufacturers, in accordance with the utility protection philosophy. In this particular installation both numerical differential relays utilize the traditional principle for differential current calculation where y/d connected interposing CTs are used on star-connected power transformer windings, as described in Section 5.1. Due to this reason, lower differential currents were measured during the turn-to-turn fault than the differential currents which are shown in this document. The existing differential relays minimum pickup current is set to 30% of the auto-transformer rating. Within approximately one year the utility had four incidents with this auto-transformer as stated below:

On 2003-04-27 at 09:39:51.199 hours, the auto-transformer 400kV bushing in phase L3 exploded causing a heavy internal fault. The fault was tripped extremely quickly by the unrestrained differential protection stage in less than one power system cycle. The fault current contribution from the 400kV network was 2500% and the fault current contribution from the 110kV network (i.e. fault current through the auto-transformer windings) was up to 500% of the auto-transformer rating. Due to fast tripping, the auto-transformer windings were not damaged. After on-site bushing replacement the auto-transformer was put back into service on 2003-05-08.

On 2004-01-04 at 00:35:07.189 hours, a nearby external fault on the 110kV side in phase L1 appeared. The auto-transformer through-fault current was around 280% of its rating. Both auto-transformer differential protections were stable.

On 2004-05-04 at 05:10:30.614 hours, a nearby external fault on the 110kV side in phase L3 happened. The auto-transformer through-fault current was around 310% of its rating. Both auto-transformer differential protections were stable.

On 2004-05-04 at 05:28:46.736 hours, approximately eighteen minutes after the external fault previously mentioned, the auto-transformer was tripped by the Buchholtz relay. Both numerical differential protections did not operate, and no other current or impedance measuring backup protection had started. By oil analysis it was confirmed that extensive and long-lasting electrical arcing within the auto-transformer tank had caused

the Buchholtz relay operation. The auto-transformer was shipped to the factory for repair and during inspection, a winding fault in phase L3 was found. It was concluded that it was a turn-to-turn fault which had involved only four turns at the auto-transformer neutral point in the common winding of phase L3. Figure 101 shows the affected common winding part in phase L3.

Figure 101: Common auto-transformer winding internal fault in phase L3 at the winding neutral point.

In order to calculate the differential currents for this auto-transformer in accordance with equation (4.30), the base currents and compensation matrixes as shown in the following table, shall be used.

Table 23: Compensation data for the 300MVA; 400/115kV auto-transformer

	Base Current Ib	Compensation Matrix MX
W1, 400kV	433A	$M0(0^o)=\frac{1}{3}\cdot\begin{bmatrix}2&-1&-1\\-1&2&-1\\-1&-1&2\end{bmatrix}$
W2, 115kV	1506A	$M0(0^o)=\frac{1}{3}\cdot\begin{bmatrix}2&-1&-1\\-1&2&-1\\-1&-1&2\end{bmatrix}$

The disturbance recordings, from all aforementioned fault cases for the auto-transformer were available from the two numerical differential relays. By merging the disturbance recording files for fault cases three and four, one overall disturbance file has been made. This merged disturbance file, with 20 samples per power system cycle, was used to specifically test the proposed algorithms for turn-to-turn fault detection.
In Figure 102, relevant instantaneous currents are shown. During the entire turn-to-turn fault, all measured phase currents are smaller than 60% of the auto-transformer rating. Therefore the traditional differential currents were smaller than the pre-set differential minimum operational level, and traditional differential protection could not operate for this fault. However, from Figure 103 it is obvious that the low-level turn-to-turn fault was definitely internal. Operation of the internal/external fault discriminator consistently indicates an internal fault. This independent but sensitive negative-sequence-current-based differential protection detects the fault and characterizes it as internal.

In Figure 102 the following waveforms, either extracted or calculated from this DR file, are presented:

- W1- and W2-side individual phase current waveforms; and
- RMS values of the differential currents.

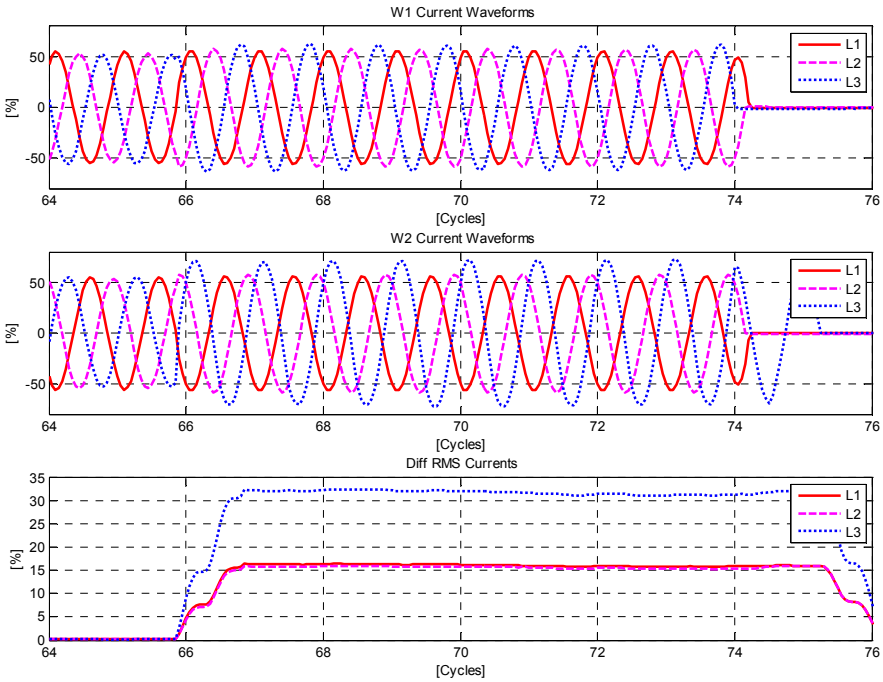

Figure 102: Current waveforms during turn-to-turn fault field case #1.

In Figure 103 the following waveforms, either extracted or calculated from this DR file, are presented:

- phase angle between the two negative sequence phasors, as defined in formula (10.5);
- phase angle between the two phase-wise phasors, as defined in formula (10.4); and,
- phase angle between the two phase-wise phasors, very similar to the one defined in formula (10.4), but with only M type compensation matrices applied on all sides of the protected transformer.

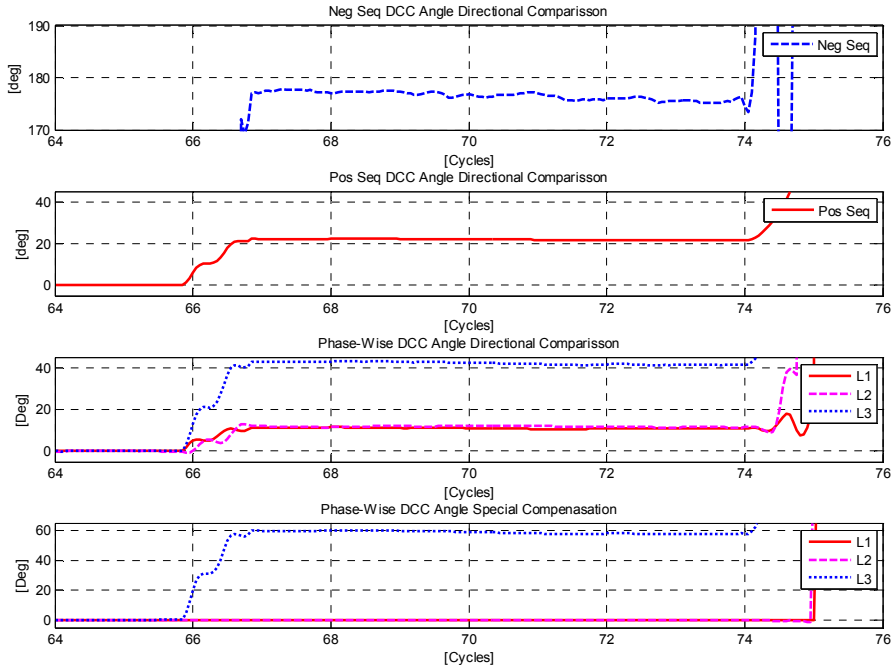

Figure 103: Directional comparison during turn-to-turn fault field case #1.

Note that all types of directional comparison can detect that something is wrong with the protected power transformer. However only the negative sequence based directional comparison has seen the complete angle inversion (i.e. angle of 180^{o}) during this winding fault. What is quite interesting is that the phase-wise directional comparison based on M matrices, being used on all transformer sides can clearly identify the faulty phase.

Field Case #2

This field case was captured on an auto-transformer with the following rating data 300/300/100MVA; 400/115/10.5kV; YNautod5; 50Hz. It should be noted that this auto-transformer tertiary winding is not loaded and is used as a delta-connected equalizer winding. This auto-transformer is protected with one numerical, two-winding differential protection. The differential relays minimum pickup current is set to 20% of the auto-transformer rating.

A serial auto-transformer winding internal fault occurred in phase L2 close to the 110kV connection point as shown in Figure 104. The exact turn-to-turn fault location in one winding disc of the serial winding is shown in Figure 105.

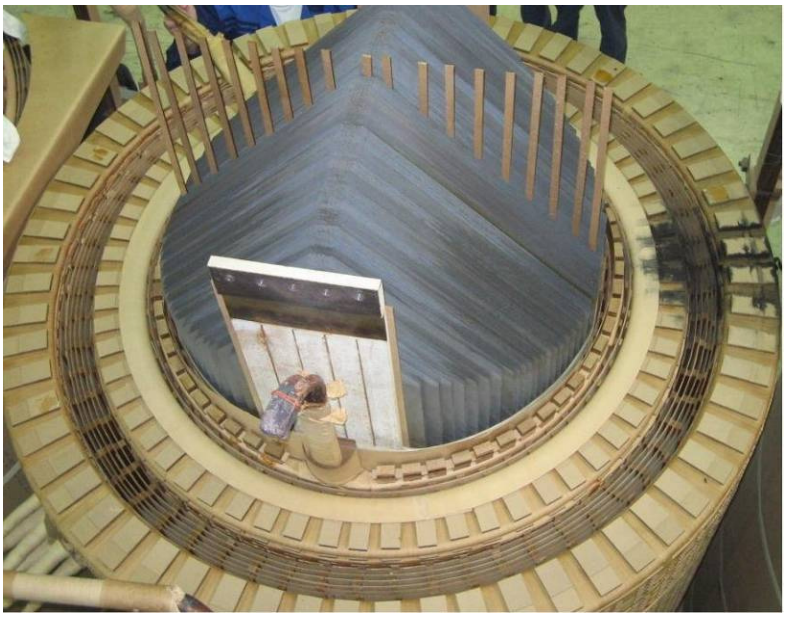

Figure 104: Serial auto-transformer winding internal fault in phase L2 was close to the 110kV connection point.

In order to calculate the differential currents for this auto-transformer in accordance with equation (4.30), the base currents and compensation matrixes as shown in Table 24 shall be used.

Figure 105: Exact location of the internal turn-to-turn fault in phase L2.

Table 24: Compensation data for the 300MVA; 400/115kV auto-transformer

	Base Current Ib	Compensation Matrix MX
W1, 400kV	433A	$M0(0^o) = \frac{1}{3} \cdot \begin{bmatrix} 2 & -1 & -1 \\ -1 & 2 & -1 \\ -1 & -1 & 2 \end{bmatrix}$
W2, 115kV	1506A	$M0(0^o) = \frac{1}{3} \cdot \begin{bmatrix} 2 & -1 & -1 \\ -1 & 2 & -1 \\ -1 & -1 & 2 \end{bmatrix}$

In Figure 106 the following waveforms, either extracted or calculated from this DR file, are presented:

- W1- and W2-side individual phase current waveforms; and
- RMS values of the differential currents.

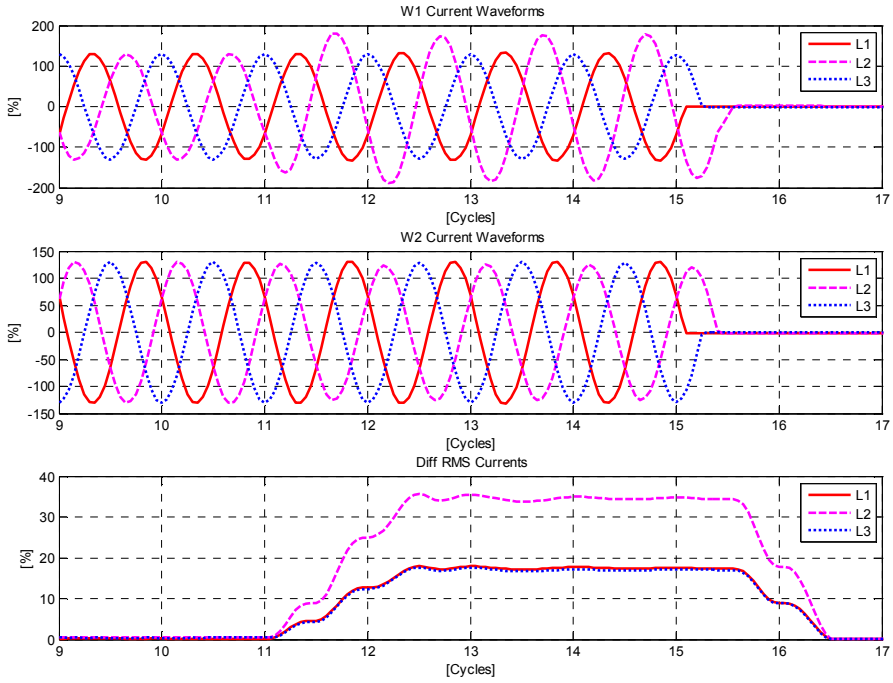

Figure 106: Current waveforms during a turn-to-turn fault, field case #2.

In Figure 107 the following waveforms, either extracted or calculated from this DR file, are presented:

- phase angle between the two negative sequence phasors, as defined in formula (10.5);
- phase angle between the two phase-wise phasors, as defined in formula (10.4); and
- phase angle between the two phase-wise phasors, very similar to the one defined in formula (10.4), but with only M type compensation matrices applied on all sides of the protected transformer.

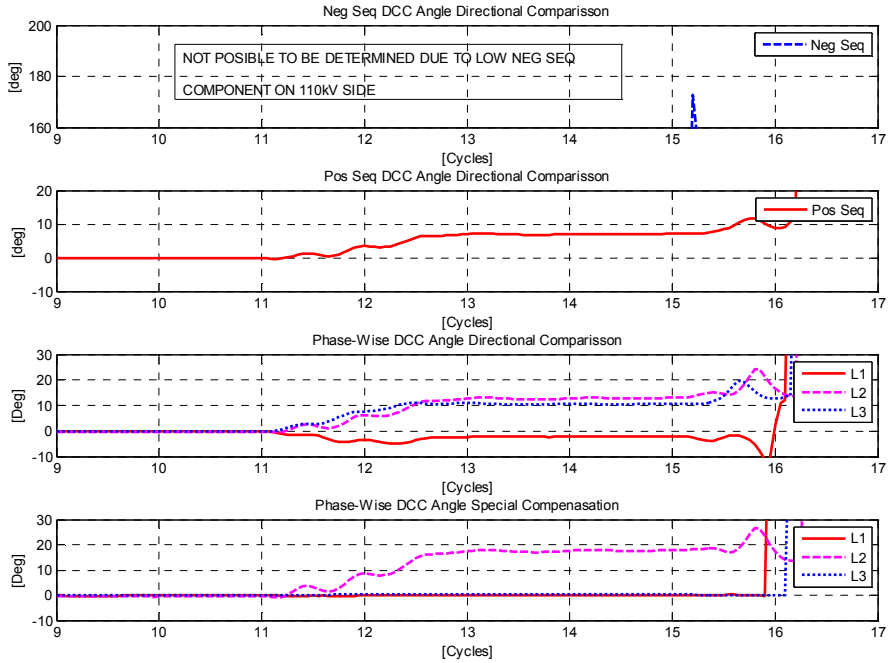

Figure 107: Directional comparison during a turn-to-turn fault, field case #2.

Note that all types of directional comparison, except the one based on the negative sequence current components, could detect that something is wrong within the protected power transformer. The reason for failure of the negative sequence directional comparison is no change of currents on the 110kV side during this fault. While other directional comparison methods could determine that something is wrong only the one where M matrices are used (i.e. without the zero sequence current reduction) on all transformer sides could clearly identify the faulty phase.

Field Case #3

This field case was captured on a three-winding power transformer with the following rating data 25MVA; 115/38.5/6.6kV; Yy0d11; 50Hz, in accordance with IEC terminology [58]. It shall be noted that all three windings are loaded. Because the transformer is installed in an industrial complex, quite high harmonic content is present in individual phase currents during normal through-load conditions. This transformer was protected with a numerical, three-winding differential protection. The 35kV winding internal fault occurred in phase L2 as shown in Figure 108.

Figure 108: 35kV winding internal fault in phase L2.

In order to calculate the differential currents in accordance with equation (4.30), the base currents and compensation matrixes as shown in Table 25 shall be used.

Table 25: Compensation data for a 25MVA; 115/38.5/6.6kV; Transformer

	Base Current Ib	Compensation Matrix MX
W1, 115kV	125.5A	$M0(0^o) = \frac{1}{3} \cdot \begin{bmatrix} 2 & -1 & -1 \\ -1 & 2 & -1 \\ -1 & -1 & 2 \end{bmatrix}$
W2, 38.5kV	374.9A	$M0(0^o) = \frac{1}{3} \cdot \begin{bmatrix} 2 & -1 & -1 \\ -1 & 2 & -1 \\ -1 & -1 & 2 \end{bmatrix}$
W3, 6.6kV	2186.9A	$M(-30^o) = \begin{bmatrix} 0.911 & 0.333 & -0.244 \\ -0.244 & 0.911 & 0.333 \\ 0.333 & -0.244 & 0.911 \end{bmatrix}$

In Figure 109 the following waveforms, either extracted or calculated from this DR file, are presented:

- W1-, W2- and W3-side individual phase current waveforms; and
- RMS values of the differential currents.

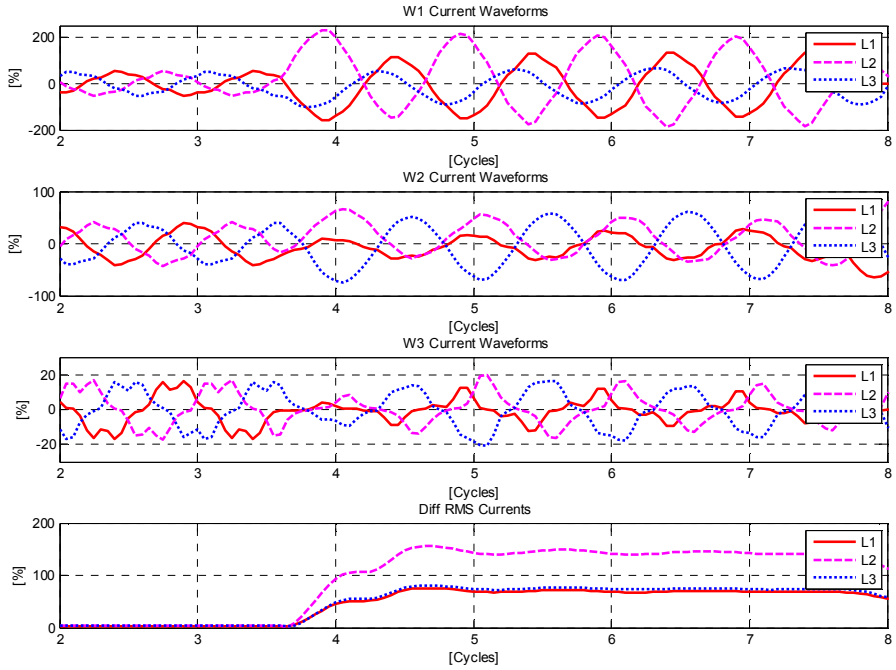

Figure 109: Current waveforms during a turn-to-turn fault, field case #3.

In Figure 110 the following waveforms, either extracted or calculated from this DR file, are presented:

- phase angle between the two negative sequence phasors, as defined in formula (10.5);
- phase angle between the two phase-wise phasors, as defined in formula (10.4); and,
- phase angle between the two phase-wise phasors, very similar to the one defined in formula (10.4), but with only M type compensation matrices applied on all sides of the protected transformer.

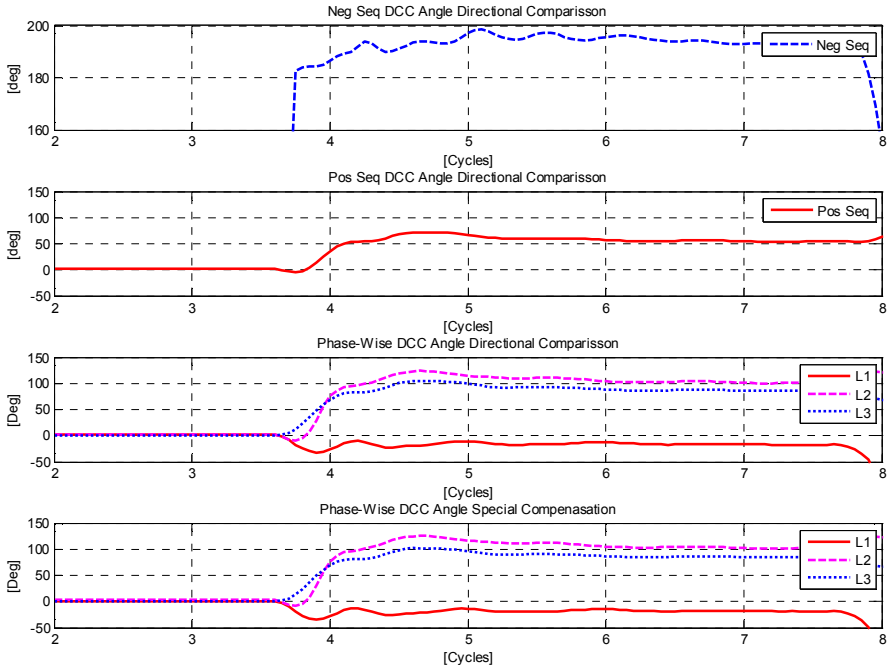

Figure 110: Directional comparison during a turn-to-turn fault, field case #3.

Note that all types of directional comparison could detect that something is wrong with the protected power transformer. Due to the relatively big fault current, all directional methods could see a quite big phase angle change for this fault. However, the phase-wise directional comparison, based only on M matrices being applied to all transformer sides, could not clearly identify the faulty phase in this case.

Field Case #4

This field case was captured on a three-winding transformer with the following rating data 20MVA, 110±13*1,15%/21/10,5kV, YNyn0(d5), 50Hz. Note that this transformer tertiary winding is not loaded and is used as a delta-connected equalizer winding. The 110kV winding neutral point is directly grounded while the 20kV winding neutral point is grounded via a 40Ω resistor. This transformer was protected with a numerical, two-winding differential protection. The differential relay minimum pickup current is set to 23% of the transformer rating. The 110kV winding internal fault occurred in phase L2 when the OLTC was four steps from the mid-position.

In order to calculate the differential currents in accordance with equation (4.30), the base currents and compensation matrixes as shown in Table 26 shall be used.

Table 26: Compensation data for the 20MVA transformer

	Base Current Ib	Compensation Matrix MX
W1, 110kV	100.5A	$M0(0^o)=\frac{1}{3}\cdot\begin{bmatrix}2&-1&-1\\-1&2&-1\\-1&-1&2\end{bmatrix}$
W2, 21kV	550A	$M0(0^o)=\frac{1}{3}\cdot\begin{bmatrix}2&-1&-1\\-1&2&-1\\-1&-1&2\end{bmatrix}$

In Figure 111 the following waveforms, either extracted or calculated from this DR file, are presented:

- W1- and W2-side individual phase current waveforms; and,
- RMS values of the differential currents.

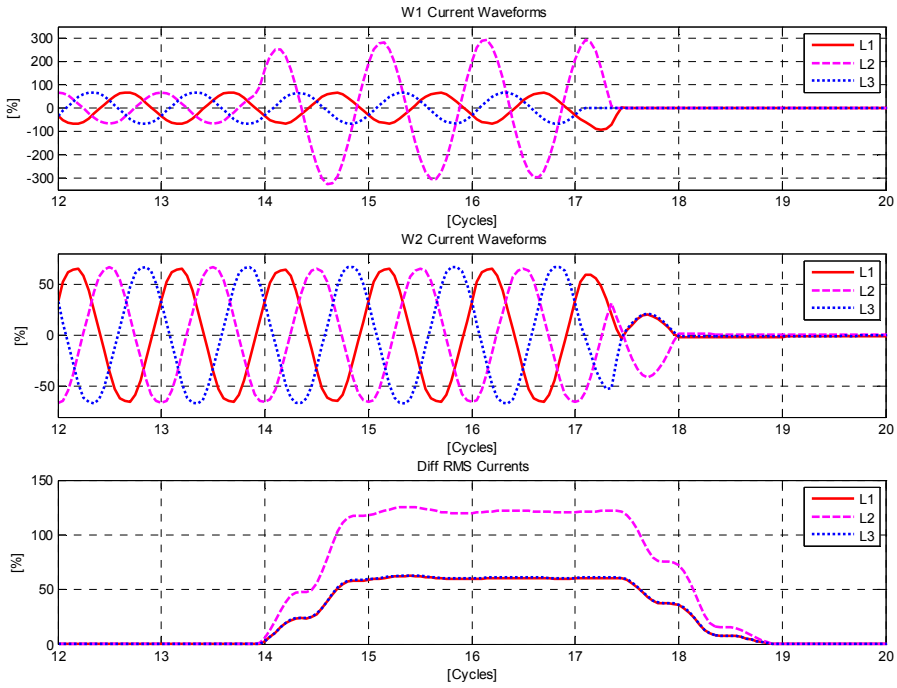

Figure 111: Current waveforms during a turn-to-turn fault, field case #4.

In Figure 112 the following waveforms, either extracted or calculated from this DR file, are presented:

- phase angle between the two negative sequence phasors, as defined in formula (10.5);
- phase angle between the two phase-wise phasors, as defined in formula (10.4); and,
- phase angle between the two phase-wise phasors, very similar to the one defined in formula (10.4), but with only M type compensation matrices applied on all sides of the protected transformer.

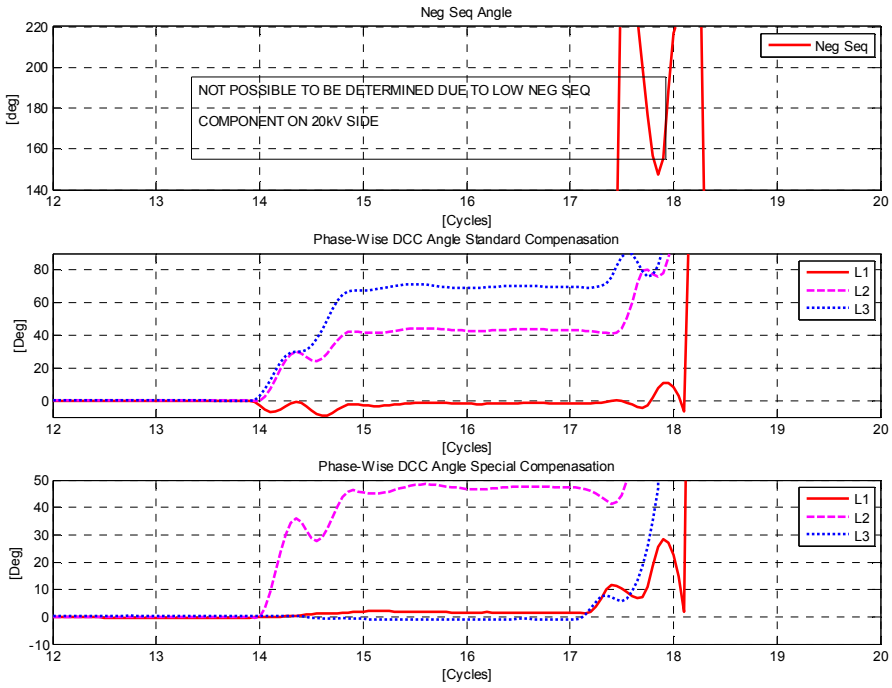

Figure 112: Directional comparison during a turn-to-turn fault, field case #4.

Note that all types of directional comparison except the one based on negative sequence current components could detect that something is wrong within the protected power transformer. The reason for failure of the negative sequence directional comparison is no change in currents on the 20kV side during this internal fault. While all other directional comparison methods could determine that something is wrong, only the one where M matrices are used on all transformer sides could clearly identify the faulty phase.

For this case, large phase L2 110kV current and differential currents appeared during the fault. However, it is interesting to note practically no change in 20kV currents during this internal fault. Similar observations were reported in [30] and [31]. Thus it can be concluded that the phase-wise directional criteria seems to be more dependable in detecting winding

turn-to-turn faults than the negative sequence component based directional criterion.

Case #5

This case is the same test case as presented in Figure 64 and Figure 65, Section 7.2. It is a single-phase to ground fault on the secondary side of the regulating transformer for 2.5° phase angle shift across a PST. It was shown that standard differential protection alone was not sufficiently sensitive to detect this fault. However, by using the directional comparison principle, it is actually possible to detect that something is wrong within the protected PST.

In Figure 113 the following waveforms, from this simulation file, are presented:

- phase angle between the two negative sequence phasors, as defined in formula (10.5); and,
- phase angle between the two positive sequence phasors, as defined in formula (10.5).

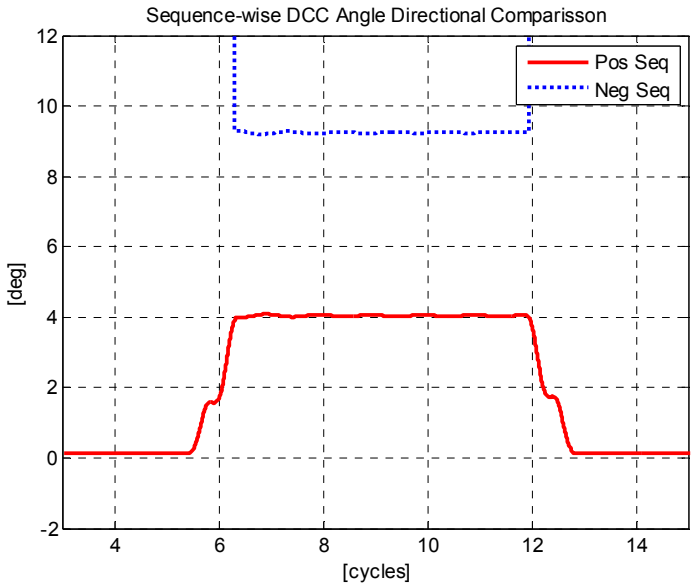

Figure 113: Sequence-wise directional comparison.

In Figure 114 the following waveforms, from this simulation file, are presented:

- phase angle between the two phase-wise phasors, as defined in formula (10.4).

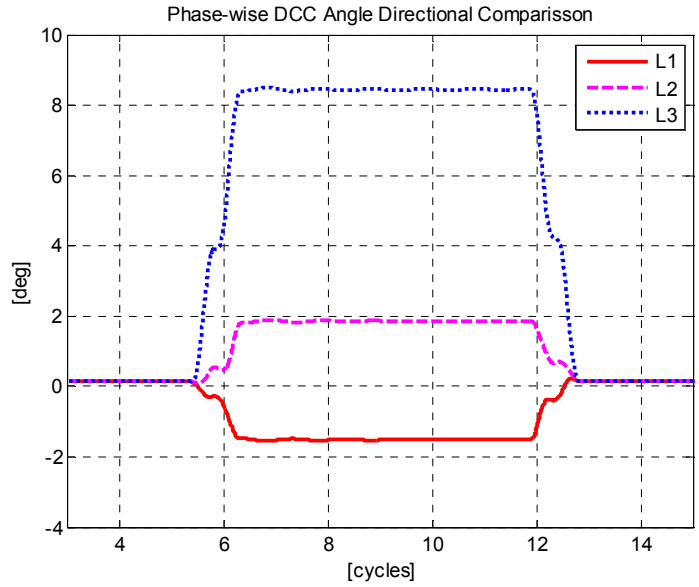

Figure 114: Phase-wise directional comparison.

Note that all types of directional comparison have indicated a deviation from a value of zero degrees, which in principle shall suggest existence an internal fault. However, the negative sequence based internal/external fault discriminator did not completely reverse (i.e. theoretically it should have a value close to 180^{o}). The phase-wise directional comparison in phase L3 had the biggest deviation from 0^{o} phase shift and can therefore be used to detect that something is wrong within the protected PST. It should also be noted that the individual phase currents are in the order of 10-14% of the PST rating during this fault.

Chapter 12

Conclusions

The equations (4.29) and (4.30) represent the universal method to calculate the differential currents for an arbitrary three-phase power transformers. This new method can be used to calculate:

- differential currents, in accordance with Figure 14, for any multi-winding, standard or non-standard power transformers and PSTs with arbitrary phase angle shifts and current magnitude variations;
- differential currents for overall differential protection of two or more series connected power transformers and/or PSTs; and,
- differential currents, in accordance with Figure 14, for any FACTS device, which comply with the assumptions for sequence no-load voltages and load currents, shown in Figure 18 and Figure 19.

The presented method provides a clear relationship between the sequence and the phase quantities for an arbitrary three-phase power transformer. By using this method the differential protection for arbitrary three-phase power transformers will be ideally balanced for all symmetrical and non-symmetrical through-load conditions and external faults, irrespective of the actual OLTC position. Note that inrush and over-excitation stabilization (e.g. 2^{nd} and 5^{th} harmonic blocking) is still required for such differential protection.
The method is also not dependent on individual winding connection details (i.e. star, delta, zigzag), but it might be dependent on correct information regarding the actual OLTC position. On-line reading of the OLTC position and compensation for phase current magnitude variations caused by OLTC movement has been used for numerical power transformer differential protection relays since 1998 [11]. This approach has shown an excellent track record and is the de-facto industry standard in many countries. In this thesis the feasibility of advanced on-line compensation for non-standard or variable phase angle shifts across a power transformer has been

demonstrated. Thus, differential protection for an arbitrary three-phase power transformer can be provided in accordance with Figure 14. By doing so, simple but effective differential protection for special converter transformers and PSTs can be achieved, which is very similar to already well-established numerical differential protection relays for standard power transformers [11] and [12]. The only difference is that elements of M(Θ) or M0(Θ) matrices used to provide the phase angle shift compensation and the zero sequence current reduction are not standard or fixed, but instead dynamically calculated based on the actual OLTC position. Due to the relatively slow operating sequence of the OLTC, these matrix elements can be computed within the differential relay on a slow cycle (e.g. once per second). That should not pose any additional burden on the processing capability of modern numerical differential protection relays.

The presented method has been extensively tested by using disturbance files captured in actual PST installations and RTDS simulations based on practical PST data. All tests indicate excellent performance of this method for all types of external and internal faults.

Any previous publications regarding such a differential protection relay could not be found. Thus, it seems that this work is unique and completely new in the field of power transformer protective relaying.

The presented differential method can also be used to check the output calculations from any short circuit and/or load flow software packages for power systems, which incorporate arbitrary power transformers and/or PSTs. Finally, the method can be used in software packages of modern secondary injection test equipment, in order to make automatic testing routines for the differential protection of any power transformer.

It has also been shown that by using supplementary directional criteria the dependability and the security of the traditional power transformer differential protection can be improved. At the same time, these directional criteria significantly improve the sensitivity of the power transformer differential protection for low level transformer internal faults such as turn-to-turn faults.

Chapter 13

Future Work

From the theoretical point of view it would be interesting to look further into the possibility to apply this universal differential protection method for an m-phase power transformer ($m \neq 3$) and subsequently to derive the equivalent M and M0 matrix transformations for such multi-phase transformers. Afterwards, the possibility to use the presented method for transformer differential protection of special railway transformers, which convert a three-phase power system into a two-phase power system (e.g. Scott and Le-blanc transformers), can be tested.

From the practical application point of view it would be interesting to investigate the influence of incorrect OLTC position feedback from a PST on the presented differential protection method and a way to automatically detect such a condition. Further the behaviour of the presented differential protection for PST series transformer saturation during heavy external faults can be investigated.

For the differential protection of standard power transformers it can be interesting to look further into the presented possibility to arrange the phase angle compensation for a protected power transformer in more than one way. Especially the behaviour of the different phase angle compensation possibilities during transformer initial inrush, sympathetic inrush and evolving faults can be further investigated.

Finally, the influence of the modern FACTS devices (such as HVDC connections and series capacitors installed in the vicinity of the protected power transformer or PST) on the operation of the presented universal transformer differential protection method can be further investigated.

References

[1] Å. Carlson, “Power Transformer Design Fundamentals”, ABB Transformers, Ludvika 2000-08-25.

[2] A. dos Santos, J. Afonso, J. Damásio, “Phase Shift Autotransformer Protection System”, 15th International Conference on Power System protection, Bled-Slovenia, September 2006.

[3] A. Girgis, D. Hart, C. Burnette “Transformer Turn-to-Turn Fault Detection Using Hybrid Parameters”, IEEE Proceedings of SSST/CSA 92 Conference, pp. 402-406, March 1992.

[4] A. Krämer, D. Dohnal, B. Herrmann, ”Special Considerations on the Selection of On-load Tap-changers for Phase-Shifting Transformers”, CIGRÉ SC A2-205, Session 2006, Paris France.

[5] A. R. van C. Warrington, Protective Relays: Their Theory and Practice, Volume One and Two, London: Chapman and Hall, 1962 & 1969.

[6] A. Sapin, P. Allenbach, J.-J. Simond, “Modeling of Multi-Winding Phase Shifting Transformers Applications to DC and Multi-Level VSI Supplies”, PCIM 2002.

[7] A.G. Phadke, J.S. Thorp “A New Computer-Based Flux-Restrained Current-Differential Relay for Power Transformer Protection”, IEEE Transactions on Power Apparatus and Systems Volume PAS-102, Issue 11, pp. 3624-3629, Nov. 1983.

[8] A.G. Phadke, S.H Horowitz “Adaptive relaying”, IEEE Computer Applications in Power Volume 3, Issue 3, pp. 47-51, July 1990.

[9] ABB Book, “Transformer Handbook”, 1LAC 000 010, ABB Power Technologies Management Ltd. Transformers, Switzerland.

[10] ABB Document 1MRK 504 002-UEN, "User´s Guide Transformer differential protection RADSB", September 1997, ABB Network Partner AB, Västerås, Sweden.

[11] ABB Document 1MRK 504 037-UEN, "Application Manual, RET 521*2.5", ABB Automation Technology Products AB, Västerås, Sweden, 2003; (www.abb.com/substationautomation).

[12] ABB Document 1MRK 504 086-UEN, "Technical reference manual, Transformer Protection IED RET 670", Product version: 1.1, ABB Power Technologies AB, Västerås, Sweden, Issued: March 2007.

[13] ABB Guide, "AC Drives Technical Guide Book", ABB Oy, Drives, (www.abb.com/motors&drives).

[14] ABB Leaflet 1LAB 000 019, "Industrial Transformers", ABB Transformers AG, Bad Honnef, Germany.

[15] ABB Leaflet 1LFI2011-en, "Special Transformers-Converter Duty Transformers for Variable Speed Drive Application", ABB Oy Transformers, Vaasa, Finland.

[16] B. Kasztenny, A. Kulidjian “An Improved Transformer Inrush Restraint Algorithm Increases Security while Maintaining Fault Response Performance”, 53rd Annual Conference for Protective Relay Engineers, College Station, Texas, April 2001.

[17] B. Kasztenny, A. Kulidjian, B. Campbell, M. Pozzuoli “Operate and Restraint Signals of Transformer Differential Relay”, 54th Annual Georgia Tech Protective Relaying Conference, Atlanta, Georgia, April 2000.

[18] B. Kasztenny, M. Kezunovic “Digital relays improve protection of large transformers”, IEEE Computer Applications in Power, Vol. 11, Issue 4, pp. 39-45, Oct. 1998.

[19] B. Stenborg, et All., “Fasregleringstransformatorer”, VAST, Stockholm-Sweden, 1988 (in Swedish).

[20] B. Sweeney, “Application of phase-shifting transformers for the enhanced interconnection between Northern Ireland and the Republic of Ireland”, IEEE Power Engineering Journal, Volume 16, Issue 3, pp. 161-167, June 2002.

[21] C.F. Wagner, R.D. Evans, Symmetrical Components, McGraw-Hill, New York & London, 1933.

[22] Converter Transformers – Application Guide, International Standard IEC 61378-3, First edition 2006-04.

[23] E.M. Carlini, G. Manduzio, D. Bonmann, "Power Flow Control on the Italian Network by Means of Phase-Shifting Transformers", CIGRÉ SC A2-206, Session 2006, Paris France.

[24] E.W. Weisstein, "Pseudoinverse." From MathWorld--A Wolfram Web Resource: http://mathworld.wolfram.com/Pseudoinverse.html.

[25] Electrical Transmission and Distribution Reference Book, 4th edition, Westinghouse Electric Corporation, East Pittsburgh, PA 1950, pp. 44-60.

[26] G. Benmouyal, J.B. Mooney "Advanced Sequence Elements for Line Current Differential Protection", 33rd Annual Western Protective Relay Conference, Spokane, WA, October 21–24, 2006.

[27] G. Benmouyal, T. Lee, "Securing Sequence Current Differential Elements" 31st Annual Western Protective Relay Conference, Spokane, WA, October 19–21, 2004.

[28] G. Benmouyal, "The Trajectories of Line Current Differential Faults in the Alpha Plane," 32nd Annual Western Protective Relay Conference, Spokane, WA, October 25–27, 2005.

[29] G. Bertagnolli, "Short-Circuit Duty of Power Transformers; The ABB Approach", Second Edition, Legnano-Italy, 1996.

[30] G. Diaz, A. Barbon, J. Gomez-Aleixandre, J. Coto "Currents Sequence Analyzes of a Transformer under Turn-to-Turn Faults", 14th PSCC Conference, Sevilla-Spain, June 2002.

[31] G. Diaz, J. Gomez-Aleixandre, P. Arboleya "Diagnosis of a turn-to-turn short circuit in power transformers by means of zero sequence current analysis", Electric Power System Research, Vol. 69, Issue 2-3, pp. 321-329, May 2004.

[32] G. Zigler, Siemens, Numerical Differential Protection, March 2005, Book, ISBN 3-89578-234-3.

[33] GE Publication No: GET-8431A, "ACB versus ABC Power System Rotation in the T60", (pm.geindustrial.com/FAQ/FAQ.asp).

[34] GT. Hayder, U. Schaerli, K. Feser, L. Schiel "New algorithms to improve the sensitivity of differential protection of regulating transformers", IEEE Power Tech Conference, Bologna-Italy, Vol. 2, 4 pp., June 2003.

[35] Guide for the application, specification, and testing of phase-shifting transformers, International Standard IEC 62032/IEEE C57.135, First edition 2005-03.

[36] H. K. Høidalen, R. Sporild, "Using Zigzag Transformers with Phase-shift to reduce Harmonics in AC-DC Systems", International Conference on Power Systems Transients (IPST'05) in Montreal, Canada, June 2005.

[37] IEEE Special Publication, "Protection of Phase Angle Regulating Transformers (PAR)," A report to the Substation Subcommittee of the IEEE Power System Relaying Committee prepared by Working Group K1, Oct. 1999.

[38] J. Brochu, F. Beauregard, R. Cloutier, A. Bergeron, L. Garant, "Innovative Applications of Phase-Shifting Transformers Supplemented with Series Reactive Elements", CIGRÉ SC A2-203, Session 2006, Paris France.

[39] J. Johansson, Fast Estimation of Symmetrical Components, M.Sc. Thesis, Department of Industrial Electrical Engineering , Lund University, Sweden, 2002.

[40] J. Pihler, B. Grcar, D. Dolinar "Improved operation of power transformer protection using artificial neural network", IEEE Transactions on Power Delivery, Vol. 12, Issue 3, pp. 1128-1136, July 1997.

[41] J. Rimez, D. Wiot, E. Jottrand, R. vd Planken, G. Claessen, J. Declercq, "Grid implementation of a 400MVA 220/150kV –15°/+3° phase shifting transformer for power flow control in the Belgian network: specification and operational considerations", CIGRÉ SC A2-202, Session 2006, Paris France.

[42] J.A.B. Elston, Methods and Apparatus for Differential Current Measurement in a three-phase power system, U.S. Patent 6,507,184; 2003-01-14.

[43] J.L. Blackburn, Symmetrical Components for Power System Engineering, Marcel Dekker, New York, Basel, Hong Kong, 1993; ISBN: 0-8247-8767-6.

[44] J.L. Schiel, Differential Current Protection for a Transformer, U.S. Patent 5,790,357; 1998-08-04.

[45] J.S. Thorp, A.G. Phadke "A Microprocessor Based Three-Phase Transformer Differential Relay", IEEE Transactions on Power Apparatus and Systems Volume PAS-101, Issue 2, pp. 426-432, Feb. 1982.

[46] K. Tian, P. Liu "Improved Operation of Differential Protection of Power Transformers for Internal Faults Based on Negative Sequence Power", IEEE Proceedings of EMPD'98 Conference, Vol. 2, pp. 422-425, March 1998.

[47] K. Yabe "Power Differential Method for Discrimination between Fault and Magnetizing Inrush Current in Transformers", IEEE Transactions on Power Delivery, Vol. 12, Issue 3, pp. 1109-1118, July 1997.

[48] K.K. Sen and M.L. Sen, "Introducing the Family of Sen Transformers: A Set of Power Flow Controlling Transformers," IEEE Trans. Power Delivery, Volume 18, Issue 1, pp. 149-157, Jan 2003.

[49] L. Asiminoaei, S. Hansen, F. Blaabjerg, "Development of calculation toolbox for harmonic estimation on multi-pulse drives", IEEE Industry Applications Conference, Vol. 2, pp. 878-885, Oct. 2004.

[50] M. Tripathy, R.P. Maheshwari, H. K. Verma "Advances in Transformer Protection: A Review", Electric Power Components and Systems, Taylor & Francis, Oct. 2005.

[51] M.J. Thompson, "Apparatus and Method for Providing Differential Protection for a Phase Angle Regulating Transformer in a Power System", USA Patent Application, Pub. No: US2007/0041137 A1, USA.

[52] M.J. Thompson, H. Miller, J. Burger, "AEP Experience With Protection of Three Delta/Hex Phase Angle Regulating Transformers", 60th Annual Georgia Tech Protective Relaying Conference, April 2006, Atlanta USA.

[53] M.R. Rao, B.P. Singh "Detection and Localization of Interturn Fault in the HV Winding of a Power Transformer Using Wavelets", IEEE Transactions on Dialectrics and Electrical Insulation, Vol. 8, Issue 4, pp. 652-657, Aug. 2001.

[54] O.W. Andersen, "Large Transformers for Power Electronic Loads", IEEE Transaction on Power Delivery, Vol. 12, Issue 4, pp. 1532-1537, Oct. 1997.

[55] P. Bastard, P. Bertrand, M. Meunier "A Transformer Model for Winding Fault Studies", IEEE Transactions on Power Delivery. Vol. 9. Issue 2, pp. 690-699, April 1994.

[56] P. Hurlet, J-C. Riboud, J. Margoloff, A. Tanguy, "French Experience in Phase-Shifting Transformers", CIGRÉ SC A2-204, Session 2006, Paris France.

[57] P. Liu, O.P. Malik, D. Chen, G.S. Hope, Y. Guo "Improved Operation of Differential Protection of Power Transformer for Internal Faults", IEEE Transactions on Power Delivery, Vol. 7, Issue 4, pp.1912-1919, Oct. 1992.

[58] Power transformer, International Standard IEC 60076, First edition 1997-10.

[59] R. Grünbaum, M. Noroozian, B. Thorvaldsson, "FACTS – powerful systems for flexible power transmission", ABB Review No 5, 1999.

[60] R.G. Andrei, M.E. Rahman, C. Koeppel, J.P. Arthaud, "A novel autotransformer design improving power system operation", IEEE Transactions on Power Delivery, Volume 17, Issue 2, pp. 523-527, April 2002.

[61] R.S. Girgis, E.G. teNyenhuis "Characteristics of Inrush Current of Present Designs of Power Transformers", Power Engineering Society General Meeting, June 2007, pp. 1-6.

[62] Transformer Book, Tampere University of Technology, (http://www.e-leeh.org/transformer/).

[63] W. Bartley, "Analysis of Transformer Failures", International Association of Engineering Insurers 36th Annual Conference, Stockholm, Sweden, 2003.

[64] W. Seitlinger, "Phase Shifting Transformers", VA TECH T&D (VA TECH ELIN TRANSFORMATOREN GmbH) Publication, 2001, www.vatechtd.com.

[65] Y.C. Kang, E.S. Jin, S.H. Kang, P.A. Crossley, "Compensated-current differential relay for protection of transformers", IEE Proceedings-Generation, Transmission & Distribution, Vol. 151, No 3, pp.281-289, May 2004.

[66] Y.C. Kang, B.E. Lee, S.H. Kang, P.A. Crossley, "Transformer protection based on the increment of flux linkages", IEE Proceedings-Generation, Transmission & Distribution, Vol. 151, No 4, pp.548-554, July 2004.

[67] Z. Gajić, I. Ivanković, B. Filipović-Grčić, "Differential Protection Issues for Combined Autotransformer – Phase Shifting Transformer," IEE Conference on Developments in Power System Protection, Amsterdam, Netherlands, April 2004.